

An assessment of the relation between monitored settlements
and the face stability of a slurry-TBM

An assessment of the relation between monitored settlements and the face stability of a slurry-TBM

By

R.A.P. Verloop

Student number: 4236564

to obtain the degree of Master of Science at the Delft University of Technology,
to be defended publicly on Tuesday June 16th, 2020 at 11:00 AM.

Committee

Chair: Dr.Ir. W. Broere	TU Delft
Dr. Ir. R.B.J. Brinkgreve	TU Delft
Ir. C. Kasbergen	TU Delft
Ir. H. Mortier	COMOL5/DIMCO
Ir. M. Brugman	COMOL5/Arthe Civil & Structure

Acknowledgements

This research has been conducted at the section Geo-Engineering of the department of Geoscience & Engineering at the faculty of Civil Engineering and Geosciences at the Delft University of Technology. Great support came from my graduation committee: Dr. Ir. W. Broere, Dr. Ir. R.B.J. Brinkgreve, Ir. C. Kasbergen, Ir. H. Mortier and Ir. M. Brugman. A special thanks to my chair: Dr. Ir. W. Broere for his great guidance, advice and mentorship throughout this research and for introducing me to the topic of use of underground space 4 years ago. Also, a special thanks to Ir. H. Mortier for introducing me to this research topic while visiting the World Tunnelling Congress in 2018. I also would like to thank him for our meetings which were not often, but very useful when having them. I would like to thank Dr. Ir. R.B.J. Brinkgreve for his critical but always spot-on advice and numerous tips and tricks regarding the numerical modelling in Plaxis 3D. I am thankful for the time you spent on looking at my models with me. Ir. M. Brugman, thank you very much for your mentorship and advice throughout my entire thesis. I have learned a lot from you both technically and professionally. Also, I am really thankful you took care of me on the project site, you guided me to find the right people to go to. You also made it possible I was able to see the (cutterhead of the) TBM at a standstill. A dream came true, really. You and W. Broere were the ones who slowed me down when I was being too enthusiastic. I would like to thank Ir. B. van de Water for his always positive attitude, fun coffee breaks, walks and for helping me out providing the data I needed to fulfil my research. I also would like to thank the consortium COMOL5 for their warm welcome at the project site of the RijnlandRoute project, but also for allowing me to use their project data for my research. Within COMOL5 a special thanks to Ir. Y. Liem, D. van Hek, Ir. C. Lantinga-Vermeulen and Ir. R. Lassaux, who I was working with at the project site. They not only gave me great advice and were always willing to help me, but also made the lunch breaks a lot of fun. I would like to thank Ir. K. Reinders for her guidance during the first part of my thesis.

A special thanks to my friends and family, in particular my brother Bas for the endless support and for guiding me into the right direction when needed. Also, I would like to thank my parents for their unlimited support, encouragement and love.

Rosanne Augusta Paulina Verloop
Delft, June 2020

Abstract

During the boring of a tunnel in soft soils with a slurry TBM, support pressure is used to achieve equilibrium at the face of the TBM. When this equilibrium is not reached, when the face support pressure is too low or too high, settlements will occur. In this research settlement and pore water pressure measurements are used to monitor the behavior of the soil and estimate the stability of the tunnel face. During boring of the tunnel, the exact stability of the face is not known. The TBM driver has to rely on the provided stratigraphy data, the advised face support pressures range provided by the geotechnical engineers and the experience of the tunnel boring team. Monitoring is not yet used to determine the face stability during construction. To do so, field data from a case study at RijnlandRoute is compared with analytical and numerical models. Sensitivity of the measurement equipment, and of both the analytical (DIN) and numerical model (Plaxis 3D) with respect to soil parameters, are considered.

It has been found that the strength parameters of the layer in which the face is located have the highest influence on the minimum face support pressure. For the maximum face support pressure this is the volumetric weight of the entire soil profile above the face.

For comparing the (soft soil) field data with numerical results, a Plaxis 3D model is built, and it is determined that HSsmall is a suitable constitutive model to capture the interaction between face stability, tunneling operations and soil behavior. It is shown that the tail void injection influences the settlements above and in front of the cutter head, but this influence is discarded and replaced by a wished in place lining, to simplify the numerical model.

A scenario analysis on the sensitivity of soil parameters shows settlements do not vary significantly between the characteristic low and high values. In this analysis correlation of parameters is taken into account. The failure mechanism for the minimum face support pressure coincides with the active cave-in failure mechanism found in literature. For the maximum face support pressure the failure mechanism found in Plaxis 3D does not coincide with the expected hydraulic fracturing failure mode. The continuum representation of the soil in Plaxis 3D does not allow a hydraulic fracturing like failure mechanism to develop. Instead, a blow-out approximately 10 m. in front of the cutterhead occurs. This behaviour better resembles the failure mechanism of a EPB TBM.

The field data gathered from the case study shows a thrust wave in front of the cutter head in both settlement and pore water pressure measurements. This thrust wave reaches up to 20 to 40 meters in front of the TBM. The heave induced by the thrust wave reduces the amount of settlements after the TBM passage. Excess pore pressures, induced by a high thrust wave, affect the face stability negatively. The excess pore pressure mainly depends on the advance rate. The higher the advance rate, the less time the pore pressures have to dissipate, leading to an increase in excess pore pressure. The accuracy of the settlements measurement devices is 0.8 mm., and of the spade cells 1.0 kPa. In general, the field data shows settlement curves corresponding to the Peck (1969) Gaussian curve (in lateral and longitudinal direction).

Comparing the case study settlements with the numerically generated settlement curves show similar trends. The field data shows lower settlements than the numerical results. This can be due to the presence of excess pore pressures, the accuracy of the TBM data or its interpretation. A method to increase the accuracy, which is expected to result in a better fit with the numerical results, was found in a late phase of the research. This method takes into account the settlements which are induced by the thrust wave in front of the TBM.

Comparing the numerical and analytically determined limit support pressures, it is found that the minimum face support pressure are similar in both methods. As similar failure mechanisms are found, numerical modelling seems a reliable way of determining the face stability. However, due to the limited range of applied support pressures available from the TBM data set, limit states could not be fully analyzed. To assure the reliability of a numerical model to determine the actual face stability based on surface settlements during the construction phase, additional research must be done. It is suggested to extend the methods used in this research with physical modelling. For maximum face support pressures, the analytical and numerical models do not coincide. Hydraulic fracturing cannot be modelled in Plaxis 3D. It is recommended not to use numerical modelling to determine the face stability based on settlements at face pressures higher than the face pressures at which an equilibrium is achieved.

Contents

Acknowledgements	iv
Abstract	vi
List of symbols	ix
1 Introduction	1
1.1 General introduction	1
1.2 Aim of the research	5
1.3 Approach	6
1.4 Hypothesis	7
1.5 Outline of the thesis	11
2 Theoretical and practical background information	12
2.1 Face stability	12
2.2 Settlements	15
2.3 (Geo-)technical project information	17
2.4 Field monitoring	21
2.4.1 Spade Cell	21
2.4.2 Settlement Marker & Total Station	22
2.5 Practical considerations	23
2.6 Summary and Conclusions	24
3 Analytic face stability	25
3.1 Scenario analysis – Analytical	25
3.1.1 Input parameters	25
3.1.2 Results	26
3.2 Advanced Soil profile Analysis - Analytical	27
3.2.1 Input parameters	27
3.2.2 Results	28
3.3 Summary & Conclusions	28
4 Numerical modelling	29
4.1 Boundary conditions and soil model	29
4.1.1 Constitutive soil model	29
4.1.2 HSmall parameters	29
4.2 Model design properties	30
4.2.1 Tunnel designer	30
4.2.2 Mesh generation	31
4.2.3 Construction of the tunnel	32
4.3 Influence of tail void injection and the taper of the TBM shield on settlements in front of the cutterhead	32
4.4 Scenario analysis – numerical modelling	33
4.4.1 Input parameters	33
4.4.2 Results	34
4.5 Advanced soil profile analysis – numerical	36
4.5.1 Input of advanced soil profile	36
4.5.2 Results	36
4.6 Summary & Conclusions	42
5 Field data analysis	43
5.1 Settlements – Monitored Field Data	44
5.1.1 Data interpretation	44
5.1.2 Data trends	46
5.2 Pore water pressure – Monitored Field Data	47
5.2.1 Data interpretation	47
5.2.2 Data trends	47
5.3 Face support pressure – Monitored TBM Data	50
5.3.1 Data interpretation	50

5.3.2	Data trends.....	50
5.4	Summary & Conclusions.....	51
6	Case study	52
6.1	Relation between the advanced soil profile numerical model and the field data	52
6.2	Relation between the advanced soil profile numerical model and the advanced soil profile analytic face stability.....	54
6.2.1	Minimum face support pressure.....	55
6.2.2	Maximum face support pressure	56
7	Conclusions & Recommendations	58
7.1	Conclusions	58
7.2	Recommendations.....	62
	Bibliography	63
	Appendix	65

List of symbols

General

c	cohesion
c'	effective cohesion
c_u, s_u	undrained shear strength
γ	soil volumetric weight
γ'	effective soil volumetric weight
φ	Angle of internal friction
σ_v	total stress
σ'_v	effective stress

Face stability

C	overburden
C_{gem}	average cohesion of multiple soil layers
D, z_e	outer diameter of TBM/lining
e_{ah}	horizontal effective stress, including 3D effect
h	thickness of layer
K_{ach}	factor of active soil pressure for cohesion
K_{agh}	factor of active soil pressure
l_{ag}	length of arching
p_{min}, p_{max}	minimum and maximum face support pressure resp.
u	pore water pressure
Z	Distance of the middle of the layer to surface level
φ_{gem}	average friction angle of multiple soil layers

Settlements

i	point of inflection
s	settlement
S_{exc}	excavated area
$S_{v,max}$	maximum settlement at centre line of tunnel
V_L	total volume loss

Numerical modelling

c'_{ref}	effective cohesion at reference pressure
$C_{inc,axial}$	contraction increment
C_{ref}	reference contraction
C_{tot}	total contraction
e_{init}	initial void ratio
E_0	initial elasticity of Young's modulus - stiffness
E_{50ref}	secant elastic modulus
E_{oedref}	tangent oedometer stiffness
E_{ur}	unloading-reloading elasticity of Young's modulus - stiffness
E_{uref}	E_{ur} at reference stress level
G_0	initial small-strain shear modulus
G_{ur}	unloading-reloading small-strain shear modulus
p_{ref}	Reference stress level
m	Power for stress level dependency of stiffness
OCR	over-consolidation ratio
POP	pre-overburden pressure
V_{inner}	volume according diameter the at the tail of the shield
V_{outer}	volume according diameter the at the face of the shield

$X_{gem;k;low}$	average low characteristic value
$X_{gem;k}$	average characteristic value
$X_{gem;k;high}$	average high characteristic value
ν_{ur}	unloading-reloading Poisson's ratio
$\gamma_{0.7}$	reference strain
γ_{unsat}	unsaturated soil volumetric weight
γ_{sat}	Saturated soil volumetric weight

Chapter 1

Introduction

This chapter introduces the research topic and its accompanying pillars in this study. A general introduction will be given in the first paragraph, §1.1. §1.2 and §1.3 respectively, discuss the aim and approach of this research. The hypothesis is presented in §1.4, and the chapter finishes with an outline of the remainder of the thesis in §1.5.

1.1 General introduction

Following the general trend in the world, the Netherlands copes with a rapidly increasing population density [16]. This leads to less and less available space above ground and congestions at existing infrastructure networks. A tunnel is an attractive solution to increase the infrastructure capacity without using above ground (green) space. One of the possibilities to build a tunnel, is by the use of a tunnel boring machine, abbreviated a TBM. There are several types of TBM's.

This research makes use of a case study: the RijnlandRoute. Part of the RijnlandRoute project will be a new road, the N434, which connects the A44 (junction Ommedijk) and the A4 (junction Hofvliet), near Leiden, see Figure 1.1. This new connection will reduce congestion in the area. The project, commissioned by the Province of Zuid-Holland, will be carried out by COMOL5¹. Some key characteristics of the N434 project are:

- It will be a 2,247 meter long bored twin tunnel;
- At the west side a cut and cover ramp of 80 meter and a 1,346 meter deepened road connect the tunnel to the junction Ommedijk;
- At the east side a cut and cover ramp of 96 meter and a 237 meter deepened road connect the tunnel to the junction Hofvliet;
- The tubes will have an outer diameter of 10.59 meters;
- The tunnel is located in soft soil with a high ground water table.

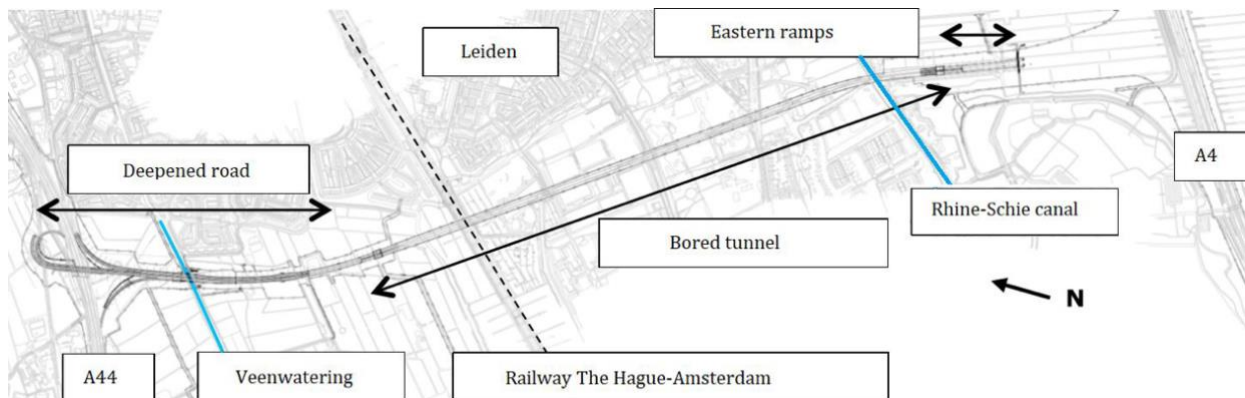


Figure 1.1: Overview of the subproject N343, part of the RijnlandRoute [15]

¹ Comol5 is an international contractor combination of the TBI companies Mobilis B.V. and Croonwolter&dros B.V, VINCI Construction Grand Projects S.A.S. and DEME Infra Marine Contractors B.V.

In this project a slurry shield TBM is used, which has a full face cutterhead which provides face support by pressurizing boring fluid inside the cutterhead chamber. This slurry prevents water and soil from flowing in. The pressure of the slurry can be adapted and regulated by the TBM operator at all times and is supported by an air bubble as shown in Figure 1.2. The slurry provides pressure on the soil and forms a filter cake in front of the shield. This cake, which is a mix of the soil and slurry, is excavated and transported to a separation plant. In the separation plant the slurry is cleaned and prepared for re-use. Slurry consists of a bentonite suspension.

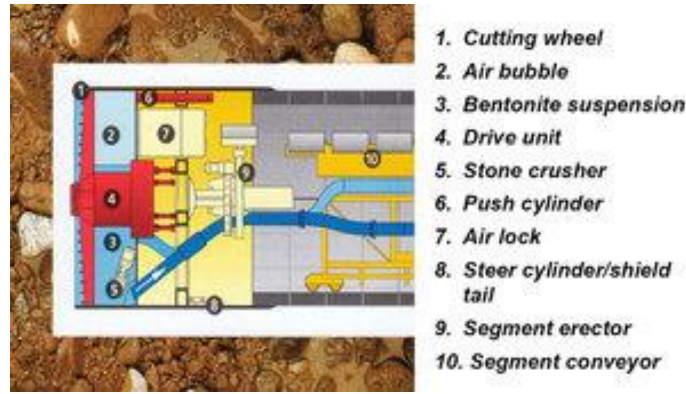


Figure 1.2: Slurry shield TBM [24]

The heterogeneity of the subsurface induces a large amount of uncertainties, which creates a risk. Not only the heterogeneity of the soil but also the design method has an influence on the preciseness of the estimation. To minimize these risks, safety factors are applied during the design of a(n) (underground) construction. These safety factors may however lead to an over conservative design which would be detrimental for the overall costs and the environmental impact of the project.

During construction, the excavations performed by the TBM are expected to lead to settlements. When displacements are negative (the surface is lowered), settlement is positive. Negative settlement equals heave (the surface is lifted). The settlements which are induced by the passage of the TBM must not exceed a maximum level of 10 cm.. This is regulated in the project contract as shown in Figure 1.3. In the project contract a serviceability limit state (SLS) and an ultimate limit state (ULS) are defined. In this case, the SLS is governing but due to this permissible SLS limit, it could very likely be (especially with low soil cover) that ULS requirements regarding face stability failure will occur more rapidly than these large settlements (SLS), which means the ULS might be leading in this case.

Requirement ID	Description	Reference
Hindrance to shipping during construction	Shipping on the Rijn-Schiekanaal shall not be hindered by construction activities for the RijnlandRoute	OSP-0187
Maximum settlements	Surface settlements caused by the construction of the Bored tunnel shall not exceed 10 cm	OSP-1069

Figure 1.3: Requirements maximum settlements [5]

The settlements can be kept below the defined limit by applying the correct bore front pressure. The bore front pressure is the pressure the slurry shield applies on the soil, which counterbalances the soil and water pressures in front of the TBM, Figure 1.4. The limits between which the bore front is stable are between the minimum- and maximum bore front pressure. During the project, there are several critical locations where staying within those limits is more critical and harder to achieve.

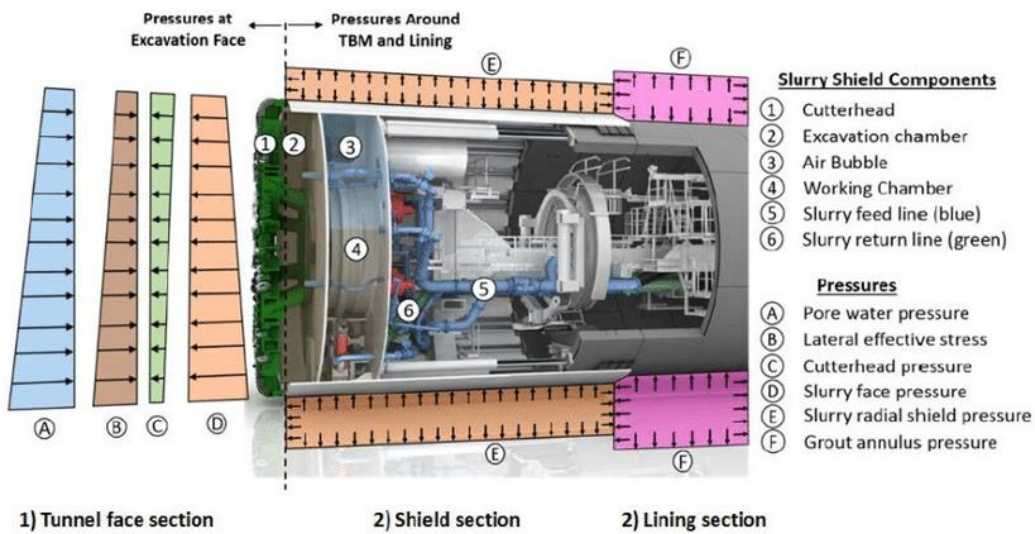


Figure 1.4: Schematic of Slurry Shield TBM and pressure components (a portion of image courtesy of Herrenknecht (after Zili LI, et al, 2015))

Due to the low and partially artificial overburden, the first critical location of the project is at the start and launch of the TBM. This first critical part will hereafter be referred to as the embankment area. The second critical location is the crossing of the Rijn-Schiekanaal at only 250 m away from the launching shaft [15]. At the location of the embankment additional measurement equipment is installed besides the regular measurement equipment which is spread along the entire route of the tunnel.

When focusing on the embankment area the artificial overburden is used to provide sufficient cover to prevent a blow-out², cave-in³, or hydraulic fracturing⁴ at the launch of the TBM. For the design of the overburden, a set of methods is available to determine the dimensions of this overburden. In prior research by Lantinga, (2018), a set of those methods are compared and discussed in detail. The methods are: Ruse-Vermeer (2002) (RV), DIN4126+4085 (2007, 2013) (DIN) and Jancsesz & Steiner (1994) (J&S). The last two have been successfully applied in Dutch projects and are both analytical methods, 2D and 3D respectively. In contrary, the RV method hasn't been applied in Dutch projects yet, however when making a design for the overburden, this method turns out to be the most optimal one due to the smallest embankment required, see Figure 1.5. The method is not applied in the RijnlandRoute project since there is no experience regarding this method on Dutch soils and therefore the reliability is unknown. The RV method is an analytical method based on numerical results. The method applied to determine the height of the overburden at the RijnlandRoute is the DIN method in combination with the EC7 (EuroCode7) which takes into account the friction of the of the failure envelope. Because this method is used for the case study, only this one will be used for the calculations in this research. With the height of the overburden known, the minimum and maximum support pressure of the bore front can be determined.

²Blow-out: when the face support pressure is too high and blows-out the soil in front of the TBM, a passive failure mechanism.

³Cave-in: when the face support pressure is too low and the tunnel face collapse into the TBM, an active failure mechanism.

⁴Hydraulic fracturing: when the face support is too high and there is a pressure loss which leads to a cave-in, a local failure mechanism as a result of micro instability. Also known as piping.

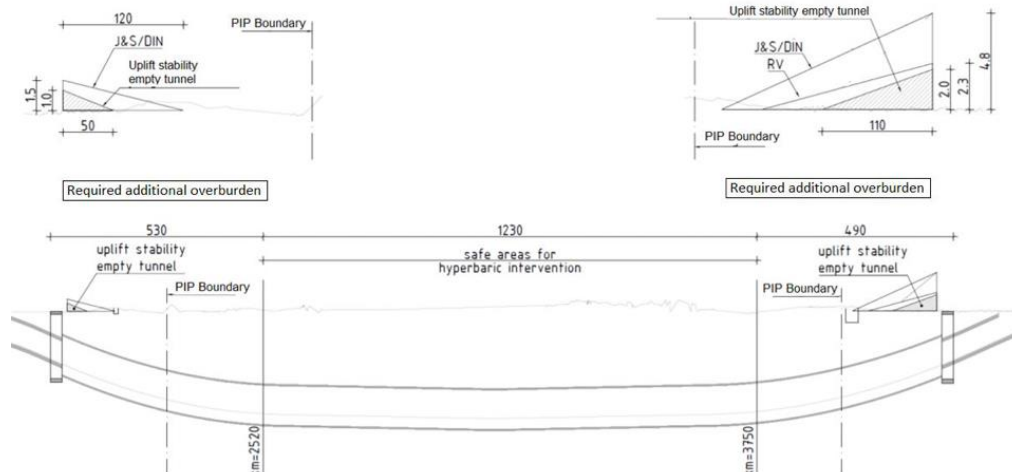


Figure 1.5: The additional overburden required for the bore front's stability and resistance against buoyancy during construction [5]

In this research, the focus lies at the stability of the bore front and the associated settlements at the face and in front of the TBM. In current projects an estimation of the settlements is based on analytical calculations, sometimes in combination with a numerical (finite element method) model.

Those analytical calculations give a range of applied face support limits with a related settlement or volume loss indication. This range is used by the TBM operator to stay within those limits to prevent a cave-in or blow-out. In reality the TBM operator has no insight in how close the applied face stability is to either one of the two limits. This is the main part of the problem that will be elaborated on in this thesis.

During a project, research is done for optimization. When this results in too complex calculations/outcomes, the findings cannot be executed in the project which is often driven by contractual constraints (time and money). It can however add significant value for future projects, basically all tunnel projects in the Netherlands, which emphasises the high relevance of this research.

1.2 Aim of the research

In order to find answers to the problems and challenges discussed in the previous paragraph, the aim of the research is to define a relation between the monitored settlements in front of the cutterhead/face of the TBM and the face stability of a slurry TBM.

The second aim of the research is to define a range of minimum and maximum face support pressures for both the analytical and numerical method to relate to the applied pressures of a case study. The aim is to find out what the safety of the applied pressure is in relation to the ranges of both the analytical and numerical methods. This can lead to a more advanced insight in the safety of the boring process.

The third aim is to check whether the analytical and numerical models are comparable and if not, investigated why not.

The research is conducted for the Dutch infrastructure project the RijnlandRoute. Due to the time limit of this research, it is suggested another student validates the results of this research by another Dutch case study: Rotterdamsebaan. The Rotterdamsebaan also provided data, which makes it feasible to perform a similar research.

The above leads to the following research question:

Is it possible to determine a relation between monitored settlements and the face stability of a slurry TBM by numerical modelling?

1. Is it possible to determine the relation between settlements and the face stability of a slurry TBM in an analytical way?
2. Is it possible to determine the relation between settlements and the face stability of a slurry TBM by numerical modelling?
 - 2.1. What are appropriate boundary conditions to set up this specific model?
 - 2.2. What are the influences of the soil profile parameters on the stability of the face of the TBM and the settlements?
 - 2.3. Does the mortar pressure of the tail void injection influence the face stability/or settlements in front of the cutterhead?
 - 2.4. Does the taper of the TBM influence (settlements in front of the cutterhead)?
3. Can trends be found in the relation between face support pressure and monitored settlements?
 - 3.1. Do the measured settlements show trends?
 - 3.2. Do the measured pore water pressures show trends?
 - 3.3. Do the applied face support pressures show trends?
 - 3.4. Can trends be found in the relation between face support pressure and settlements with support of 3D modelling?

The boundaries of this research must be monitored throughout the progress of this thesis. Those boundary conditions are due to time constraints of this thesis.

1.3 Approach

The approach of this research is built upon three pillars: Analytical approach, a numerical approach and via field data from the case study, the RijnlandRoute. The aim is to connect the three pillars with each other to find the answer to the main research question: Is it possible to determine a relation between monitored settlements and the face stability of a slurry TBM by numerical modelling?

The reason the analytical approach is included in the research is because at the moment the design limits of a soft soil tunnelling project are often based on analytical calculations. It is of interest for the reliability of the outcome of the thesis to find out if the numerical approach finds results which are similar or close to the analytical ones. In this way a reference is created.

The approach to finding an answer to the main research question starts with a literature study to form a solid base for the rest of the research. Thereafter the three pillars are discussed separately. This is followed by connecting the pillars, leading to conclusions and the ability to answer to the research question. The entire research focuses on a cross-section of the case study at which much data is available and to be able to compare each of the pillars with one another.

The analytical approach consists of a scenario analysis of a simplified soil profile. This simplified soil profile is based on the prior mentioned cross-section to study the influence of varying soil parameters on the analytically determined face support pressure limits. Second, an analytical calculation at the case study cross-section is done to determine the analytical minimum and maximum face support pressure.

The numerical approach is performed by use of Plaxis 3D modelling. The approach is similar to the analytical one, but is extended in 2 ways. First, the scenario analysis is extended because in numerical modelling a larger set of soil parameters is considered compared to in an analytical calculation. Second, influences of design properties such as tail void injection and contraction due to the taper of the TBM are considered. The numerical approach also makes a numerical model at the prior mentioned case study cross-section to determine the minimum and maximum face support pressure and the corresponding settlements and failure mechanisms.

The field data from the case study consist of measured settlements measured pore water pressures and applied face support pressures. The gathered data is separately analysed for both trends and irregularities. The aim is to find interrelated conclusions between the different type of data.

After discussing each of the three pillars, the pillars are compared and related to one another. This will happen by defining the relation between the numerical results and the field data, and between the numerical results and the analytical results.

When this is completed it is assumed to be able to answer the research questions.

1.4 Hypothesis

Before starting the research, a hypothesis is formulated. This aims to address the main research question:

Is it possible to determine a relation between monitored settlements and the face stability of a slurry TBM by numerical modelling?

The hypothesis on the main research question will be based on the sub-research questions and hypothesis which are presented below. The hypothesis relating to the main research question will be presented at the end of this paragraph.

Is it possible to determine the relation between settlements and the face stability of a slurry TBM in an analytical way?

It is expected there will be no relation between the settlements and face stability determined in an analytical way. This is because the analytical way of determining the face stability does not involve settlements parameters and vice versa.

Is it possible to determine the relation between settlements and the face stability of a slurry TBM by numerical modelling?

This relation is expected to be found, because by means of numerical modelling the settlements and face stability are (numerically) interrelated.

- ***What are appropriate boundary conditions to set up this specific model?***

Literature is consulted to find appropriate boundary conditions as well as the soil model type which is best suitable for this research. The literature results should however be validated and adapted accordingly for this case study. It is expected the Hardening Soil Small Strain model will be the most suitable constitutive model, driven by the large scale of the tunnel and TBM in combination with the relatively small displacement occurring due to mechanized tunnelling.

- ***What are the influences of the soil profile parameters on the stability of the face of the TBM and the settlements?***

The soil profile parameters are expected to be of influence on the stability of the face and the settlements. The influence is expected to be mainly locally at the cutterhead and above it with extension to in front of the cutterhead (the area of the failure wedge). With regards to the soil parameters, it is expected the strength parameters are of most influence because their high influence on the interparticle bond. This is expected to have the largest influence at the location of the failure wedge of the bore front.

- ***Does the mortar pressure of the tail void injection influence the face stability/or settlements in front of the cutterhead?***

As mentioned in the research approach, it is investigated if the tail void injection influences the displacements in front of the face of the tunnel. It is expected that the influence of the tail void injection is strongly dependent on the pressure applied. When a low-pressure tail void injection is applied, the failure plane is expected to be active. This is leading to a steep failure plane. As illustrated in the left sketch of Figure 1.6, this failure plane is not likely to interfere with the failure plane of the face. When a high-pressure tail void injection is applied, the failure plane is expected to be passive. This is leading to a flatter failure plane. As illustrated in the right sketch of Figure 1.6, this failure plane is expected to interfere with the failure plane of the face.

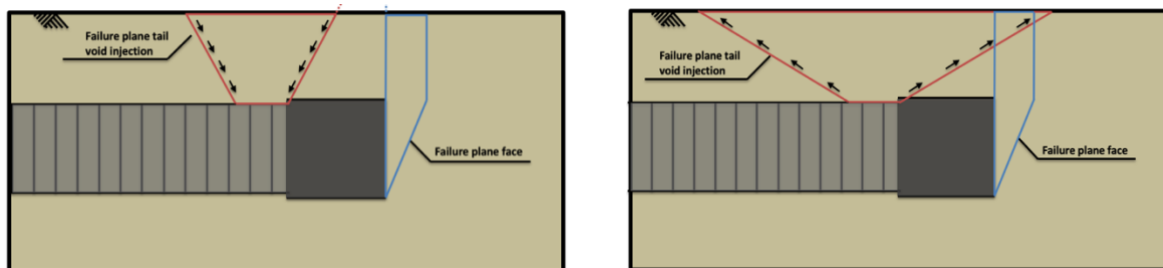


Figure 1.6: Hypothesis of the influence of the tail void injection on the face stability and settlements in front of the TBM. Left: High injection pressure. Right: Low injection pressure (personal communication, B. van de Water, Arthe Civil & Structure, 2020)

When comparing the monitored field data from the case study, with the results of the numerical model, it is not expected they match. This is expected because of the uncertainties in the soil profile and the numerical approach of the problem in the numerical model. For example, the numerical model in Plaxis tends to show a displacement curve which is wider compared to field measurement results. From experience it is known this is the case in transversal direction, but it is also expected to occur for the displacement curve in longitudinal direction. Compared to practice results, this could lead to having a larger influence of the tail void injection in the numerical model in Plaxis.

- **Does the taper of the TBM influence settlements (in front of the cutterhead)?**

When no settlements occur as a result of the ideal support pressures, it is expected there will still be settlements due to the taper of the TBM (a taps cylinder) from the moment the entire TBM is in the soil. The influence is expected to be $1 * \text{diameter (D)}$ (experience number). This is under the assumption the shield is approximately equally long as its diameter. This means $0.5 * D$ to the front from the shield and $0.5 * D$ to the back, starting from the tail gap. This will most likely be negligible for the TBM, it will however be checked by the 3D model. It is checked by comparing a model with and without a tapered TBM. In Plaxis this results in a model with and without plate contraction. This comparison gives a better understanding of the influence of the taper of the TBM and measured displacements.

Can trends be found in the relation between face support pressure and monitored settlements?

Following the line of reasoning as presented in the four sub-questions below, it is expected a trend can be found between face support pressure and settlements because the settlement through will vary along with the face support pressure (more or fewer settlements when the face support pressure is respectively increased or reduced), and because the trends which are expected to be found by means of numerical modelling. The measured settlements are expected to show similar behaviour.

- **Do the measured settlements show trends?**

It is expected the settlements will show trends. Settlements are divided in two groups, longitudinal and lateral. In lateral direction the settlements are expected to look like the Gaussian settlement trough, attributed to Peck (1969) and Schmidt (1969), which takes the form of an inverted Gaussian distribution curve transverse to the direction of the tunnel drive. This is illustrated in Figure 1.7. The 3D settlement curve in Figure 1.8 illustrates the expected settlement trough in longitudinal direction. The measured settlements are expected to show similar behaviour, including more or less settlements when the face support pressure is respectively increased or reduced, as illustrated in Figure 1.9.

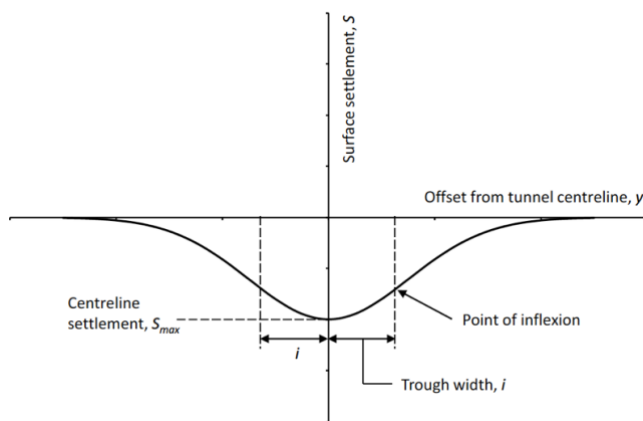


Figure 1.7: Gaussian settlement trough by Peck (1969) and Schmidt (1969)

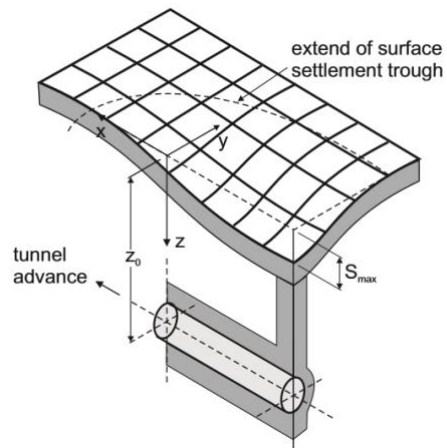


Figure 1.8: Tunnel-Induced settlement trough ([13], after [1])

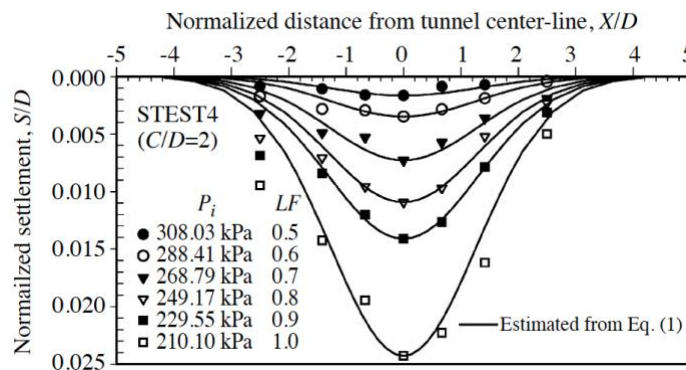


Figure 1.9: Evolution of surface settlement trough with changing support pressure [12]

s Ideal F: the face support pressure at which the face support pressure is in equilibrium with the soil pressure.

- **Do the measured pore water pressures show trends?**

It is expected the pore water pressure measurements will show trends. The trends will be in front of the TBM and are expected to have the shape of a thrust wave. This is expected since similar measurements are noted in previous soft soil tunnelling projects in the Netherlands: Botlek Rail, Figure 1.10, the Second Heineoord tunnel, Figure 1.11 and the North-South line metro project in Amsterdam, Figure 1.12. Those three figures all show the same thrust wave shaped behaviour with respect to the pore water pressure in front of the TBM. The results are not only expected due to project measurement results, but also because of a theoretical background which says the increase in piezometric head in front of the tunnel face decrease exponentially with the distance [3]. The measurement results in Figure 1.12 show a more or less similar behaviour to the back of the face as to the front, this behaviour was unexpected.

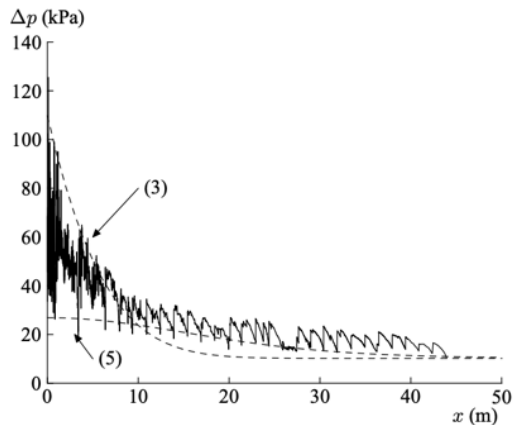


Figure 1.10: Excess pore pressure profiles according to (3) at $t = 0.75h$ and (5) at $t = 1.5h$, compared with measurements at Botlek Rail, MQ1 [4]

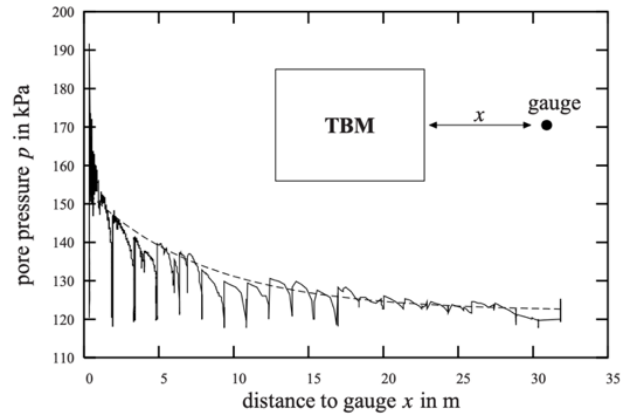


Figure 1.11: Measured excess pore pressure in front of the TBM at the COB monitoring field North at the Second Heineoord, compared with pore pressure according to Bezuijen (1998) (dashed line) [4]

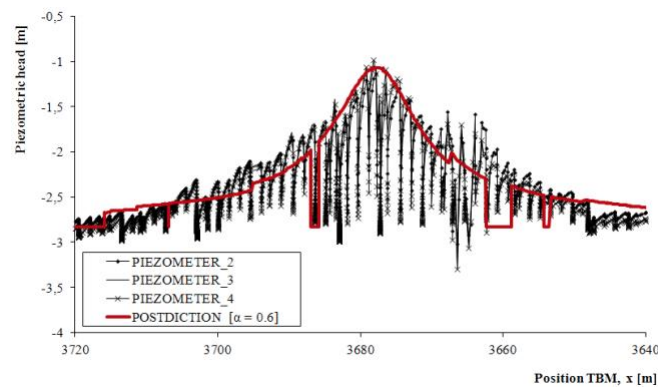


Figure 1.12: Measurements of the piezometric head of the first tunnel location [9]

- **Do the applied face support pressures show trends?**

It is expected the applied face support pressures will not show independent trends. If the face support pressures show trends of sudden in- or decrease those are expected to be related to monitored settlements.

- **Can trends be found in the relation between face support pressure and settlements with support of 3D modelling?**

It is expected there will be a relation, which will play an important role in answering the main research question. When plotting the settlements against the face support pressure as shown in Figure 1.13, the following trends are expected:

- The closer the face support pressure is to the maximum face support pressure the more heave is expected (+ surface displacement);
- The closer the face support pressure is to the minimum face support pressure the more settlement is expected (- surface displacement);
- When moving away from the ideal face support pressure the first derivative/slope is expected to deviate (red circles, Figure 1.13)

The trend shown in Figure 1.13 is expected following laboratory test results with soft soils, as illustrated in Figure 1.14. Due to the scale of supporting pressure in Figure 1.14 the displacement seems small before collapse, but with a closer look a similar curve as in Figure 1.13 can be observed.

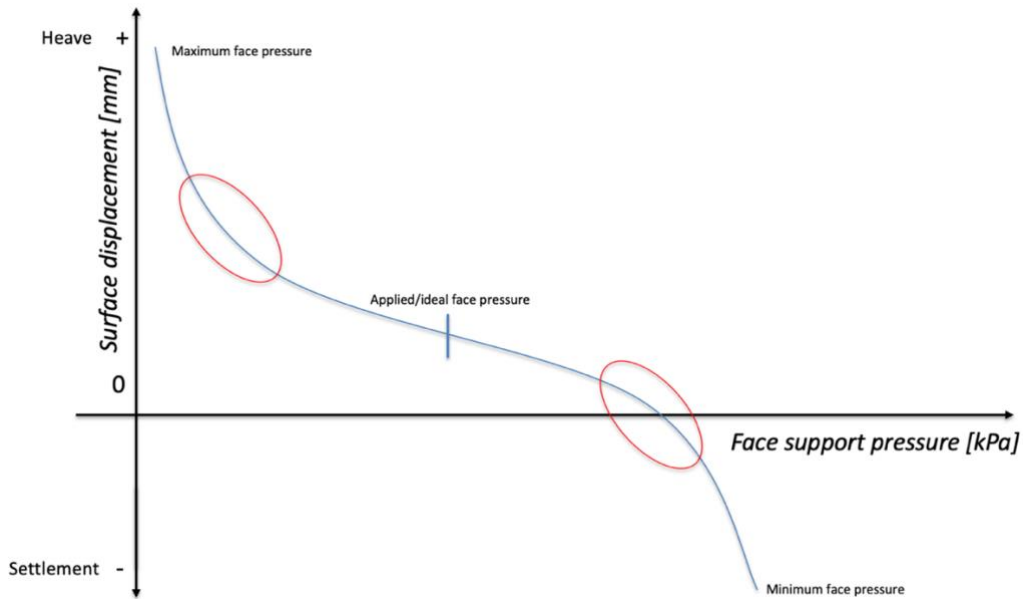


Figure 1.13: Expected trend formation between settlements and face support pressure. March 4, 2020

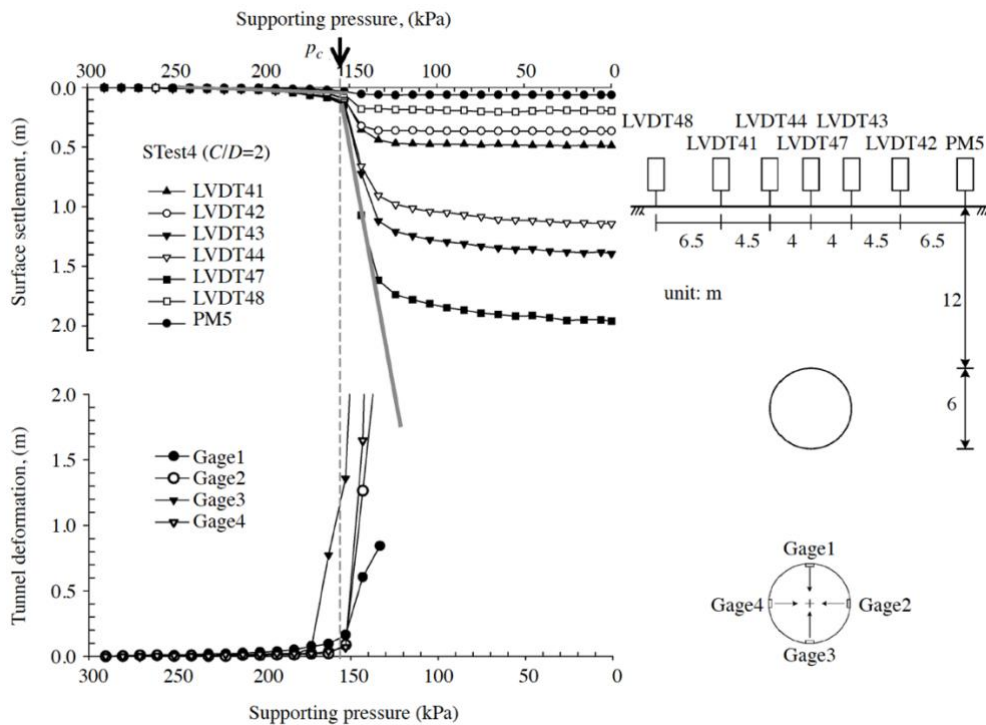
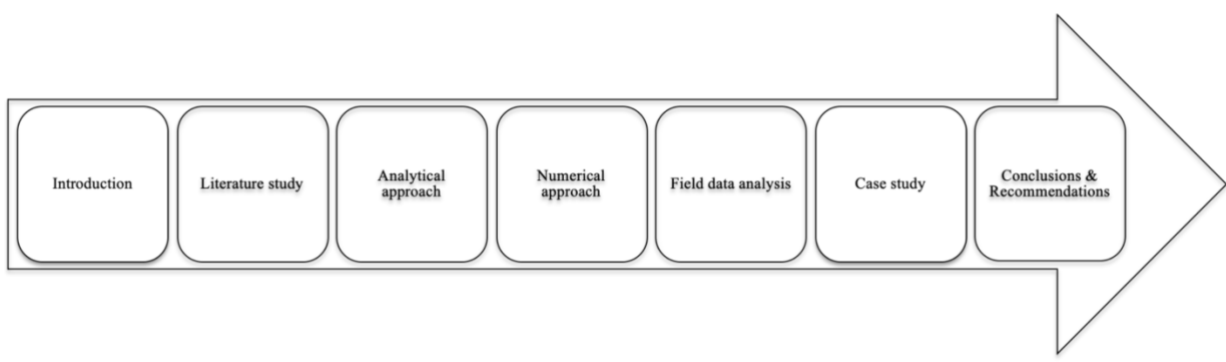


Figure 1.14: Surface settlements and tunnel displacements at various face support pressures with $p_c =$ face support pressure at collapse [12]

Overall hypothesis

Following the main-research question “Is it possible to determine a relation between monitored settlements and the face stability of a slurry TBM by numerical modelling?” and the aforementioned sub questions, the overarching hypothesis is that it is expected to be found. This is because the influence of a large group of parameters such as the soil parameters, the tail void injection and the taper of the TBM can be distinguished. In addition, it is expected that the outcome of this research will strongly depend on the results of the numerical modelling. The monitored field data will support the validation of the modelling.

1.5 Outline of the thesis



- **Chapter 1** is the introduction of the thesis, with a broad introduction of the topic, aim of the research, approach, hypothesis and an overview of the structure of the remainder of the thesis.
- **Chapter 2** is the literature study. Face stability is the first topic elaborated on in the literature study, this is followed by the expected behaviour of settlements. These two topics form the basis for this research as the aim is to find a relation between them. Paragraph 3 will cover the geotechnical project information to provide a basis for the case study. Paragraph 4 will elaborate on the field monitoring methods used in the RijnlandRoute case study project. The chapter is concluded by a summary and conclusions.
- **Chapter 3** contains the analytical determination of the face stability. The first paragraph covers a scenario analysis to define the sensitivity of the soil parameters used in the analytical calculation. The second paragraph elaborates on the analytical approach and results of the advanced soil profile analysis. The chapter is closed by a summary and conclusions.
- **Chapter 4** covers the numerical modelling analysis performed in Plaxis 3D. The chapter starts with introducing the boundary conditions and the type of soil model used. In the second paragraph the model design properties are elaborated. Paragraph 3 elaborates on the influence of the tail void injection and the taper of the TBM shield on settlements. The fourth paragraph covers a scenario analysis to define the sensitivity of the soil parameters used in the numerical calculation. The sixth paragraph discusses the numerical input parameters as well as the results of the advanced soil profile analysis. The chapter is closed by a summary and conclusions.
- **Chapter 5**, the field data analysis. In this chapter the results of the gathered field data is elaborated on. This contains settlements, (excessive) groundwater pressures and face support pressures. Those three topics are the first three paragraphs of this chapter. Each paragraph consists of the two subparagraphs data interpretation and data trends. Chapter 5 ends with a summary and conclusions.
- **Chapter 6** covers the RijnlandRoute case study. In the first paragraph the results of the numerical model are compared with the field data. Those results are compared to find out if the numerical model is a reliable way of interpreting the expected settlements. The second paragraph elaborates on comparing the analytical with numerical modelling face support pressure limits. Do they differ much? If yes, why? This will lead to a better understanding of the relation between the analytically determined face support pressures on the one hand and on the other hand generated by the numerical model. This relation is elaborated on because in projects, the face support pressure range is often determined by analytical calculations. Chapter 6 does not end with conclusions. Those will be elaborated on in chapter 7.
- **Chapter 7** contains the conclusion of Chapter 6 and the answer to the research question supported by overall conclusions & recommendations of the research.

Chapter 2

Theoretical and practical background information

This chapter covers the literature study of the research and provides both theoretical and practical background information to support the rest of the research. For a more detailed outline of this chapter, please refer to §1.5.

2.1 Face stability

The face stability can be determined by several methods. The method applied for the case study RijnlandRoute is the [DIN] as mentioned in §1.1, a method which comes from the calculation of diaphragm walls. The calculation for the soil pressures refer to (DIN 4126 + 4085).

Due to the time constraints of this thesis, the face stability calculation method discussed is the one applied in the case study RijnlandRoute. DIN is a 2D analytical method with a sliding failure wedge mechanism, but can be adapted to a 3D sliding failure wedge mechanism, as shown in Figure 2.1. To deform the 2D to a 3D method an arch length, the diameter of the tunnel, the cohesion and active earth pressures are introduced to the formula to determine the horizontal effective soil pressure.

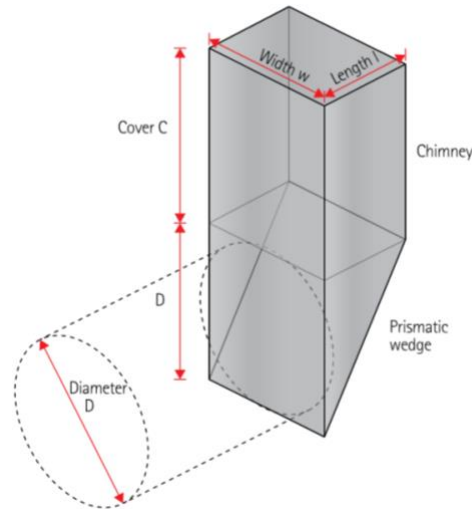


Figure 2.1: Failure mechanism: 3D wedge model ('wall length' reduction method, similar to the failure model Jancsecz-Steiner model) (Broere, 1998)

Note: In this research safety factors are not taken into account since the focus of the research aims for the actual safety. This means when determining the factor of safety no safety factors are applied to the parameters. The minimum support pressure can be determined by equation 2.1 to equation 2.6.

$$p_{min} = e_{ah} + u \quad (\text{equation 2.1})$$

$$e_{ah} = \frac{\sigma'_v * K_{agh} * l_{ag}}{D} - K_{ach} * c' \quad (\text{equation 2.2})$$

$$\sigma'_v = \sum_n \gamma'_n * h_n \quad (\text{equation 2.3})$$

$$l_{ag} = D * \left[1 - \frac{2}{\pi} * \arctan \left(\frac{\varphi * z}{2 * D} \right) \right] \quad (\text{equation 2.4})$$

$$K_{ach} = \frac{2 * \cos \varphi}{1 + \sin \varphi} \quad (\text{equation 2.5})$$

$$K_{agh} = \left[\frac{\cos \varphi}{1 + \sin \varphi} \right]^2 \quad (\text{equation 2.6})$$

With:

p_{min}	: Minimum support pressure (DIN 4126) [Broere]	[kPa]
e_{ah}	: Horizontal effective soil pressure including 3D effect (DIN 4126)	[kPa]
u	: Water pressure	[kPa]
σ'_v	: Horizontal effective soil pressure (2D)	[kPa]
K_{agh}	: Factor of active soil pressure (DIN 4085)	[-]
l_{ag}	: Length of arching (DIN 4126)	[m]
K_{ach}	: Factor of active soil pressure for cohesion (DIN 4085)	[-]
c'	: Effective cohesion	[kPa]
D	: Outer diameter of the tunnel	[m]
φ	: Friction angle of the soil	[°]
z	: Distance to surface level	[m]
h	: Thickness of the soil layer	[m]

The indices represent:

a	: Active state
c	: Due to cohesion
g	: Water pressure
h	: Horizontal component
max	: Maximum value
min	: Minimum value
n	: Number of layers
p	: Passive state or due to vertical surface load
v	: Vertical component

The maximum support pressure can be calculated by equation 2.7 – equation 2.9.

$$p_{max} = \sigma_v + \frac{C}{D} * (2 * c + \sigma'_v * K_{agh} * \tan \varphi) \quad (\text{equation 2.7})$$

$$\sigma_v = \sigma'_v + u \quad (\text{equation 2.8})$$

$$K_{agh} = \left[\frac{\cos \varphi}{1 + \sin \varphi} \right]^2 \quad (\text{equation 2.9})$$

With:

p_{max}	: Maximum support pressure (including friction) (DAUB) [6]	[kPa]
σ_v	: Horizontal soil pressure (2D)	[kPa]
C	: Soil cover on top of the tunnel	[m]
c	: Cohesion	[kPa]
σ'_v	: Horizontal effective soil pressure (2D)	[kPa]
K_{agh}	: Factor of active soil pressure (DIN 4085)	[-]
φ	: Friction angle of the soil	[°]
D	: Outer diameter of the tunnel	[m]

The soil profile is heterogeneous, therefore the determination of the input values for the friction angle (φ) and the cohesion (c) consist of a weighted soil parameter, see Figure 2.2, equation 2.10 and equation 2.11. This weighted soil parameter is used for the parameter: c_{ah} .

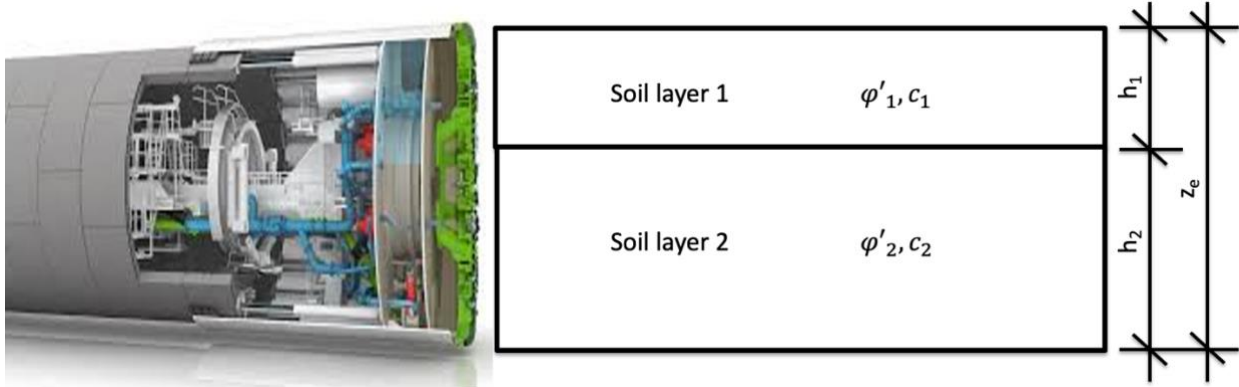


Figure 2.2: Weighted soil parameters (animation on the left from Herrenknecht)

$$\varphi'_{gem} = \frac{h_1 * \varphi'_1 * (z_e + 0.5 * h_1 - h_1) + h_2 * \varphi'_2 * (z_e + 0.5 * h_2 - h_1 - h_2)}{h_1 * (z_e + 0.5 * h_1 - h_1) + h_2 * (z_e + 0.5 * h_2 - h_1 - h_2)} \quad (\text{equation 2.10})$$

$$c_{gem} = \frac{h_1 * c_1 * (z_e + 0.5 * h_1 - h_1) + h_2 * c_2 * (z_e + 0.5 * h_2 - h_1 - h_2)}{h_1 * (z_e + 0.5 * h_1 - h_1) + h_2 * (z_e + 0.5 * h_2 - h_1 - h_2)} \quad (\text{equation 2.11})$$

In layers where excess pore pressures are expected, friction will be disregarded. This can for example be due to consolidation of the embankment.

When calculating the minimum and maximum required pressure by use of the DIN method, the entire chimney above the bore front is included in the counterforce, because it is meant for diaphragm walls, which means this method takes soil resistance all the way to the surface into consideration.

For the analytical analysis a start height has to be defined between D and D+C. By the use of Plaxis it might be possible to investigate what the height of this failure plane is, which can then be implemented in the analytical calculation.

The methodology presented above is used, amongst others, because in practice is learned that a burst or blow-out occurs before hydraulic fracturing (piping). Bursting is a vertical silo of soil being pushed up. When determining the maximum face support pressure, the pressure required for that to happen is determined. This mechanism is not likely to occur, but is an acceptable way of representing another mechanism: hydraulic fracturing. At hydraulic fracturing, slurry finds its way up to the surface via local micro instabilities. The instability of the soil skeleton tries to find its way up to the surface. Concluding from this, in the analytical method of determining the maximum face support pressure, a bursting mechanism is used to provide an allowable pressure for a totally different failure mechanism. The reason for this methodology is because when determining the maximum face support pressure for hydraulic fracturing, an even lower pressure is the result. A lower pressure leads to very small working pressures for the TBM driver and are easily exceeded if the limits are extremely close to one another.

2.2 Settlements

Settlements induced by mechanized tunnelling (slurry) depend on the soil profile and its engineering properties, the height of the tunnel cover (C), the diameter (D), the face support pressure (P), the tail void injection, the advance rate of the TBM and the experience of the TBM driver. The settlements occurring by a TBM drive occur in both longitudinal and transverse directions. This research mainly has its focus on the longitudinal direction because a relation between settlements in front of the face is assessed to determine the face stability of a slurry TBM.

There are multiple methods to predict ground movement due to tunnelling. The methods can be divided into three groups: empirical, analytical and numerical methods. The analytical method by Loganathan & Poulos (1998) will not be elaborated on because this method is not applied/used in this research.

Empirical

The empirical method, developed by Peck (1969), assumes a transverse settlement trough which resembles an inverted normal Gaussian distribution curve as presented in Figure 2.3. The curve depends on two parameters, $S_{v,max}$: the maximum settlement at the tunnel centre and i : the distance to the inflection point. Half an inverted normal Gaussian distribution curve is assumed in longitudinal direction [6]. This leads to a 3D assumption as shown in Figure 2.4.

Based on $S_{v,max}$ and i , the volume loss V_L , induced by mechanised tunnelling can be determined.

$V_L = \frac{100 \cdot \sqrt{2\pi} \cdot S_{max} \cdot i}{S_{exc}}$ with S_{exc} is the excavated area. By measured settlements, s , at locations, y , the point of inflection can be determined. $s = S_{max} * e^{-\frac{y^2}{2i^2}}$.

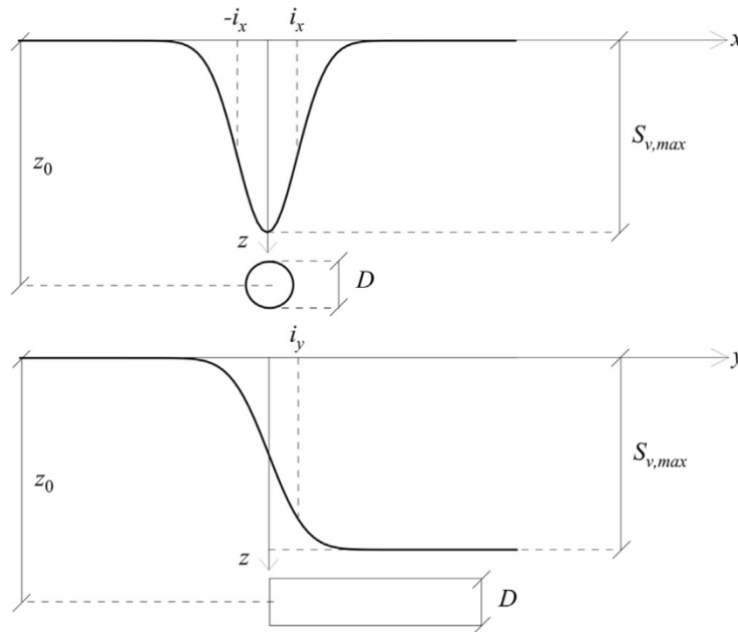


Figure 2.3: Gaussian settlement curve in horizontal (top) and longitudinal (bottom) direction [6]

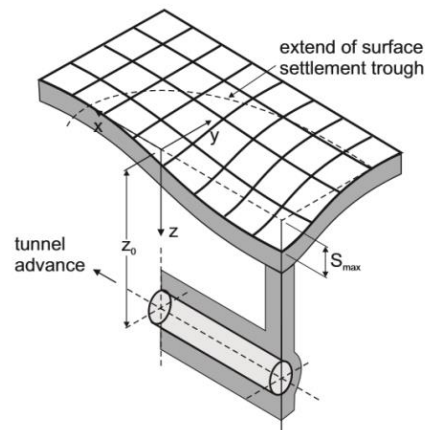


Figure 2.4: Tunnel-induced settlement trough ([13], after [1])

Volume loss can be divided in 5 components contributing to settlements, as shown in Figure 2.5:

1. Settlements in front of the face of the TBM;
2. Settlements at the cutterhead of the TBM;
3. Settlements at the shield passage;
4. Settlements due to the annular gap grouting/tail void injection;
5. Settlements due to long term settlement, such as consolidation.

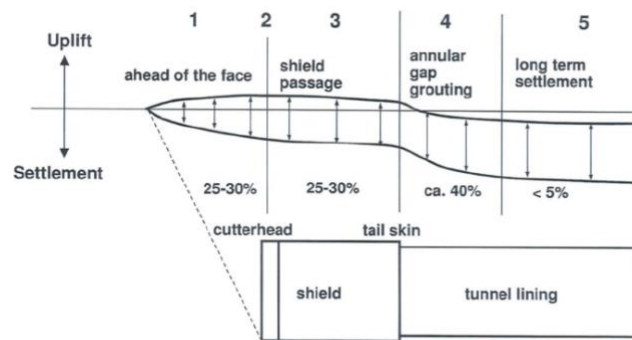


Figure 2.5: Settlements at occurring at tunnel construction

The volume loss distribution as presented in Figure 2.5 can be used to parse the numerical and/or field settlements.

Numerical

Settlement prediction by numerical modelling is broadly used in this research. Numerical modelling makes use of the finite element method and takes into account realistic soil behaviour [19], including the interaction between the soil, the TBM and lining. By means of numerical modelling the influence of TBM properties as mentioned in the introduction are determined. The properties analysed in this research are: the tail void injection, the taper of the TBM and soil properties.

2.3 (Geo-)technical project information

The geotechnical project information includes the following subjects:

- Geology
- Geotechnical profile
- Design parameter determination
- Hydraulic head
- TBM specifications
- Lining specifications

Geology

The western part (A44) of the RijnlandRoute tunnel project lies at the interface of old beach walls (Formation of Naaldwijk – Lagoon deposit environment (coastal barrier: beach and dune deposits)) and the deposits of the Old Rhine (Formation of Nieuwkoop – Lagoon deposit environment). The eastern part of the RijnlandRoute tunnel project (A4) is almost entirely located in the peat meadow area behind it (Formation of Echteld – Fluvial deposits). This variability leads to a very diverse ground structure along the route of the (tunnel) project. Figure 2.6 illustrates the schematic overview of the geology in Zuid-Holland.

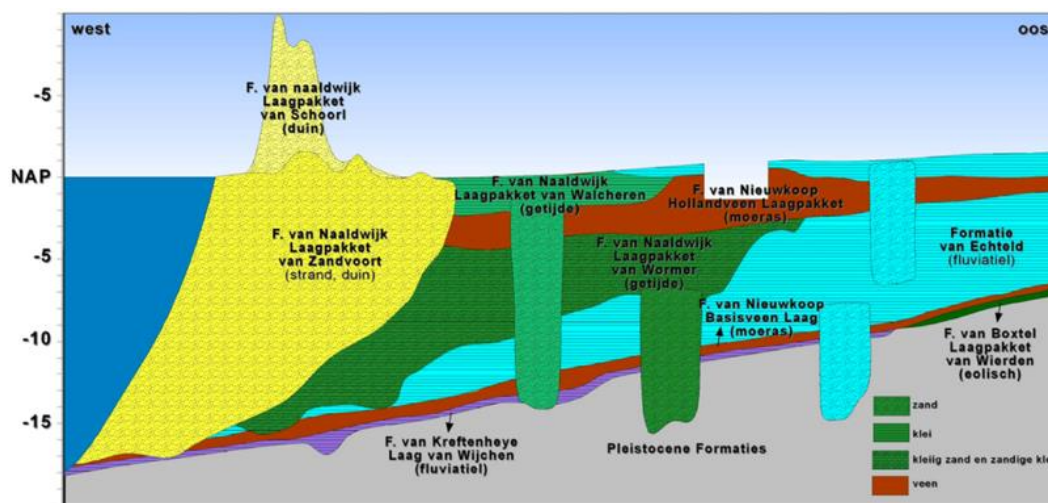


Figure 2.6: Schematic geological cross-section Zuid-Holland (Geotechnisch Basisrapport Systeem RijnlandRoute) [5]

Geotechnical profile

The geotechnical profile for the trace of the tunnel is based on the results gained by CPT's (cone penetration tests) performed in the surrounding of the trace. The names of the layers are based on the formation names from Figure 2.6.

Based on these CPT's 7 different layers were defined, layer 0 is added for anthropogenic layers (man-made). The layers are defined as:

- Layer 0: Anthropogenic layers
 - Sand (e.g.: Existing track body or road cunet)
 - a. Clay (e.g.: Covering layer, top agricultural use)
- Layer 1: Naaldwijk formation - Laagpakket van Zandvoort
 - Sand - fine
- Layer 2: Naaldwijk formation- Laagpakket van Walcheren
 - a. Clay – very organic
 - b. Clay – organic
 - c. Clay – silty
- Layer 3: Nieuwkoop formation - Hollandveen
 - Peat
- Layer 4: Naaldwijk formation - Laagpakket van Wormer (incl. Echteld formation)
 - a. Clay – very organic
 - b. Clay - organic
 - c. Clay - silty
 - d. Sand - very clayey
 - e. Sand - medium fine
- Layer 5: Nieuwkoop formation - Basisveen
 - Peat
- Layer 6: Pleistocene formation (Urk, Delwijnen, Kreftenheye, Bostel, incl. dekzanden)
 - a. Sand – loose
 - b. Sand – medium
 - c. Sand - dense
- Layer 7: Pleistocene formation (Stamproy, Sterksel, Bostel, incl. Dekzanden)
 - Clay- and loam layers

Figure 2.7 illustrated what the configuration of layering is at the start location of the tunnel.

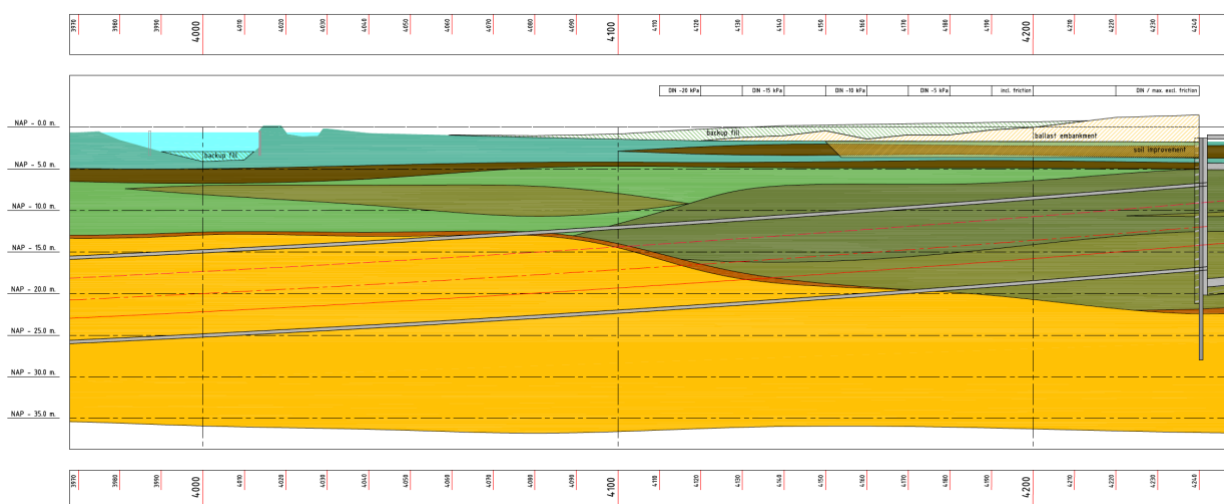


Figure 2.7: Schematic geotechnical profile cross-section at the location of the tunnel [5]

Hydraulic head

The normative hydraulic head is the one in the first aquifer, the Pleistocene sand layer. The hydraulic head in this Pleistocene sand layer at the area of interest for this research (\pm first 200 meters), is around -2.0 meter below NAP.

The hydraulic head is determined by a detailed analysis of standpipes near the trajectory of the tunnel. The hydraulic head is measured in the sandy layers. No differences in hydraulic head between those layers occurred [5]

Design parameter determination

The design parameters of the projects are determined by use of laboratory tests, correlations or codes/regulations, or a combination of those. Table 2.1 shows the design parameters of the project used in for this research and how they have been determined.

Table 2.1: Required design parameters [5]			
Parameter	Laboratory test	Correlation	Other
<i>Unit weight</i>			
γ , volumetric weight	Determination of volumetric weight	-	NEN9997-1 Table 2b
<i>Strength parameters</i>			
ϕ at 2% strain	Triaxial	-	NEN9997-1 Table 2b
c at 2% strain	Triaxial	-	NEN9997-1 Table 2b
s_u	Torvane test, triaxial test, DSS test	-	-
<i>Compressibility</i>			
POP	Compression tests	-	-
OCR	Compression tests	-	-
<i>Stiffness parameters</i>			
e_0 (dilatancy)	-	Correlation with ϕ	-
ν_{ur}	-	-	Plaxis manual, CUR 2003-7
E'_{oed}	Compression tests (Oedometer)	Correlation with E'_{50}	-
E'_{50}	Triaxial test	Correlation with E'_{oed}	-
E'_{ur}	-	Correlation with E'_{50}	-
m	-	-	Via E-moduli
<i>Consolidation and permeability</i>			
Permeability	Compression tests, permeability tests	Correlation with E'_{oes}	CUR 2003-7

TBM dimensions

The shield of the slurry TBM has a length of 11.5 m. The diameter is almost 11 meters. An overview of the TBM dimension is shown in Figure 2.8.

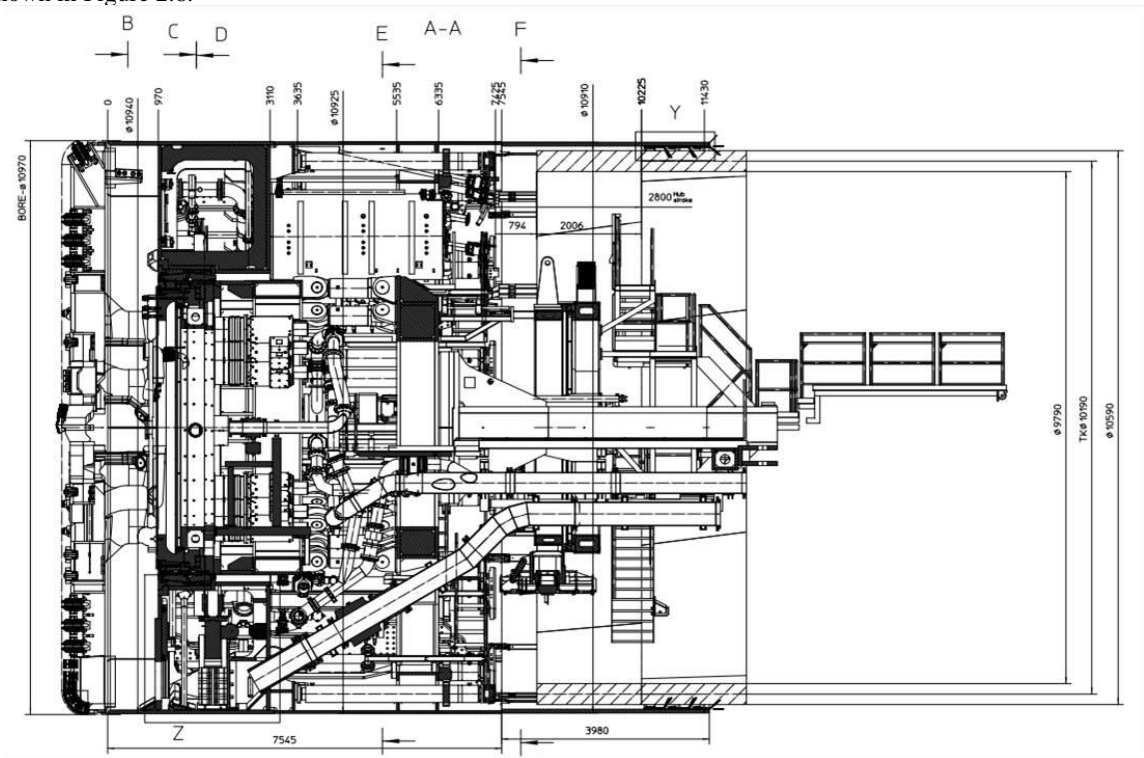
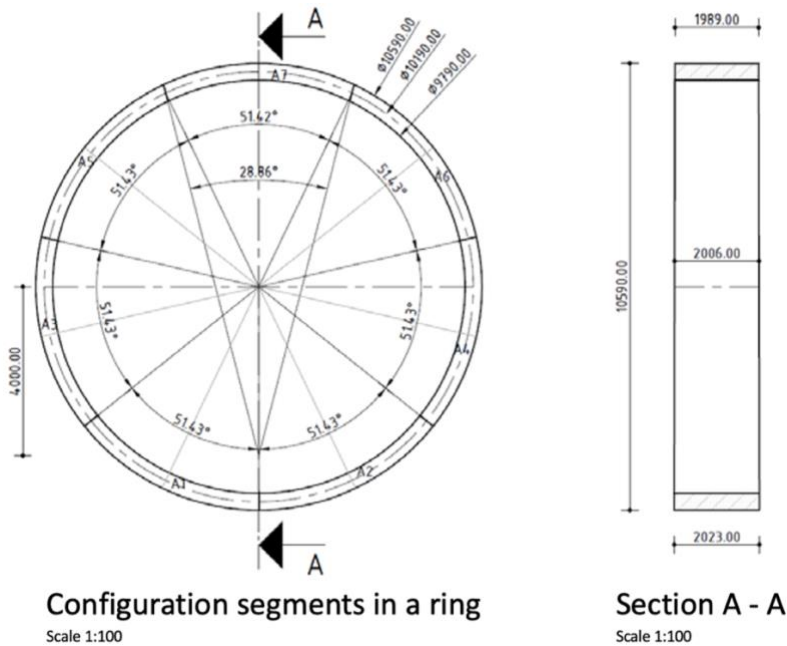


Figure 2.8: TBM overview of dimensions [5]

Lining specifications

The concrete lining is 400 mm thick. With an internal diameter of the tunnel of 9.79 m., this gives an external diameter of 10.59 m. This diameter corresponds to the diameter of the cutting wheel [5]. Each ring is build up from 7 segments. The width of the lining is 2006 mm. The geometric specifications are shown in Figure 2.9. The volume of a tunnel ring is 25.61 m³/m' and the volume weight of the reinforced concrete is 23.8 kN/m³ which is equal to a dead weight of a ring of 305 kN.



Configuration segments in a ring
Scale 1:100

Section A - A
Scale 1:100

Figure 2.9: Geometry tunnel [5]

2.4 Field monitoring

The field monitoring equipment at the RijnlandRoute tunnel project site consists of spade cells, settlement markers and total stations. Those devices will be discussed in this paragraph.

2.4.1 Spade Cell

A spade cell, Figure 2.10, is a push-in pressure cell measuring the total horizontal stress in the soil. Within the cell is a piezometer, defining the piezometric head, allowing for a derivation of the effective stress. The spade cell consists of two longitudinal stainless-steel plates, welded together around their periphery [10]. The gap between the plates is filled by oil which is used to determine the total horizontal stress [22] The horizontal effective stress is determined by the subtraction of the pore water pressure from the total horizontal stress.



Figure 2.10: Left: Spade cell RijnlandRoute (Verloop, 2019). Middle: Spade cell information RijnlandRoute (Verloop, 2019). Right: Spade cell head [21]

At the RijnlandRoute tunnel project, 8 spade cells are located at 4 cross sections, 20 metres apart from one another, Figure 2.11. Spade cells 1, 3, 5 and 7 are located 1 meter south of the tunnel crown, hereafter referred to as tunnel crown. The spade cells 2, 4, 6 and 8 are located between the two tubes, 7 meters from the axis of the southern tube axis. The depth of the spade cells are presented in Table 2.2.

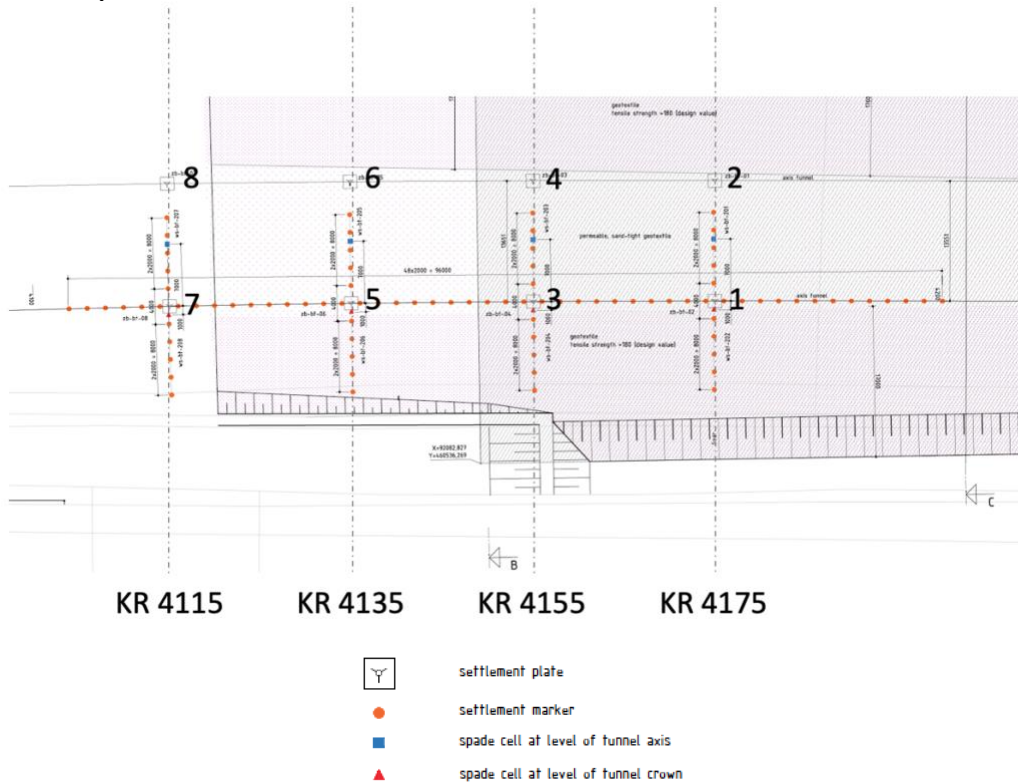


Figure 2.11: Locations of the field measurement equipment [5]

Table 2.2: Locations of spade cells at tunnel crown [5]

Spade cell number	Depth of cell below NAP [m]	Chainage
1	-14.500	4175
2	-8.000	4175
3	-15.200	4155
4	-8.700	4155
5	-15.900	4135
6	-9.400	4135
7	-16.600	4115
8	-10.100	4115

2.4.2 Settlement Marker & Total Station

The first 96 meters after the start of the tunnel, settlement markers are placed above the tunnel crown with a 2-meter interval. At similar chainages as the location of the spade cells, rows of settlement markers perpendicular to the route of the tunnel are placed, orange dots in Figure 2.11, also with a 2-meter interval.

A total station is located in the start area. The total station is prone to settlements, due to the soft soil below it. A total station outside the start settlement area is used as a calibration point.

Along the rest of the route of the tunnel, settlement plates and total stations are placed, Figure 2.12. At the Rijn-Schie Canal a higher frequency of markers is installed (along the canal).



Figure 2.12: Left: Total station. Middle: Settlement marker. Right: Total station + settlement marker (Verloop. 2019 July 16)

2.5 Practical considerations

During the construction process of a slurry TBM tunnel, the prevention of cave-in, a blow-out or hydraulic fracturing is of great importance, though definitely not the only thing. A set of practical considerations while executing a slurry TBM driven tunnel project, which are also relevant for this research, are discussed below:

- The cutter tools of the shield can get damaged. If so, they need to be replaced. To replace cutter tools, the pressurised slurry must be lowered. To maintain sufficient face support pressure, the excavation chamber is filled with compressed air. The chance of the air traveling through the soil leading to a pressure drop at the face increases the risk of face instability [10]. Secondly, the air has a volumetric weight close to 0 kN/m³. This means there is no pressure increase from the tunnel crown down to the level to which the slurry is lowered. The result is often a higher air pressure at crown than during full slurry support, which reduces the bandwidth between (air) face support pressure at the crown and the maximum allowable face support pressure (blow-out pressure). The risk is mitigated by the COMOL5 tunnel team by knowing the cutter tools will at least last the first 800 meters. After the first 800 meter the TBM will be in a safe zone because of its depth. At sufficient depth, the margin between the minimum and maximum face support pressure is large. Therefore it is not a problem if the air pressure is higher than the initially applied slurry face support pressure. If the cutting tools fail, when there is little soil cover maintenance can be done. In this case the chamber is filled with bentonite instead of air. The maintenance is performed by divers.
- The influence of the tail void injection to the settlements in front of the tail needs to be considered. In a shallow model the failure planes of the face stability and tail will most likely not interfere. When it is known how far the influence is to the front, this is assumed to be similar to the back. Also, the influence of the tail void injection in front of the shield can be defined by switching the tail void injection on and off. This only accounts for the modelling of the problem. In the field switching the tail void injection of is not an option in a soft soil ground profile.
- The relation between the face stability and the settlements in front depends on a set of multiple components. To make a numerical model suitable for validation by an analytical model, the model has to be for a shallow tunnel ($C/D < 2$) [23].
- The analytical model will not include the influence of the tail void injection in the calculations. Therefore it must be considered what the influence is of the tail void injection in numerical modelling.

2.6 Summary and Conclusions

The analytical calculation method is a 2D method based on the DIN4126 and DIN4085 methods including friction [Broere]. Safety factors are not taken into account in this research. The methodology for the maximum face support pressure calculates for a blow-out (a silo of soil being pushed up). This is a global passive failure mechanism. From experience it is known that hydraulic fracturing (piping) is a more likely failure mechanism to occur. This is a local failure mechanism due to micro instability of the soil particles. However, because the method to determine the maximum face support pressure due to piping results in a too conservative limit, it is generally expected within the tunnel industry the blow-out mechanism is used to determine the maximum face support pressure.

Settlements induced by mechanized tunnelling (slurry) depend on the soil profile and its engineering properties, the height of the tunnel cover (C), the diameter (D), the face support pressure (P), the tail void injection, the advance rate of the TBM and the experience of the TBM driver. There are multiple methods to predict ground movement due to tunnelling. The methods can be divided into three groups: empirical, analytical and numerical methods. The analytical method by Loganathan & Poulos (1998) is not elaborated on because this method is not applied/used in this research. The analytical method assumes an inverted Gaussian distribution curve in transversal direction, and half of this in longitudinal direction. Based on Peck's (1969) method, the volume loss can be determined. Volume loss distribution can be used to parse the numerical and/or field settlements. The numerical prediction of settlements is done by use of the finite element method and takes into account realistic soil behaviour [19], including the interaction between the soil and the TBM and lining. The effect of multiple properties of soil and TBM properties are analysed in this research.

The soil types in which the TBM is mainly located in this research are sand, clay and peat, in order of magnitude presence. The normative hydraulic head of the case study, is the one in the first aquifer, the Pleistocene sand layer. The hydraulic head in this Pleistocene sand layer at the area of interest for this research (\pm first 200 meters), is around -2.0 m. below NAP. The shield of the slurry TBM has a length of 11.5 m. The concrete lining is 400 mm. thick. The internal diameter of the tunnel is 9.79 m., and the external diameter is 10.59 m. The width of the lining is 2006 mm. The field monitoring equipment at the RijnlandRoute tunnel project site consists of spade cells, settlement markers and total stations.

COMOL5 reduced the chance of necessary maintenance at locations at which maintenance proposes a high risk. Differences between the analytical and numerical method must be taken into consideration while analysing results.

Chapter 3

Analytic face stability

This chapter covers the analytical determination of the face stability, including a scenario analysis. For a more detailed outline of this chapter, please refer to §1.5.



3.1 Scenario analysis – Analytical

The scenario analysis is performed to investigate the sensitivity of soil parameters used in an analytical face stability calculation by the DIN 4126 method. For example: If a small value change of a soil parameter has a large impact on the minimum and maximum face stability, it is important this parameter gets the highest priority during the site investigation of a project. The numerical scenarios performed in the next chapter will be of similar kind for consistency throughout the report.

3.1.1 Input parameters

The scenario analysis focusses at the chainage 4115. The location of chainage 4115 is displayed in Appendix 3. This location lies within the first 250 meter of the project where the TBM is still at relatively shallow depth. This location chainage 4115 is chosen, because there is a high-density of measurement equipment, the man-made overburden is not present and possible start-up problems are not likely to occur. The high-density of measurement equipment makes it an optimal location to compare field results with analytical and numerical modelling results later in this research. The soil profile at the chainage 4115 location is simplified for the scenario analysis to get a better understanding of individual soil parameters. It is assumed the sand layers which are not considered in the scenario analysis, will show similar trends regarding their sensitivity. The same accounts for the other clay layers present at chainage 4115. Because the peat layers are very thin compared to the clay and sand layers these are not considered for the scenario analysis. It is assumed the peat layers will have little influence on the failure mechanism and limit states of the face stability. The simplified soil profile at chainage 4115 consists of a thick layer of sand with clay on top of it. The tunnel crown has a cover of 8.96 m. The hydraulic head is at 2.0 m. below N.A.P. Figure 3.1 and Table 3.1 provide an overview.

Table 3.1: Simplified soil profile for the scenario analysis at chainage 4115

Top of layer [N.A.P. +m.]	Bottom of layer [N.A.P. +m.]	Geotechnical unit and main soil type	Legend
-1.60 (surface)	-6.0	4C – Clay	
-6.0	-30.00	6 – Sand	

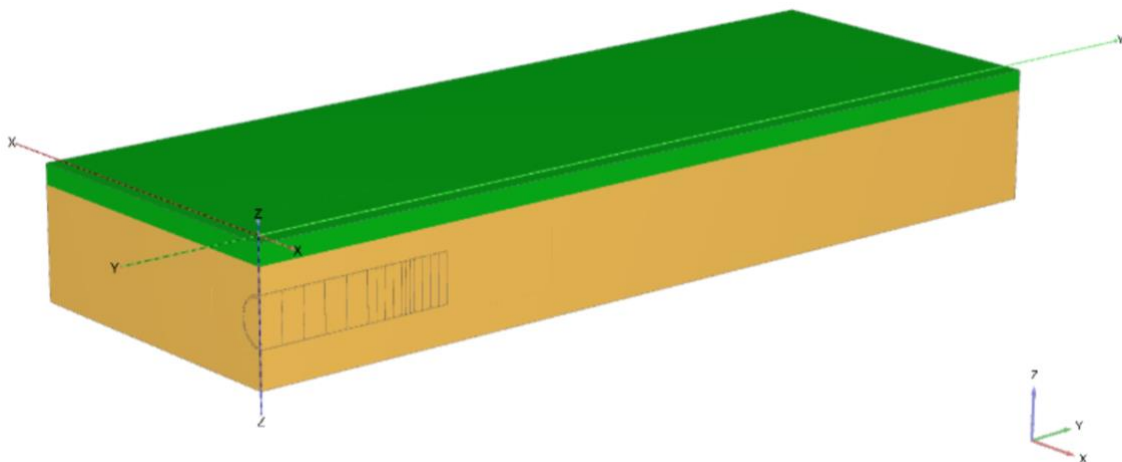


Figure 3.1: Simplified soil profile for the scenario analysis analyses at chainage 4115

To perform the scenario analysis, the following formulas are used (and will be elaborated on in §2.1):

$$p_{min} = \sigma'_v * \left[\frac{\cos \varphi}{1 + \sin \varphi} \right]^2 * \left[1 - \frac{2}{\pi} * \arctan \left(\frac{\varphi * z}{2 * D} \right) \right] - \left(\frac{2 * \cos \varphi}{1 + \sin \varphi} * c' \right) + u$$

$$p_{max} = (\sigma'_v + u) + \frac{C}{D} * (2 * c + \sigma'_v * \left[\frac{\cos \varphi}{1 + \sin \varphi} \right]^2 * \tan \varphi)$$

The scenario analysis uses the geotechnical parameter set in which each layer has three values (please refer to Appendix 2 for further background). The geotechnical parameter set is in Dutch, the indices used in this report remain similar to the ones used in Appendix 2. Gem. stands for average and k. for characteristic:

- X, average and characteristic = $X_{gem;k}$
- X, average and low characteristic = $X_{gem;k;low}$
- X, average and high characteristic = $X_{gem;k;high}$

To be able to compare the set of scenarios, a reference model is created. The reference model is based on the characteristic average, $X_{gem;k}$, soil parameters.

The scenario analysis considers 4 scenarios in total, 2 for the clay and 2 for the sand layer. The scenarios analyse the following geotechnical parameters:

1. Unit weight (γ). This leads to one scenario with $X_{gem;k;low}$ for the unit weight and one scenario with $X_{gem;k;high}$ for unit weight;
2. Strength parameters: the friction angle (φ) and cohesion (c) are considered in one scenario due to their correlation. The parameters are correlated crosswise. This leads to a scenario with $X_{gem;k;low}$ for the friction angle and $X_{gem;k;high}$ for the cohesion, and vice versa for the other scenario.

All scenarios will be compared with a reference scenario.

3.1.2 Results

The minimum and maximum face support pressures, respectively P_{min} and P_{max} , are compared at the tunnel crown. The limit face support pressures for the reference scenario are:

$$p_{min} = 97 \text{ kPa}$$

$$p_{max} = 168 \text{ kPa}$$

Table 3.2 displays the results of the scenario analysis. The results of the minimum face support pressure show minimal influence with respect to the clay scenarios and the volumetric weight of the sand. The largest, but still very small influence comes from the sand strength parameter scenario. The governing parameter on the determination of the minimum face support pressure is the horizontal effective soil pressure (including the 3D effect), e_{ah} . e_{ah} consists amongst others of the length of arching, l_{ag} , the factor of active soil pressure, K_{agh} and the factor of active soil pressure for cohesion, K_{ach} , which at their turn also have strength parameters in their formula. The parameters e_{ah} , l_{ag} , K_{agh} and K_{ach} are influenced by the soil strength properties of the soil layers in which the cutterhead is located. As in this scenario analysis the cutterhead is completely in sand, this explains the large contribution of the sands strength parameters on the parameters e_{ah} , l_{ag} , K_{agh} and K_{ach} . The contribution of the clay strength parameter on the settlements in the scenarios is negligible.

For the maximum face support pressure, the influence is minimal for the strength parameter scenarios of both sand and clay. The volumetric weight scenarios are of more influence, but are still small. This means that the volumetric weight has the highest influence on the determination of the maximum face support pressure, independent of the soil at the location of the cutterhead. This is the contrary of what accounts for the minimum face support pressure.

Because the influence of the strength parameters is of little to no influence on the maximum face support pressure, it can be concluded that for the minimum face support pressure the K_{agh} is expected not to be of influence worth mentioning. If parameters would be of influence it would be the parameters l_{ag} and K_{ach} . It has to be kept in mind that the determination of a soil profile has an inaccuracy. The measurement inaccuracy of the soil parameters is considered in the geotechnical parameter set, which is set up following the rules of the Eurocode 7. The determination of the thickness of the layers remains an inaccuracy.

Table 3.2: Results scenario analysis

Parameter	Unit	Reference scenario	Sand				Clay			
			γ low	γ high	c high, ϕ low	c low, ϕ high	γ low	γ high	c high, ϕ low	c low, ϕ high
Pmin	[kPa]	97.4	97.2	97.6	98.5	96.3	97.1	97.7	97.4	97.4
Pmax	[kPa]	167.6	166.0	169.2	167.7	167.4	165.7	169.9	167.6	167.6
Relative difference between Pmin and Pmin, reference scenario	[kPa]	0.0	0.2	0.2	1.1	1.1	0.3	0.3	0.0	0.0
Relative difference between Pmax and Pmax, reference scenario	[kPa]	0.0	1.6	1.6	0.1	0.2	1.9	2.3	0.0	0.0







3.2 Advanced Soil profile Analysis - Analytical

3.2.1 Input parameters

The advanced soil profile analysis aims to find a soil profile that comes close to a representation of the soil profile at chainage 4115, as presented in Appendix 3. The soil profile is more detailed compared to the one of the scenario analyses. The choice to make a soil profile which does not vary throughout the model is made to be able to have a clear or better view on what induces certain behaviour. One could argue it would be more realistic to add more boreholes, which in essence is valid, however does not serve the purpose of this research.

The calculation method remains similar compared to the previous paragraph. For each soil layer the average and characteristic value is used for the calculation as presented in Appendix 2. Table 3.3 and Figure 3.2 show an overview of the advanced soil profile.

Table 3.3: Soil profile for the advanced soil profile analysis at chainage 4115

Top of layer [N.A.P. +m.]	Bottom of layer [N.A.P. +m.]	Geotechnical unit and main soil type	Legend
-1.60 (surface)	-2.30	2A – Clay	
-2.30	-5.40	3 – Peat	
-5.40	-7.40	4C – Clay	
-7.40	-17.50	4D – Sand	
-17.50	-18.30	5 – Peat	
-18.30	-30.00	6 – Sand	

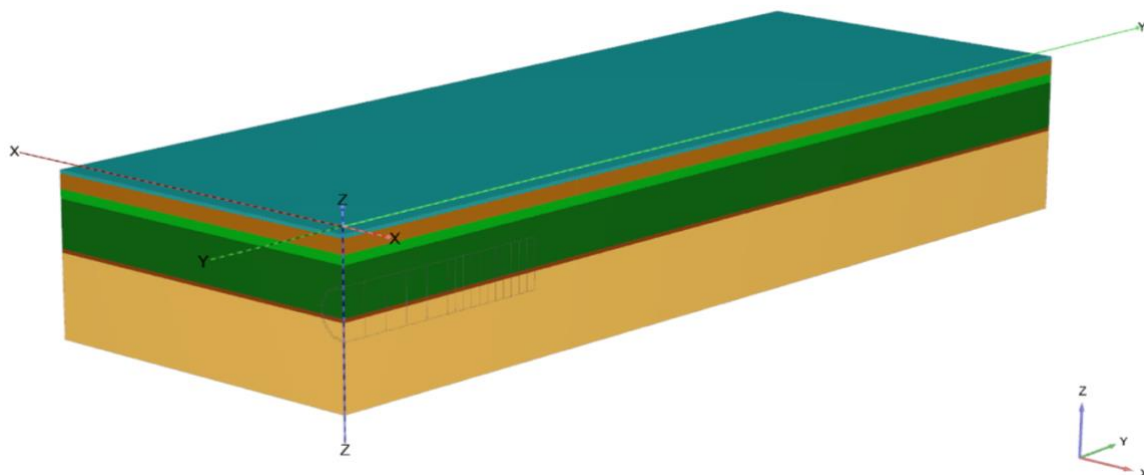


Figure 3.2: Soil profile for the advanced soil profile analysis at chainage 4115

For this calculation the average characteristic values from the geotechnical parameter set are used, as elaborated on in Appendix 2.

3.2.2 Results

The minimum and maximum face support pressures, respectively P_{\min} and P_{\max} at the tunnel crown are:

$$\begin{aligned}p_{\min} &= 92 \text{ kPa} \\p_{\max} &= 136 \text{ kPa}\end{aligned}$$

In §6.2 the result of this calculation will be compared with the numerical modelling results. It shows the advanced soil profile analysis differs significantly on the maximum face support pressure. This can be concluded from the fact the volumetric weight throughout the entire soil profile has a large contribution to the outcome of the maximum face support pressure. The composition of volumetric weight differs much between the simplified and advanced soil profile. For the minimum support pressure the difference in results is smaller. This can be concluded from the fact that the main influence comes from the strength parameters of the soil layer where the cutterhead is in. In case of the advanced soil profile, the strength parameters of the governing layers in which the cutterhead is in do not vary much. Therefore the difference in minimum face support pressure is also small.

3.3 Summary & Conclusions

The scenario analysis is performed to investigate the sensitivity of soil parameters used in an analytical face stability calculation by the DIN 4126 method. The results show that for the minimum support pressure, the strength parameters of the layer in which the cutterhead is located have the highest influence. The horizontal effective soil pressure including 3D effect, e_{ah} , represents the largest contributor to the sensitivity of the scenario analysis for the minimum face support pressure. For the maximum face support pressure this is the volumetric weight throughout the entire soil profile. Because the influence of the strength parameters is of little to no influence on the maximum face support pressure, it can be concluded that for the minimum face support pressure the K_{agh} is likely not to be of big influence, however the parameters: l_{ag} and K_{ach} are.

The above conclusions are confirmed by the differences in minimum and maximum face support pressure between the simplified and advanced soil profile.

The advanced soil profile analysis aims to find a soil profile that comes close to a representation of the soil profile of the case study. The soil profile is more detailed compared to the one of the scenario analyses. The choice to make a soil profile which does not vary throughout the model is made to be able to have a clear or better view on what induces certain behaviour. One could argue it would be more realistic to add more boreholes, which in essence is valid, however does not serve the purpose of this research.

Chapter 4

Numerical modelling

This chapter covers the numerical modelling of the problem and provides the base of the modelling part for the case study. For a more detailed outline of this chapter, please refer to §1.5.

4.1 Boundary conditions and soil model

To reduce the calculation time of the model, the vertical axis is used as a symmetry plane, which reduces half of the model's size. According to Ring (2018) the boundary conditions of the model can be set at 5 times the diameter from the vertical boundary to the tunnel side for the width. The depth below the tunnel invert should be approximated 2 times the diameter.

The principle of unloading is not assumed in the model because the focus lies at settlements in front of the TBM. In a numerical study, Ring & Comulada (2018) found the displacements in front of the TBM decrease rapidly over increasing distance from the shield.

4.1.1 Constitutive soil model

To get a first overview of the expected displacements and to implement the TBM in a suitable way for the purpose of this research the constitutive model chosen is a Mohr-Coulomb (MC) model. This is a linear elastic perfectly-plastic model which is often used for a first analysis of a problem. The model runs relatively fast due to a constant average stiffness estimated for each soil layer.

The model's outcome showed only very little settlements (millimetre level). Based on the results, the switch is made to a Hardening Soil model with small-strain stiffness (HSsmall). The HSsmall soil model is a modification of the Hardening Soil model (HS). HS is an advanced model which is of elastoplastic kind of hyperbolic modelling, formulated in the framework of shear hardening plasticity. Compression hardening is involved in the model to simulate irreversible compaction of soil under primary compression. Within tunnelling and for the aim of this research, which relates to settlements and failure mechanisms, compression hardening and elastoplastic behaviour are preferred to be included in the model. In addition to the HS model, the HSsmall model adds a strain dependent stiffness moduli. This simulates the different reaction of soils from all levels of strain.

4.1.2 HSsmall parameters

There are two small strain input parameters, G_0 and $\gamma_{0.7}$, respectively the reference shear modulus at very small strains ($\varepsilon < 10^{-6}$) and the shear strain at which $G_s = 0.722 * G_0$. G_s is the secant shear modulus. The small strain parameters are determined by the relations shown in equation 4.1 to 4.4. It is known that the stiffer the soil, the less difference between small-strain stiffness and large strains occur vice versa. For very dense sands this leads to: $G_0 = 2.5 * G_{ur}$ and $\gamma_{0.7} = 1 * 10^{-4}$. For a normally consolidated clay: $G_0 = 10 * G_{ur}$ and $\gamma_{0.7} = 5 * 10^{-4}$. Note: These are indicative numbers to provide guidance.

The small strain input parameters used for this research are presented in Table 4.1. For the undrained layers (clay) an undrained (A) is chosen. Undrained (A) is an undrained effective stress analysis with effective stiffness as well as effective strength parameters⁶. For the drained layers (sand), the properties are set to drained. The effective properties are used as input for this research. The hydraulic head is at -2.00 m. below N.A.P.

⁶ The other method in Plaxis 3D is Undrained (B), which is an undrained effective stress analysis with effective stiffness parameters and undrained strength parameters.

$$E_0 = 2 * G_0(1 + \nu_{ur}) \quad (\text{equation 4.1})$$

$$G_{ur} = \frac{E_{ur}}{2(1 + \nu_{ur})} \quad (\text{equation 4.2})$$

$$G_0 = 2.5 \text{ to } 10 * G_{ur} \quad (\text{equation 4.3})$$

$$\gamma_{0.7} = 1 \text{ to } 5 * 10^{-4} \quad (\text{equation 4.4})$$

**Table 4.1: Estimation small strain parameters set 1 [8],
(Dr. Ir. R.B.J. Brinkgreve, personal communication, 2019)**

Sand	Clay
$G_0 = 1.5 * G_{ur}$	$G_0 = 9 * G_{ur}$
$\gamma_{0.7} = 1.5 * 10^{-4}$	$\gamma_{0.7} = 4.5 * 10^{-4}$

4.2 Model design properties

Model design properties and considerations are discussed in this paragraph. Tunnel design properties, such as tail void injection, taper of the TBM, jack forces and tunnel face support pressure are discussed. Second, why a local mesh refinement is applied around the face of the TBM shield and at last why the setup of a pre-build tunnel of 25 meter followed up by 5 rings being build is chosen.

4.2.1 Tunnel designer

In Plaxis, the tunnel is designed with the tunnel designer function. As mentioned before, only one symmetric half of the tunnel is build. The design starts with the design of the segments in the segments sheet. The input for the inner radius is: $r_i = 4.895$ m. The thickness of the lining is set to 0.4 m. The tail void injection, in Plaxis referred to as grout pressure, is switched of in the majority of the scenarios. In the scenario which includes a grout pressure, a reference tail void injection pressure of $\sigma_{n,ref} = -140$ kPa is applied. Reference refers to the pressure applied at the tunnel crown. The pressures increases linearly over depth with a vertical increment of $\sigma_{n,inc} = -12$ kPa/m. This increment represents the volumetric weight of the grout. The values are negative due to the chosen axis system. Jack forces are left out in the model. The face support pressure vertical increment, $\sigma_{n,inc} = -11.02$ kPa/m. and also represents the volumetric weight. The reference face support pressure varies for almost every model. For the case study the reference face support pressure, $\sigma_{n,ref} = -122.4$ kPa. Due to the taper of the TBM, a contraction is applied on the plates which represent the TBM. This contraction is based on the determined volume loss as a result of this taper. The length of the TBM is 9.0 m. A sketch of the TBM is provided in Figure 4.1. All values are gathered from the COMOL5 TBM data.

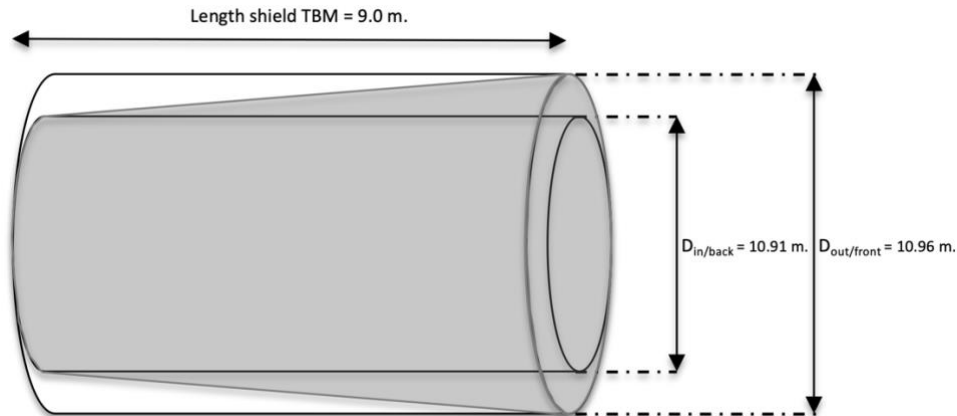


Figure 4.1: Dimensions of the shield of the TBM and its taper (not to scale!)

The total contraction, c_{tot} , of the TBM is determined by dividing the volume loss by the volume as if there would be no contraction. In addition the contraction increment, $c_{inc,axial}$, is determined. The contraction increment is the contraction applied over the width of the ring. The reference contraction, c_{ref} , of each ring can be determined by subtracting $c_{inc,axial}$ from c_{tot} . This leads to the reference contractions as shown in Table 4.2. Ring one being the ring closest to the cutterhead. At the tail of the shield the contraction becomes uniform at a c_{ref} of 0.91039 %.

$$c_{tot} = \frac{V_{loss}}{V_{outer}} * 100\% = \frac{V_{outer} - V_{inner}}{V_{outer}} * 100\% = 0.91039 \%$$

$$c_{inc,axial} = \frac{c_{tot}}{length\ shield\ TBM} = 0.10115 \%/m.$$

Table 4.2: c_{ref} for each ring

Ring number	c_{ref} [%/m]
1	0.0000
2	0.2022
3	0.4044
4	0.6067
5	0.8089

4.2.2 Mesh generation

To perform a numerical calculation in Plaxis 3D a mesh is created. This mesh is built up from a by the computer determined amount of tetrahedral elements, each containing 10 nodes (in Plaxis 3D modelling, this is the only type of element possible). The nodes in each element are at fixed positions, see Figure 4.2. The elements provide a second-order interpolation of displacements. Each element consist of three local coordinates: ξ, η and ζ . Each of the nodes has three degrees of freedom, being in x, y and z direction. Each element contains 4 integration points, x.

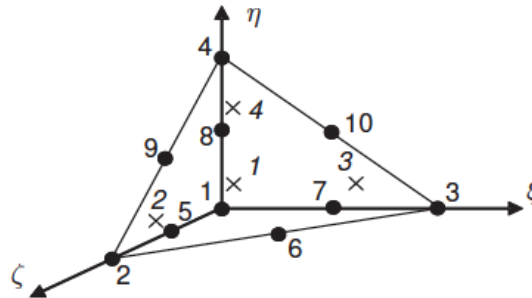


Figure 4.2: Local numbering and positioning of nodes (•) and integration points (x) of a 10-node tetrahedral element [18]

The amount of elements has a big influence on the calculation time of the numerical model, the more elements the higher the calculation time. The number of elements can be controlled by the refinement of the mesh. By increasing the refinement of the mesh, the smaller the elements, so the more elements required to fill the model. The accuracy increases by refinement. For this research a local mesh refinement is applied. By a local mesh refinement an indicated area of the mesh is refined. By this a balance between accuracy and calculation time can be reached. For most of this research, a local mesh refinement is applied around the cutterhead of the TBM with extension to the back and to the front. This is the failure zone including the zone of interest for settlements. Figure 4.3 shows the local refinement box in which the mesh is locally refined. This refinement box is used for the majority of the models of this research. The size of the area is 10.0 m. wide, from the centre of the tunnel to 10.0 m. in x direction. The refinement area starts at a location of 10.0 m. behind the cutterhead and continues to up to 10.0 m. in front of it. In z direction the local refinement is applied from surface level (-1.6 m.) to -22.0 m. Those dimensions and a local refinement factor of 0.125 are assumed to be sufficient for the aim of this research. Appendix 6 shows the steps taken to get to this assumption. On the edge of the refinement a sudden jump in deformation was found above the shield. For the model containing the applied face support pressure, which is being compared to the monitored field data, the refinement area is increased: x = 0.0 m. up to x = -15.0m., y = 0.0 m. up to y = 70.0 m. and z = -1.6 m. up to z = -24.0 m. The refinement is increased to increase the accuracy of the case study models.

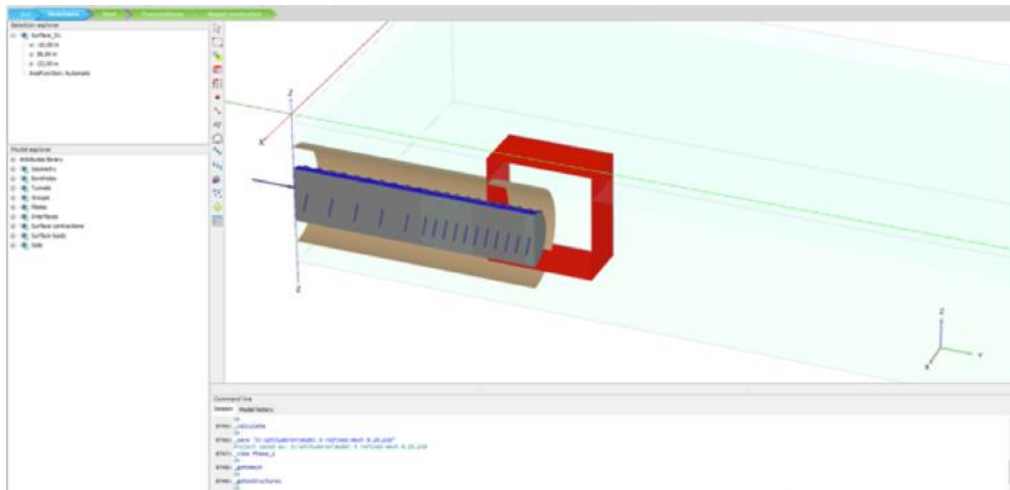


Figure 4.3: Refinement box (Plaxis 3D)

4.2.3 Construction of the tunnel

Building of the TBM in Plaxis 3D is done in phases. Each phase represents a construction step. To discard the influence of boundary conditions of the model in the first phase, an as built part of the tunnel is constructed. In this model it is assumed 25 m. is sufficient to discard the influence of boundary conditions. A uniform contraction is applied to this as built part in a separate phase. The 25 m. of constructed tunnel is followed up by the building of multiple rings. Multiple rings must be modelled to discard start-up influence of the TBM. In this research it is assumed a number of 5 rings is sufficient to discard the start-up influence of the TBM, which means reaching a steady state when it comes to settlements not induced by the components as elaborated on in this research. Appendix 1 contains the figures supporting this assumption. After the last ring is build, an extra phase is added which is similar to the previous one. This increases the accuracy of the outcome. From that point forward, failure mechanisms are looked for by varying the face support pressure.

4.3 Influence of tail void injection and the taper of the TBM shield on settlements in front of the cutterhead

It is preferable to reduce the amount of variables in the numerical model. Therefore the influence of the tail void injection and taper of the shield are analysed. The analysis checks if both have impact on the settlements above the cutterhead and in front of it.

Tail void injection

The tail void injection is the mortar being injected between the TBM shield and the lining. The mortar prevents the soil from collapsing while the TBM is excavating, or building a ring. For the analysis 5 scenarios are compared. 1 of them is without a tail void injection. In this scenario the tail void injection is replaced by a wished in place lining. No tail void injection is not a realistic situation in a soft soil tunnelling project, but gives an insight of its influence in numerical modelling. The other 4 scenarios represent a varying set of mortar pressures. At ring 64 the applied mortar pressure is about 140 kPa, with a peak pressure of 340 kPa. The mortar pressures 100 kPa and 120 kPa are to check what the influence is for a drop in mortar pressure.

A 4.5 mm. settlement difference above the cutterhead is measured between the results of the models with and without tail void injection. This is illustrated in Figure 4.4. An in- or decrease in mortar pressure does not influence this number at this location. 14 meters in front of the TBM the difference between with and without tail void injection is below 1 mm. This falls within the range of measurement inaccuracy of measurement equipment in the field. Therefore, to reduce the number of variables in the model, the tail void injection is left out of the model of this research.

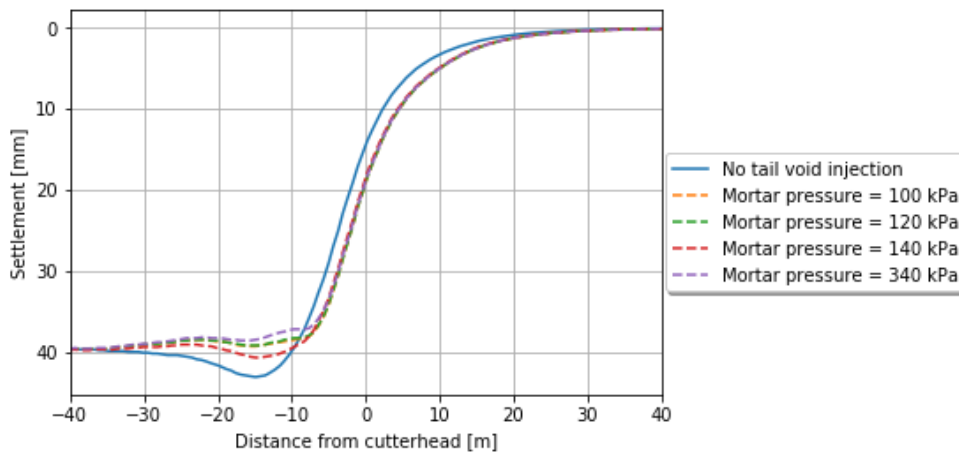


Figure 4.4: Settlements with and without tail void injection. With varying mortar pressure at the tail void

Taper of the TBM shield

The taper of the TBM shield, also known as contraction, is shown in Figure 4.1. In numerical modelling, contraction can be switched off. In numerical modelling the TBM shield is represented by plate elements. To see the influence of the contraction, two scenarios are compared: with and without plate contraction applied, see Figure 4.5. 12 meters in front of the TBM the difference between with and without TBM plate contraction is below 1 mm. Above the cutterhead the influence of the contraction is 8.7 mm, which is not within the range of measurement inaccuracy. Therefore this property should not be left out of the numerical model.

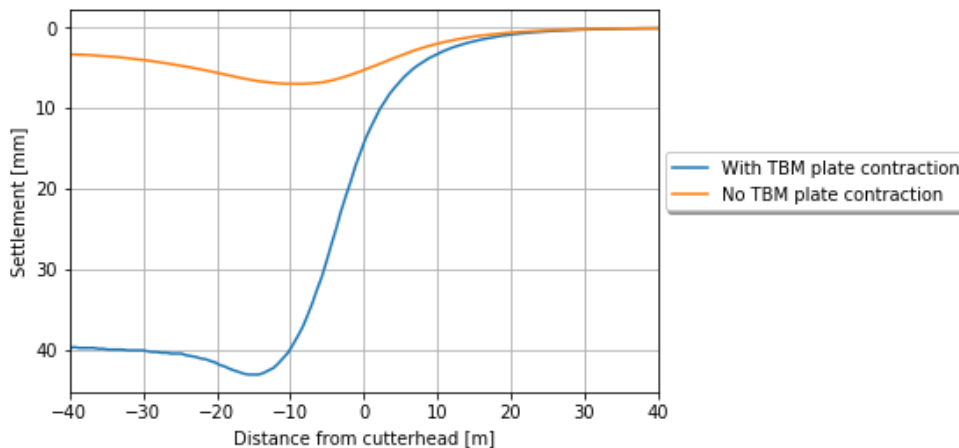


Figure 4.5: Settlements with and without TBM plate contraction

4.4 Scenario analysis – numerical modelling

Similar to the analytical approach, this chapter elaborates on a scenario analysis. The scenario uses the soil profile as presented in Table 3.1 and Figure 3.1, and the geotechnical parameter set of COMOL5 (Appendix 2).

4.4.1 Input parameters

For the numerical analysis, the parameter set is extended by parameters which are taken into account by numerical modelling, but not with the analytical method of this research. The scenario analysis considers two scenarios for both the clay and the sand layer. The scenarios analyse the following geotechnical parameters:

1. Unit weight (γ) and stiffness (E_{50} , E_{ur} , E_{oed}): unit weight and stiffness (E-moduli) are considered in one scenario due to their correlation. The higher the unit weight, the stiffer the material is. This leads to one sub-scenario with $X_{gem;k:low}$ for both unit weight and stiffness and one scenario with $X_{gem;k:high}$ for both unit weight and stiffness. The sub-scenarios are called the lower bound and higher bound respectively;

2. Strength parameters: the friction angle (ϕ) and cohesion (c) are considered in one scenario due to their correlation. Unlike in scenario 1, the parameters are correlated in a different way. This leads to one scenario with $X_{gem;k;low}$ for the friction angle and $X_{gem;k;high}$ for the cohesion. The second sub-scenario is the other way around. The sub-scenarios are called the lower bound and higher bound respectively.

The above mentioned parameters are analysed because these are the parameters which are included in the analytical scenario analysis. This does not account for the stiffness parameters. Due to its correlation with the unit weight this parameter is included in the scenario analysis of the numerical modelling. The vertical permeability is considered but did show 0.0 mm. influence and is therefore not further elaborated on.

4.4.2 Results

The results of the scenario analysis are displayed for the four sub-scenarios. Figure 4.6 until Figure 4.9 display the relative displacement at both the surface and at the TBM crown. The relative displacement is displayed from the cutterhead until 20.0 m. in front of it. The results show that:

- For all scenarios the relative displacement is larger at the TBM crown compared to the relative displacement at surface;
- For the first scenario, the unit weight and stiffness scenarios, the lower bound shows more relative displacement compared to the higher bound. It can be concluded a conservative assumption of the unit weight and stiffness parameters is preferred. This accounts for both clay and sand;
- The strength parameter scenario shows more relative displacement compared to the unit weight and stiffness parameter scenario. It can be concluded the strength parameters have a larger influence on the displacement. This accounts for both the sand and clay scenario;
- The differences are very small. Finding inaccuracies in the numerical model soil parameter input based on field data is not possible in this case. This is not possible due to the inaccuracy of field data;
- For all (sub-)scenarios, both at surface level and TBM crown level, the relative displacement of the lower and higher bound approach each other;
- The largest influence in changing soil parameters lies at the cutterhead for the unit weight and stiffness parameters of clay and for the strength parameters of sand. For the unit weight and stiffness parameters of sand and the strength parameters of clay the largest influence of changing soil parameters lies around 5m. in front of the cutterhead.

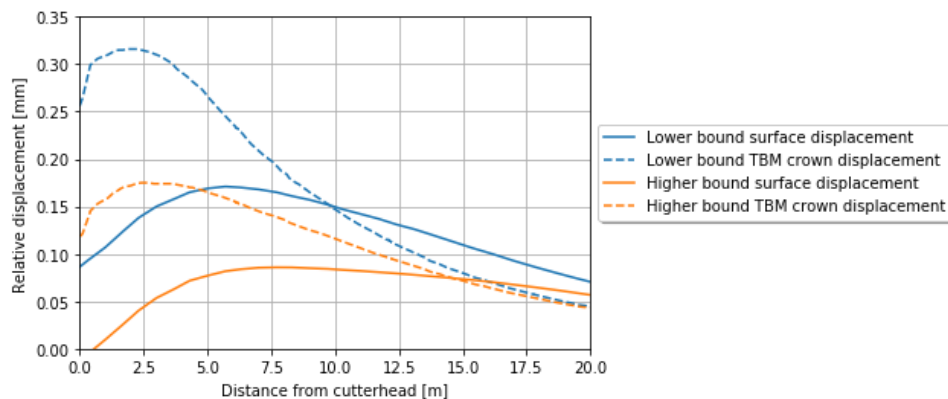


Figure 4.6: Unit weight and stiffness parameters sand:
Lower bound: Relative displacement between $X_{gem;k}$ and $X_{gem;k;low}$
Higher bound: Relative displacement between $X_{gem;k}$ and $X_{gem;k;high}$

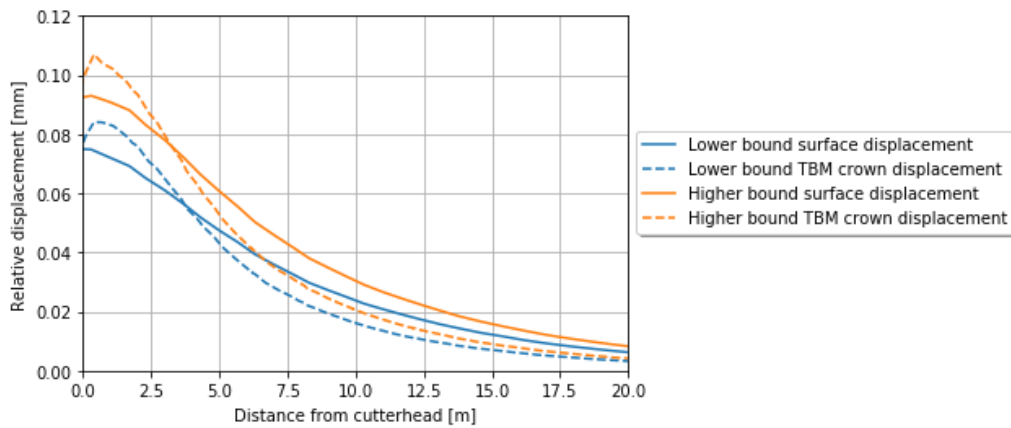


Figure 4.7: Unit weight and stiffness parameters clay:
Lower bound: Relative displacement between $X_{gem;k}$ and $X_{gem;k;low}$
Higher bound: Relative displacement between $X_{gem;k}$ and $X_{gem;k;high}$

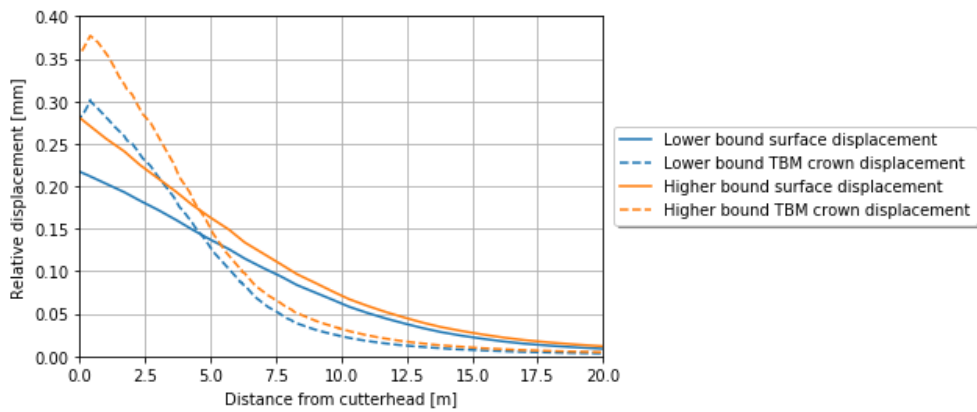


Figure 4.8: Strength parameters sand:
Lower bound: Relative displacement between $X_{gem;k}$ and φ : $X_{gem;k;low}$ and c : $X_{gem;k;high}$
Higher bound: Relative displacement between $X_{gem;k}$ and φ : $X_{gem;k;high}$ and c : $X_{gem;k;low}$

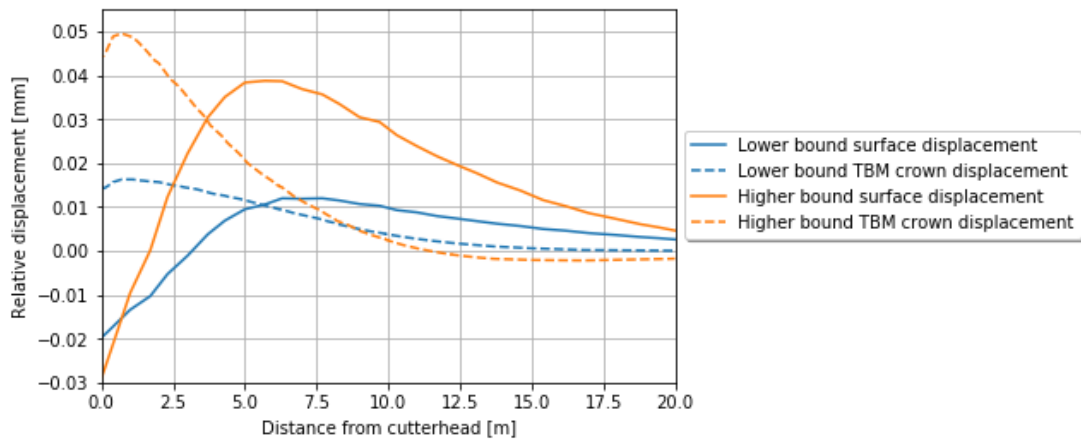


Figure 4.9: Strength parameters clay
Lower bound: Relative displacement between $X_{gem;k}$ and φ : $X_{gem;k;low}$ and c : $X_{gem;k;high}$
Higher bound: Relative displacement between $X_{gem;k}$ and φ : $X_{gem;k;high}$ and c : $X_{gem;k;low}$

4.5 Advanced soil profile analysis – numerical

4.5.1 Input of advanced soil profile

Similar to the analytical approach, this chapter elaborates on an advanced soil profile analysis. The scenario uses the soil profile as presented in Table 3.3, Figure 3.2 and the geotechnical parameter set of COMOL5 (please refer to Appendix 2). The corresponding reference pressure and small strain and K_0 parameters can be found in Appendix 4. For the advanced soil profile analysis not only the minimal and maximum face support pressure are looked for, but also the type of failure mechanisms and trends regarding face pressure in relation to settlements.

4.5.2 Results

To find a minimum and maximum face support pressure numerically, two face support pressures have to be used as an input. Those face support pressures must be so low or high, the soil body failure will occur. This number is chosen based on common sense and logical reasoning. The model will fail in finishing the entire calculation. In Plaxis Output the ΣM_{stage} gives back a value between 0.0 and 1.0. If a model is able to complete the calculation, the $\Sigma M_{stage} = 1.0$. If the calculation failed to finish the calculation due to soil body failure, the value presented by the ΣM_{stage} is below 1.0. The minimum and maximum face support pressure thereafter can be determined by: $\Sigma M_{stage} * \text{applied face support pressure} + \text{the applied face support pressure of the previous phase}$. With the applied face support pressure being an extremely low value (for the minimum) and extremely high value (for the maximum face support pressure). The applied face support pressure of the previous phase must be a face support pressure which is guaranteed to be stable. Therefore the applied face support pressure from the case study is used. The minimum face support pressure can be determined by: $\Sigma M_{stage} * \text{applied face support pressure}$,

The minimum face support pressure

The minimum face support pressure in the numerical model is found at 91 kPa. This is only 1 kPa lower compared to the analytical determined minimal face support pressure. The failure mechanism is an active soil failure mechanism, a cave-in, and is as expected. Figure 4.10 and Figure 4.11 show the total phase displacement. Total phase displacement is the displacement occurring only in the last calculated phase. In this case the building of the last ring. The zone of influence is rather small in transversal direction compared to the influence in longitudinal direction where the influence is both to the front and (little) to the back (for visual support, refer to Appendix 7).

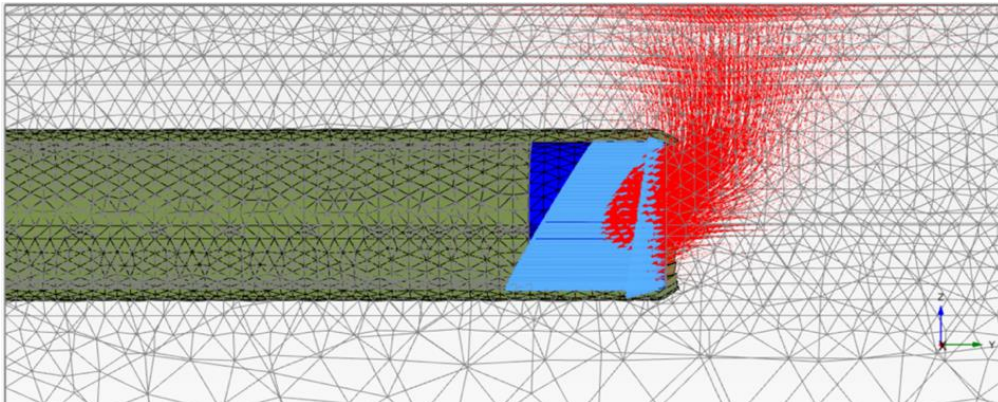


Figure 4.10: Soil body failure mechanism at the numerical lower face support pressure limit. Total phase displacements, P_u . Including soil movement direction arrows

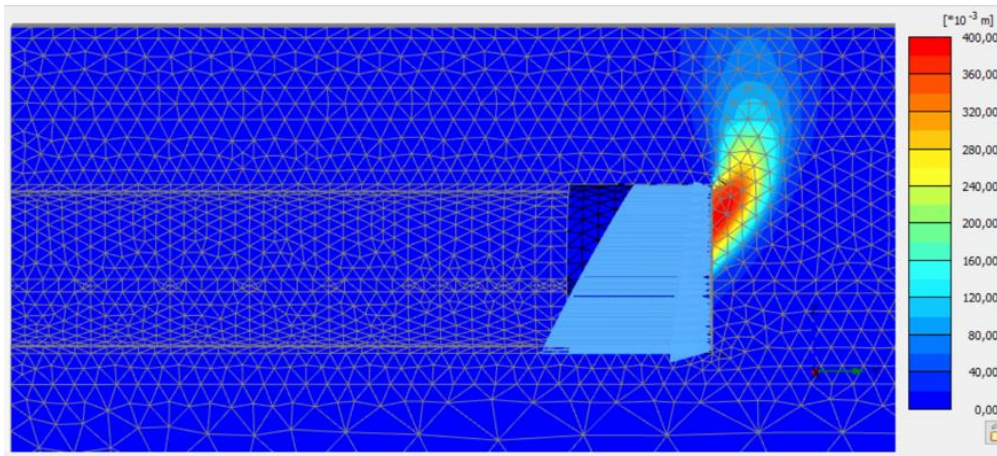


Figure 4.11: Soil body failure mechanism at the numerical lower face support pressure limit. Total phase displacements, P_u . Including deformation scale

The maximum face support pressure

The maximum face support pressure in the numerical is model found at 794 kPa. This is 658 kPa higher than the analytically found maximum face support pressure. The failure mechanism is a passive soil failure mechanism, a blow-out, and is as expected. Figure 4.12 and Figure 4.13 show the total phase displacement. The zone of influence in transversal direction reached just outside the width of the TBM (for virtual support, refer to appendix 7). In longitudinal direction the influence is completely in front of the TBM.

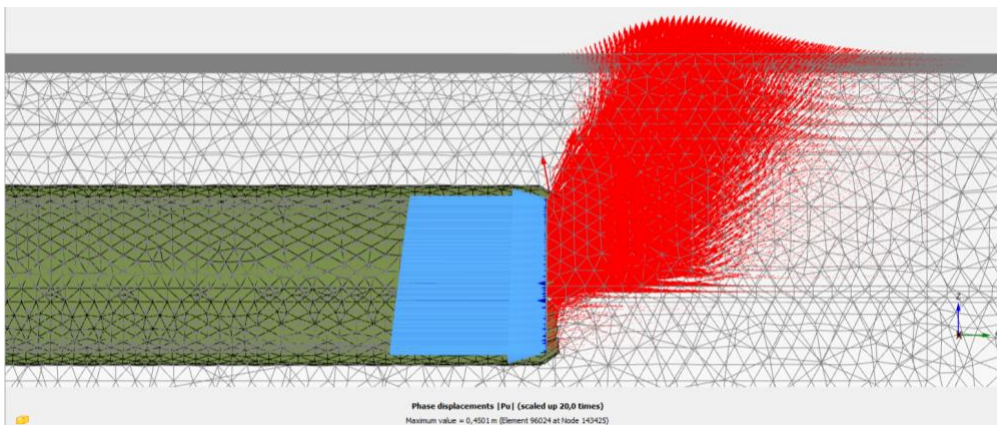


Figure 4.12: Soil body failure mechanism at the numerical upper face support pressure limit. Total phase displacements, P_u . Including soil movement direction arrows.

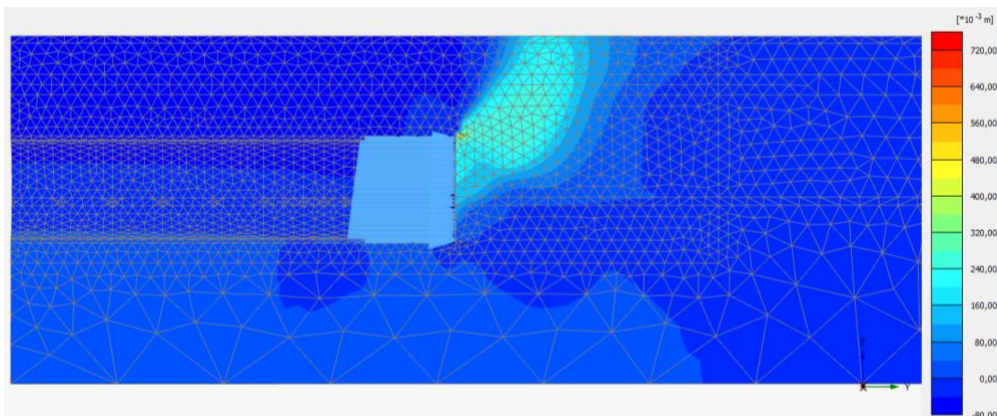


Figure 4.13: Soil body failure mechanism at the numerical upper face support pressure limit. Total phase displacements, P_u . Including deformation scale

Behaviour, mechanisms and trends

A set of trends is discussed, starting with the trends of the face support pressure in relation to the settlements. Figure 4.14 displays the settlements above the cutterhead vs. the applied face support pressure applied at the crown of the cutterhead. When traveling from the left hand side to the right hand side of the curve in Figure 4.14, two inclination points are present. At a face support pressure of around 120 kPa, the curve flips over for the first time as can be seen in a close up in Figure 4.15. The second flipping point is at a face support pressure 600 kPa. A decrease in settlements occurs when traveling from the minimum face support pressure to the first flipping point at around 120 kPa. From there on, an increase in settlements occur. At face support pressures higher than 600 kPa the settlement decreases again until failure occurs. This divides Figure 4.14 into 3 phases.

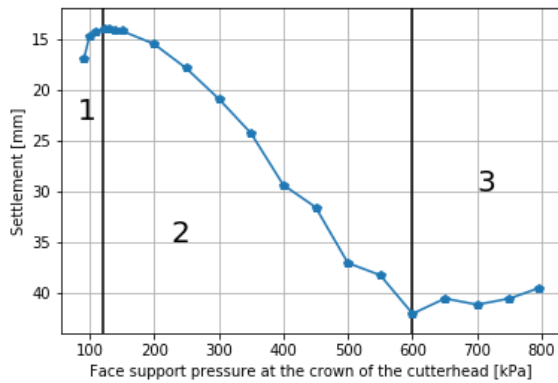


Figure 4.14: Settlements above the cutterhead for a varying set of applied face support pressures

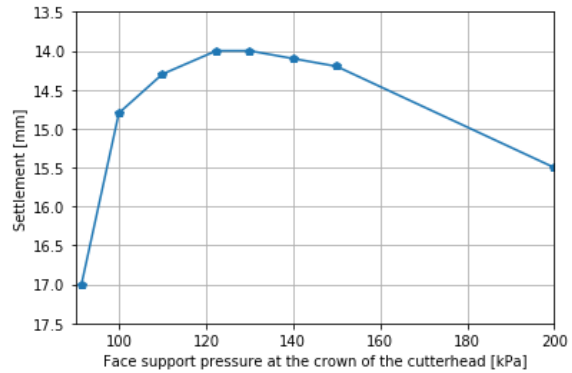


Figure 4.15: Zoom on the area between minimum face support pressure and a face support pressure of 200 kPa

Trends of the three phases will be elaborated separately.

Phase 1: The increased settlement while lowering the face support pressure from around 120 kPa is expected behaviour. This is anticipated because the lower the face support pressure, the less resistance against the soil body will. The lower the face support pressure, the more the soil body will move towards the face. This leads to an increase in settlements. Below the in the case study applied face support pressure of 122 kPa, the numerical model shows an active failure mechanism. An exponential trend is observed.

Based on the results, the slope (m) of the settlement curve between the different support pressures is determined, presented in Figure 4.16. The difference between m_1 and m_2 is relatively large. It is most likely this is due to the low density of results. If the density is increased, the curve is expected to smoothen. The red line in Figure 4.16 represents such line (NOTE: this is just an example and not based on scientific results). Based on common sense, it is expected there will be an inclination point between the 100 and 110 kPa. The location of this inclination point can be found by increasing the density of the result, which also leads to a higher accuracy. The red line in Figure 4.16 shows: $m_2 < m_{red\ line} < m_1$. Based on the results gathered in this research, the TBM operator should be alarmed at a slope of $m = -0.1$, based on the results shown in Figure 4.17. Again the note must be made that this is an indication based on a non-scientific curve, but most likely is a reasonable indication for a curve with a higher density in results. This slope becomes more accurate when increasing the density of the results.

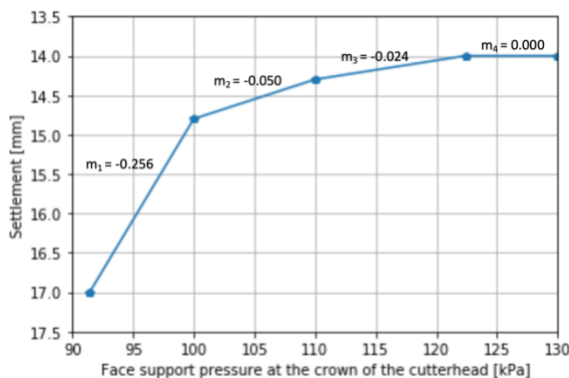


Figure 4.16: Slope (m) at low face support pressures

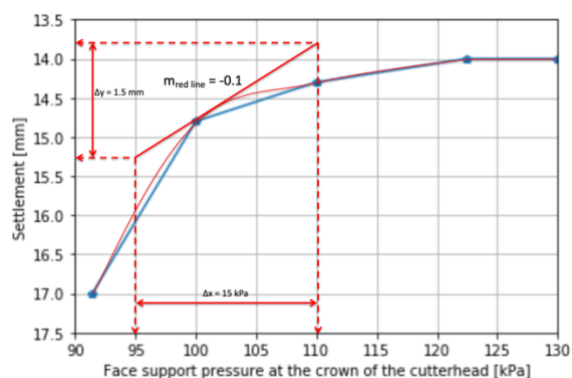


Figure 4.17: Determination of slope (m) of the red line which represents the expected behavior of the curve when a higher measurement density is achieved

Phase 2: The settlement occurring when increasing the face support pressure from 120 kPa up to 600 kPa is not the expected behaviour. It is expected to see heave occurring. The increase in settlements as shown in Figure 4.14 originates from an active local mechanism, which is expected to be plastic of kind.

It seems plastic deformation takes place which induces settlements at surface. The more increase in face support pressure the closer the mechanism gets to the surface. This mechanism is presented in Figure 4.14, Figure 4.18 and Figure 4.19 for a face support pressure of 150 kPa, and in Figure 4.20 and Figure 4.21 for a face support pressure of 500 kPa.

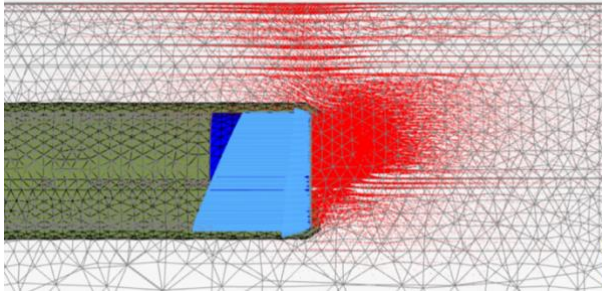


Figure 4.18 Total phase displacement at a face support pressure of 150 kPa.
Local displacement behaviour

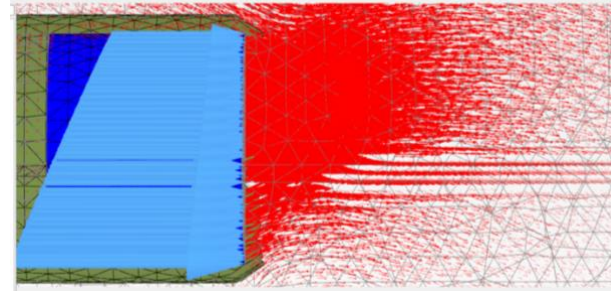


Figure 4.19: Total phase displacement at a face support pressure of 150 kPa.
Local displacement behaviour, zoom

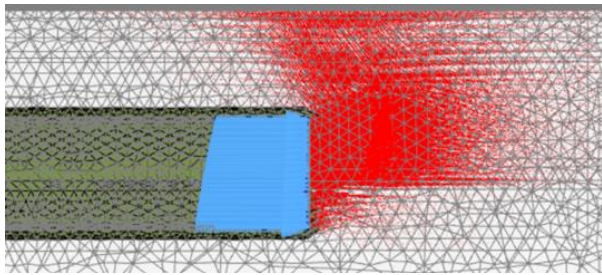


Figure 4.20: Total phase displacement at a face support pressure of 500 kPa.
Local displacement behaviour

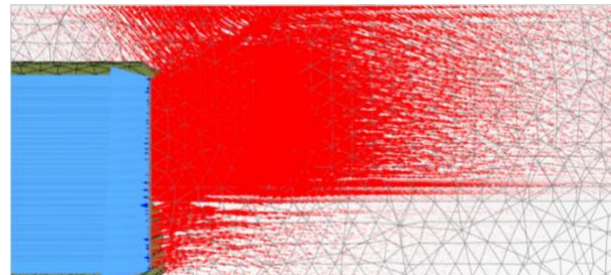


Figure 4.21: Total phase displacement at a face support pressure of 500 kPa.
Local displacement behaviour, zoom

Phase 3: From a face support pressure of 600 kPa and higher, up to the maximum face support pressure, a passive global mechanism occurs. The settlements reduce and a soil body is pushed up in front of the TBM. This causes heave in front of the TBM. This is the expected mechanism for high face support pressures.

Figure 4.14 shows the influence of the settlements right above the cutterhead. To see the influence of the varying face support pressure at different locations, Figure 4.22 is presented. The results in Figure 4.22 show that 10 meters in front of the cutterhead the most heave, representing the blow-out, take place. This matches the results presented in Figure 4.12 and Figure 4.13. Further ahead of the cutterhead, for most face support pressures, the settlements damp out. Around the tail void an increase in settlements occur.

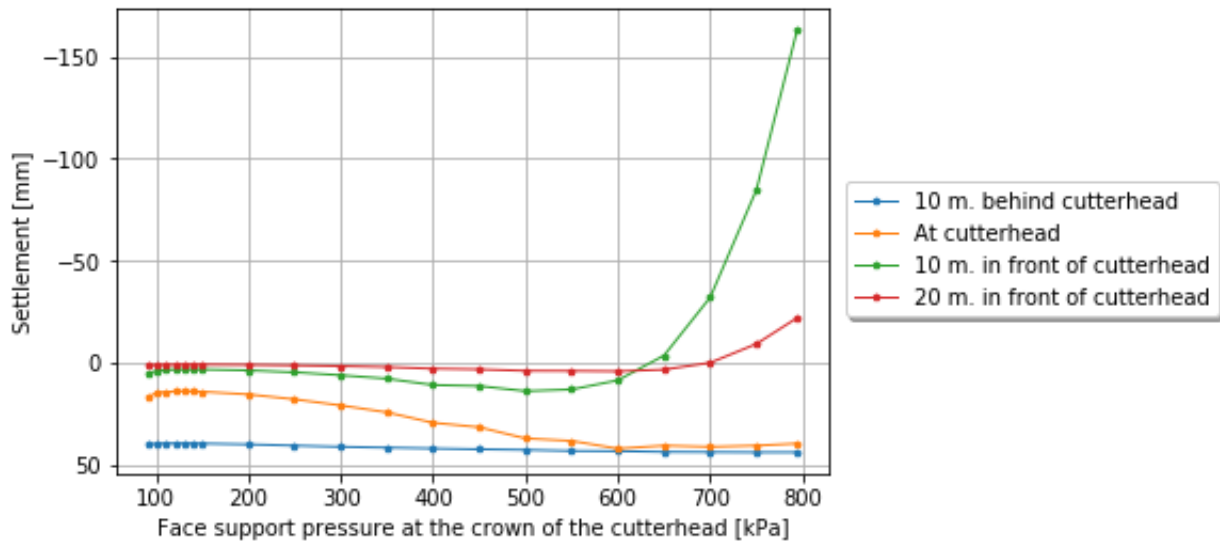


Figure 4.22: Settlements at different locations from the cutterhead for a set of different face support pressures

The settlement curves in longitudinal direction in Figure 4.23 to Figure 4.26 show a similar trend. The settlement curves presented in those figures show the minimum face support pressure = 91.4 kPa (analytically and numerically), the applied face support pressure during the construction of ring 64 = 122.5 kPa, the analytical maximum face support pressure = 136.0 kPa and the numerical maximum face support pressure = 794.0 kPa.

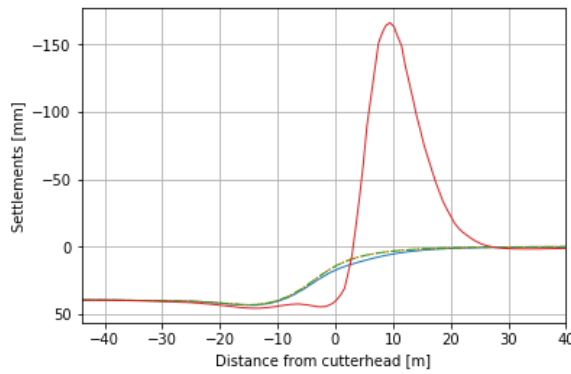


Figure 4.23: Settlements for 4 different support pressures

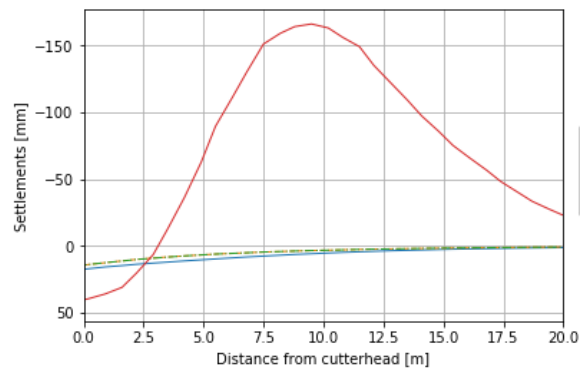


Figure 4.24: Settlements for 4 different support pressures, zoom to cutterhead and in front of it

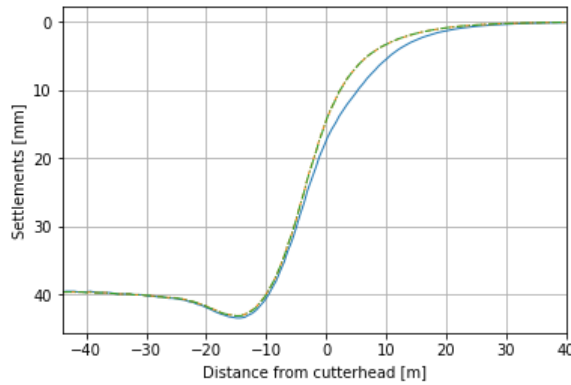
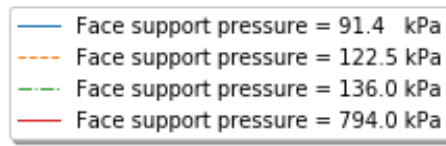


Figure 4.25: Settlements for 4 different support pressures (fp = 794.0 kPa excluded)

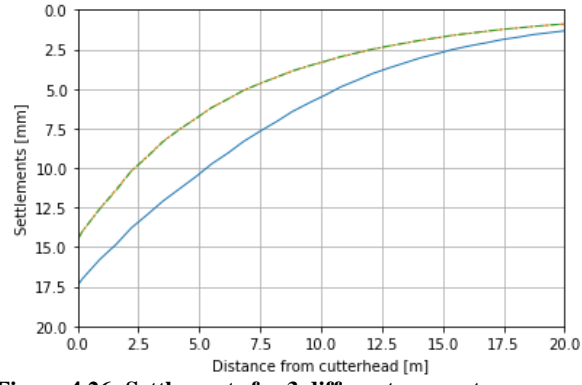


Figure 4.26: Settlements for 3 different support pressures, zoom to cutterhead and in front of it (fp = 794.0 kPa excluded)

Behind the cutterhead (= above the shield of the TBM), the settlements increase more for high face support pressures compared to the low face support pressures when taking the cutterhead as a reference. This is shown in Figure 4.22 and can be caused by several things. The several hypotheses are listed below:

- The face support pressure influences the ground surrounding the cutterhead. This means the face support pressure does not only apply pressure in horizontal direction in front of the cutterhead, but also to the sides. It is possible the high face support pressure deforms the surrounding soil plastically which causes an increase in settlements after the cutterhead is passed. This is caused due to the fact the face support pressure is not applied anymore which leaves a gap around the TBM, which is filled by the plastically deformed (and densified) soil;
- An increase in settlements can be caused by overcutting of the cutterhead. Since the cutterhead has almost the same diameter as the lining, this is not likely to be the reason of the increase in settlements. The only decrease in diameter is due to the taper of the TBM.
- Steering losses can lead to an increase in settlements behind the cutterhead. Steering losses occur when the TBM is not going straight through the ground. Going straight means neither vertical nor horizontal inclination/angles of the TBM. Steering losses are not possible in the used numerical model since the tunnel lies horizontal in the ground and does not make any turns/goes straight through the ground. Steering losses could be modelled by letting the TBM make a turn or incline deeper into the ground. For sake of simplification of the model this is not done.

Based on prior soft soil slurry tunnelling projects it is known that the failure mechanism found by numerical modelling is not the one occurring in the field. In soft soil projects, active instabilities such as piping are much more likely to occur.

4.6 Summary & Conclusions

For the numerical modelling of this soft soil slurry TBM project, HSsmall is used as constitutive model. This constitutive model is elastoplastic of kind in the framework of shear hardening plasticity. The HSsmall model takes into account strain dependent stiffness moduli.

From the results of varying meshes it can be concluded that for research behind the cutterhead, the local refinement of the mesh needs to be extended beyond the zone of interest. A local refinement of about 10m. in front of the cutterhead is sufficient for a first impression. When comparing the results to field data, a larger local refinement is suggested/required to increase the accuracy of the results. The distance from the cutterhead depends on how far in front of the cutterhead the field data is gathered.

The tail void injection is of influence on the settlement above and in front of the cutterhead, but for simplification of the model, the tail void is replaced by wished in place lining for this research. The applied mortar pressure at the tail void does not show settlement differences worth mentioning when analysing the settlements in front of the TBM. The taper of the TBM should not be switched off, the influence is large with respect to settlements at and in front of the cutterhead. Behind the shield of the TBM the settlements reduce enormously when no plate contraction is applied.

From the scenario analysis it can be concluded the hypothesis that a small change in soil parameter properties leads to a significant change in settlements was incorrect. The influence of varying soil parameters has a negligible influence on settlements in this case study in which the characteristic low and high values of the geotechnical parameter set are used to perform the scenario analysis.

It is recommended to also take into account the parameters that are correlated to the varying scenario parameters as far Plaxis does not do this itself.

When looking for minimum and maximum face support pressures in a similar kind of numerical model, the ΣM stage function is recommended to use. The limit face pressures can be found by running a modelling phase with an applied face support pressure (from for example, the case study) with an extremely low and high face support pressure, of which one is sure the model will fail to finish the calculation. By use of the resulting ΣM stage of those extreme face support pressures and the applied face support pressure of the case study, the numerical minimum and maximum face support pressures can be determined.

For low face support pressures, the behaviour of settlements and the active soil mechanisms are as expected. A cave-in occurs when reaching the minimum face support pressure. For high face support pressures, this is not the case. Instead of heave, an increase in settlements occur when increasing the face support pressure. A local active soil mechanism occurs. Based on the settlements curve for different face pressures, the TBM operator should get a warning a cave-in is approached at a slope of $m = -0.1$. The accuracy of this warning number can be increased by increasing the density of results of the settlement curve. For the extremely high face support pressures a global (failure) mechanism in the form of a blow-out occurs. The blow-out occurs around 10 m. in front of the cutterhead and does not coincide with the expected failure mechanism which is hydraulic fracturing.

Behind the cutterhead an increase of settlements takes place. For low face support pressures there is a larger increase than for high face support pressures. Above the cutterhead it is expected an increase in pore water pressure, dilation or total soil body displacement to be the reason. Behind the cutterhead, it is assumed the settlements are due to plastic deformations around the shield, overcutting and steering losses.

Chapter 5

Field data analysis

This chapter covers the analysis of the field data. For a more detailed outline of this chapter, please refer to §1.5. Like the analytical (Chapter 3) and numerical (Chapter 4) analysis, the field data analysis has a focus on the chainage 4115/ring 64. With a focus on the moment the cutterhead is located at chainage 4115. The field data analysis starts with visualising the TBM drive. From the TBM data, the progress of the cutterhead vs. time is displayed in Figure 5.1. Figure 5.2 zooms in on the chainage 4115, at which ring 64 is build. The data interpretation is divided in three groups: settlements, pore water pressure and face support pressure. Those three components are considered because it is assumed those three topics contribute to answering the research question.

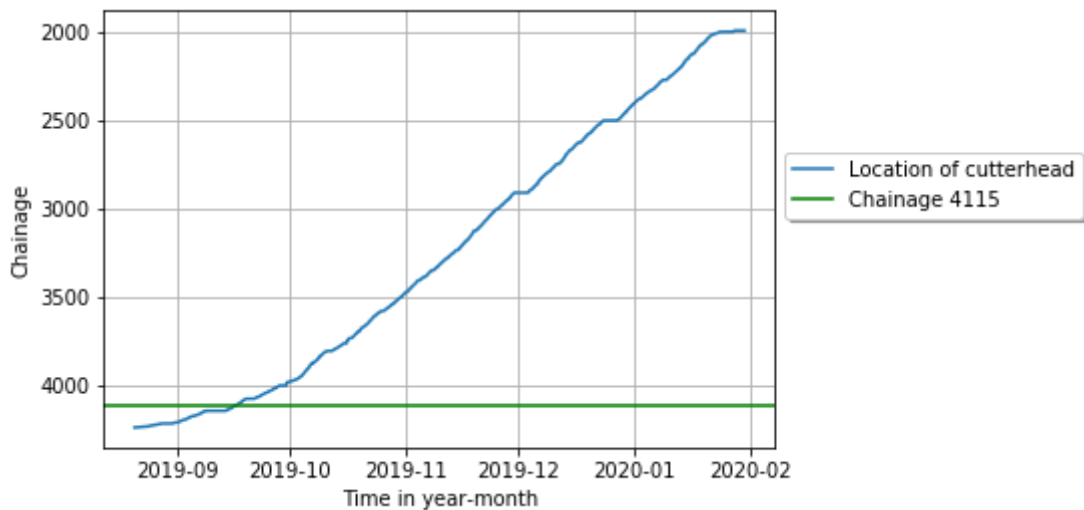


Figure 5.1: Location of the TBM Gaia through time

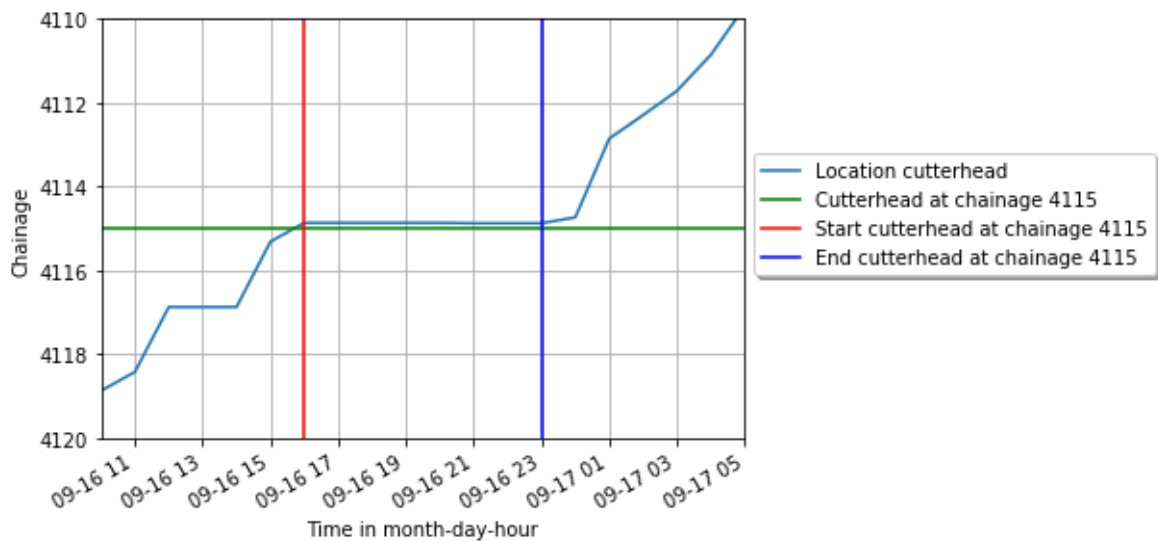


Figure 5.2: Location of the TBM Gaia through time with a focus on chainage 4115

5.1 Settlements – Monitored Field Data

5.1.1 Data interpretation

The settlements data provided by COMOL5 needed modification, prior to using it for the aim of this research. Prior to the start of excavation, a pre-load has been applied to the launch area. This is done to speed up the consolidation process so no significant excess pore pressures would remain in the cohesive soil layer when the TBM starts. Appendix 3 shows the soil profile, including the pre-load area at the location of the launch area. The pre-load is removed before the TBM started excavating. Removing the pre-load has led to swelling. The influence of the swelling is being removed from the results. This is done to discard its influence on the results of the monitored field data analysis. To do so, the resulting settlement is determined by subtracting the settlement (at the same location) from one week prior to the moment of interest.

The monitored field data provides settlements over the entire trajectory of the southern tunnel tube. A higher density of monitoring devices at the TBM launch area, gives the possibility to perform a data analysis. The monitoring layout of the TBM launch area is shown in Appendix 8. As mentioned in the introduction of this chapter, the settlements elaborated in this paragraph have a focus on chainage 4115, similar to the location of the analytical and numerical analysis. The TBM is at chainage 4115 for a time period of about 8 hours. Figure 5.3 shows the settlements (in longitudinal direction), at the moment the cutterhead is at a standstill, at chainage 4115. When the cutterhead is at chainage 4115, the 64th ring of the southern tube is constructed. In the legend of Figure 5.3 all measurements of when the TBM is at chainage 4115, are presented. All settlement measurements at the standstill are elaborated on, to know what the influence of the TBM is on settlements during the building of 1 ring.

The accuracy is determined by analysing a group of measurements of a settlement device for a time period of 10 measurements (Appendix 9). The accuracy is around 1.0 mm.

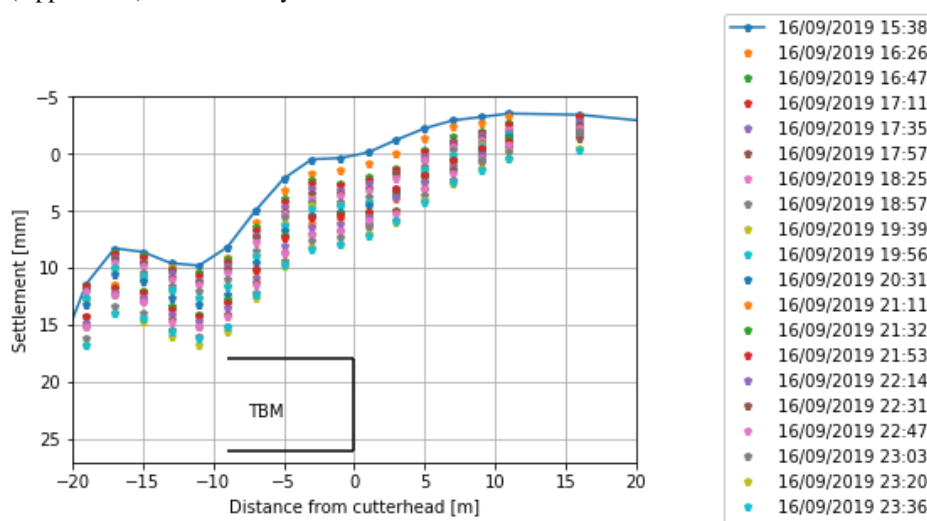


Figure 5.3: Settlements when the cutterhead of the TBM is at chainage 4115, in longitudinal direction

Beside chainage 4115, the 4 rings prior to ring 64 are elaborated on. This is done to investigate the influence of the TBM on settlements throughout a larger time span. The settlement curves for rings 60-64 are presented in Figure 5.4 and Figure 5.5.

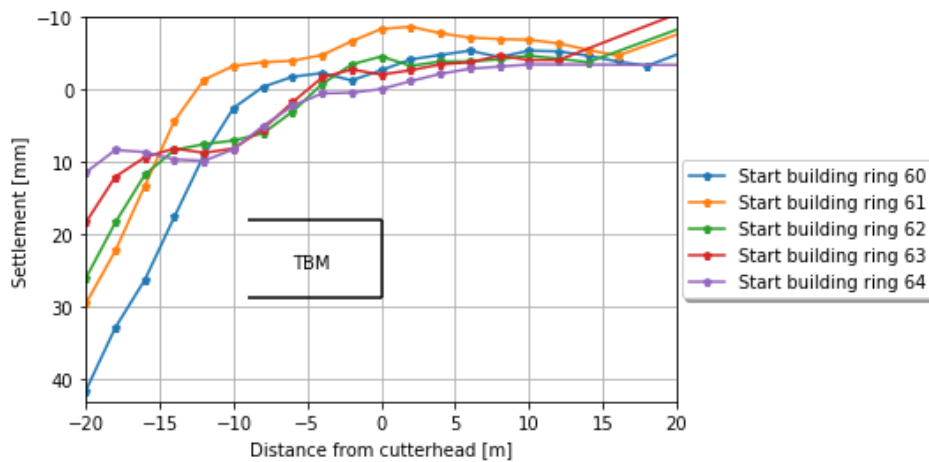


Figure 5.4: Settlements during the construction of ring 60-64.

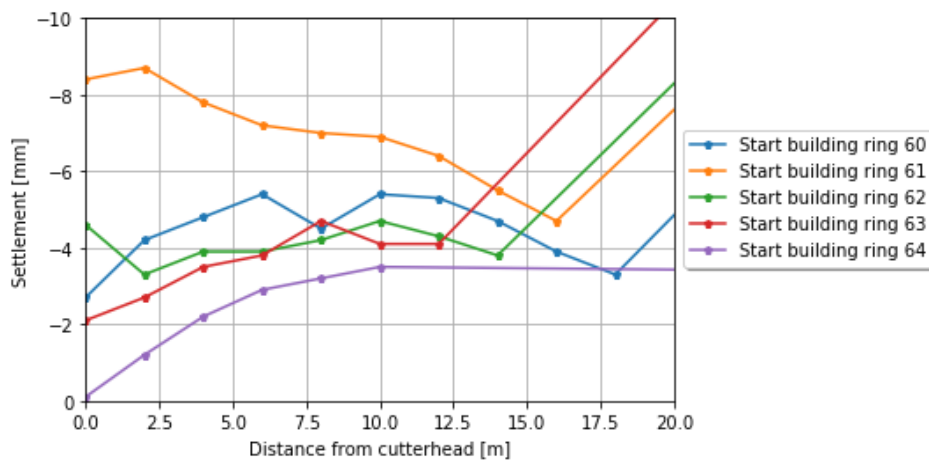


Figure 5.5: Settlements during the construction of rings 60 – 64, behaviour in front of the cutterhead

For the sake of the completeness of this settlement analysis, the transversal displacement curve at chainage 4115 is analysed. The results are shown in Figure 5.6. The displacement is not meeting the expectations. It is expected to have less or no heave occurring. Also the point of highest settlements is not in the centre of the the TBM.

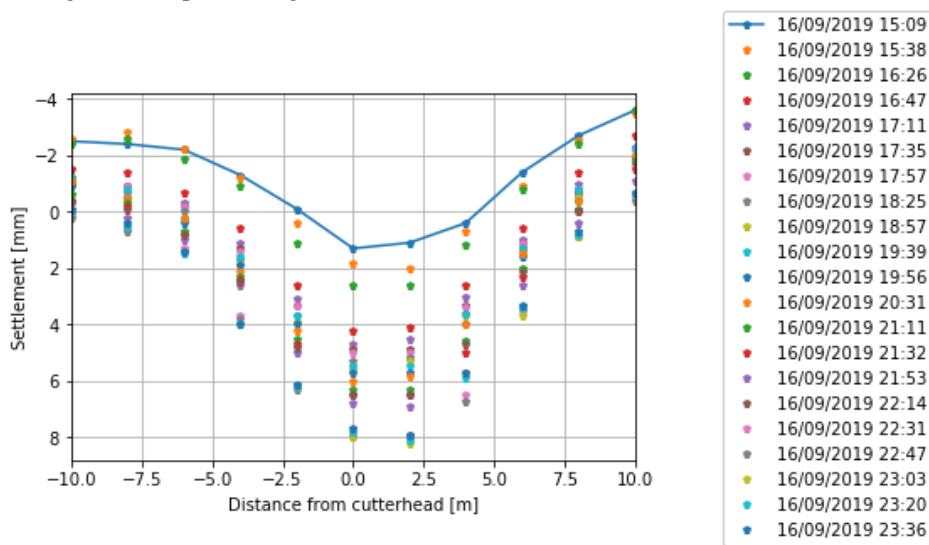


Figure 5.6: Settlements when the cutterhead of the TBM is at chainage 4115, in transversal direction

To analyse what the influence of the TBM is throughout a larger time span, the settlements in transversal direction are analysed prior and after the cutterhead is at chainage 4115. The results are presented in Figure 5.7.

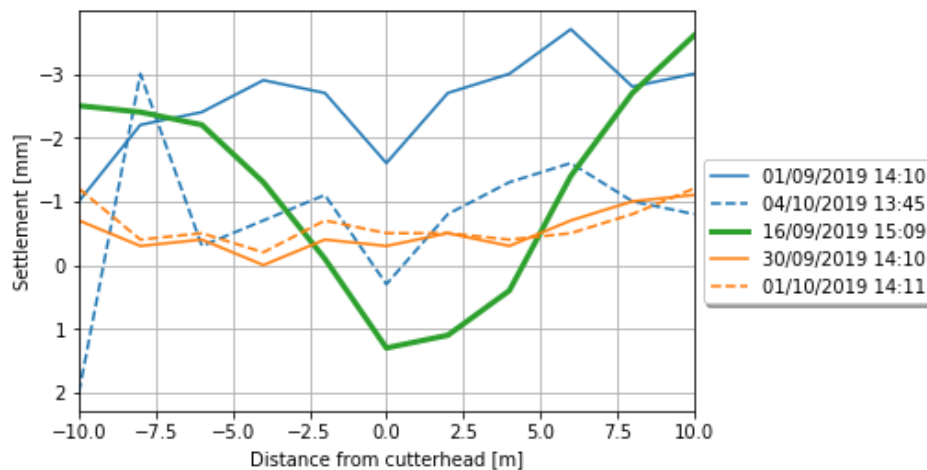


Figure 5.7: Settlements 2.5 weeks prior and after the cutterhead has past chainage 4115

5.1.2 Data trends

The measured settlement data shows multiple trends.

Figure 5.3 shows that at a standstill, there is an increase in settlements. This can be explained by the TBM sinking due to its high weight in the soft soil. The sinking of the TBM explains why the increase in displacements over time mainly occurs behind the cutterhead. This effect also works in front of the TBM, but damps out.

Various trends can be observed from the results presented in Figure 5.4. The settlement decreases behind the shield of the TBM, which can be explained by the soil being pushed up between 0 and 10 mm. in front of the TBM. This reduces the settlement for the rings that follow. It can also play a role that there has been a change in applied face pressure, tail void injection pressure and the soil profile. Also the steering of the TBM could be of influence, but this topic is left out of the scope of this research.

Figure 5.6 has the same set-up as Figure 5.3. Those two figures show comparable/similar trends during a standstill. From the transversal displacement curve in Figure 5.6, a trend as expected occurs. The shape of the settlement curve roughly meets the expected Gaussian settlement trough by Peck (1969) and Schmidt (1969), like in Figure 1.7. The lowest point of the settlement curve is not at $x = 0$ m. which can be caused by several things. First, the accuracy of the measurement equipment can be too low for the aim of this research. Second, it is possible the TBM did not go exactly under the measurement equipment. A third origin of the deviation could be the measurement equipment is not placed right above the trajectory of the TBM.

The fact heave is occurring can mean the soil is being pushed away, not only in longitudinal direction, but also in transversal direction.

It is assumed this means the TBM was between 0.0 m. and 2.5 m. off the planned trajectory, or the measurement equipment was not placed above the centre of the TBM trajectory.

5.2 Pore water pressure – Monitored Field Data

5.2.1 Data interpretation

To perform a reliable analysis of the monitored pore water pressure, the accuracy of the measurement device is determined. The measurement device used for measurement of the pore water pressure is the spade cell (§2.4). The accuracy is 0.9 kPa, 0.8 kPa, 0.9 kPa & 1.1 kPa respectively for measurement devices 1, 3, 5 & 7. The location of the spade cells are shown in Figure 5.8. Only the spade cells 1, 3, 5 & 7 are considered because they are placed above the centreline of the trajectory of the southern tube.

The accuracy is determined by analysing all measurements of a spade cell for a time period of 5 days (Appendix 10). 5 days are selected after the TBM has passed for at least 2.5 weeks. It is assumed the influence of the TBM passage is no longer of influence after this period of time. Both the 5 days and 2.5 week time periods are an assumption based on common sense. To analyse the presence of excess pore water pressure, a reference pore water pressure is determined. This is done by taking an average of all measurements for the same period of time (2.5 weeks) as for the accuracy. The reference pore water pressures measured by the spade cells are 49.37 kPa, 60.07 kPa, 68.51 kPa & 76.30 kPa for the spade cells 1, 3, 5 & 7 respectively.

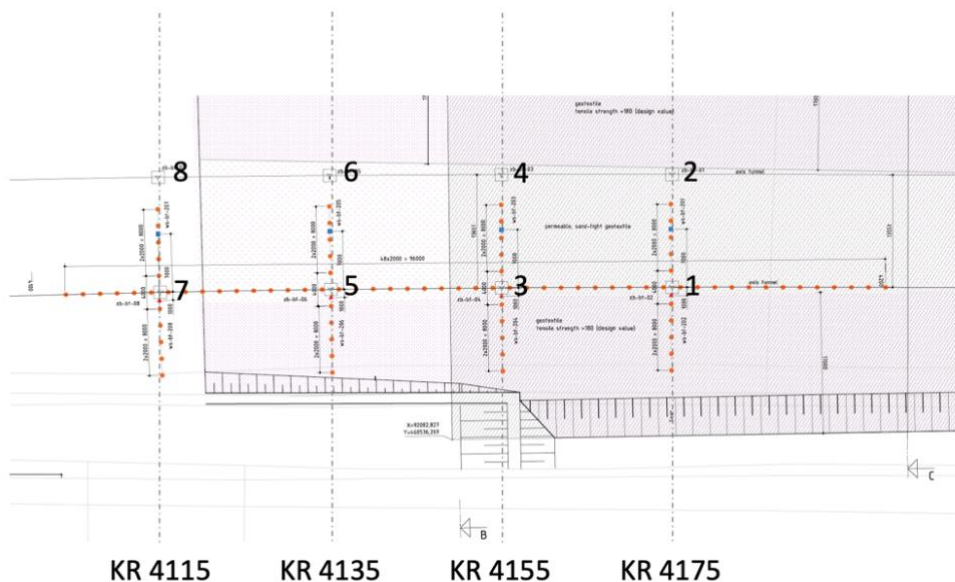


Figure 5.8: Overview of spade cells

If higher pore pressures are measured (relative to the prior mentioned reference values), excess pore water pressures are present. This is the result of the slurry infiltrating and transferring the face pressure onto the soil body/silo in front of the TBM. The groundwater flow generated by this process induces excess pore water pressures. It is of interest for this research to know if excess pore water pressure occurs because excess pore water pressures lead to a reduction in effectiveness of the face support medium/slurry and the face stability as a result of the excess pore pressure reducing the friction in the soil wedge in front of the cutterhead (in vertical direction) [4].

5.2.2 Data trends

Trends in the data are found in the form of a thrust wave. This means, when the TBM is approaching, a thrust wave of excess pore pressure is induced. The further away from the TBM, the lower the influence on the pore water pressure. When the TBM is at a standstill, the excess pore pressure has time to dissipate. Figure 5.9 to Figure 5.12 show pore water pressures against the time at 4 locations. The 4 locations are the location of the spade cells 1, 3, 5 and 7, which coincide with chainage 4175, 4155, 4135 and 4115 respectively. The spade cells are 20 m. apart from each other. For each figure three black lines represent the building of three consecutive rings. The second ring coincides with the location and chainage of the spade cell concerned.

Figure 5.9, around spade cell 1, shows that the influence in front of the TBM reduces over distance. The (excess) pore water peaks show up delayed at the spade cells 3, 5 and 7, but more flattened.

Spade cell 5 and 7, at a distance of 40 and 60 m. respectively from spade cell 1, show almost no excess pore pressures. Around spade cell 3, at 20 meters distance from spade cell 1, a significant amount of excess pore water pressure is shown. From this it can be concluded, the higher the advance rate of the TBM, the more the influence on the pore pressure increases. At an advance rate of 4 hours between two rings, the pore water pressure close to the TBM can rise around 20 kPa and around 10 kPa around 20 meters in front of the TBM (Figure 5.9). At a lower advance rate, as between the first and second ring in Figure 5.12 (10 hours between two rings) the pore pressure has enough time to dissipate.

Figure 5.11 gives a very clear view on the fact the excess pore pressure close to spade cell 1 and 3 reduces after the TBM has past. The reason Figure 5.12 shows little fluctuation in the curves is because the TBM has past the spade cells 1, 3 & 5.

To get a feeling for what the amount of excess pore pressure is, the maximum excess pore water pressure is determined for each spade cell:

$$\begin{aligned} & \textit{Maximum excess pore pressure spade cell} \\ & = \textit{Highest measured pore water pressure} - \textit{reference pore water pressure} \end{aligned}$$

$$\textit{Maximum excess pore pressure spade cell 1} = 75.42 - 49.37 = 26.05 \textit{ kPa}$$

$$\textit{Maximum excess pore pressure spade cell 3} = 81.80 - 60.07 = 21.73 \textit{ kPa}$$

$$\textit{Maximum excess pore pressure spade cell 5} = 98.46 - 68.51 = 29.95 \textit{ kPa}$$

$$\textit{Maximum excess pore pressure spade cell 7} = 94.77 - 76.30 = 18.47 \textit{ kPa}$$

To analyse those maximum excess pore pressures, the moments in time they occur are determined. When the moment in time is known via the data of the progress of TBM Gaia, the ring being built at that certain moment can be determined. For each ring the progress speed of the TBM is known. From relating this information to the maximum excess pore pressures, it can be concluded the maximum excess pore pressures relates to multiple components. Not only the advancement speed of the ring being built at that particular moment, but also the advance rate prior to that moment. Because of this, it is possible the peak of the excess pore pressure does not necessarily have to occur when the TBM is close to the spade cell. For example, the peak of spade cell 7 occurs at around the same time as the peak of spade cell 5. The peak of spade cell 7 occurs delayed due to the distance and time the thrust wave has to travel. By the time the cutterhead reached spade cell 7, a large part of the excess pore pressure dissipated. The peaks of spade cell 1 and 3 occurred just before the TBM reached both spade cells which matches the thrust wave theory mentioned at the start of this paragraph.

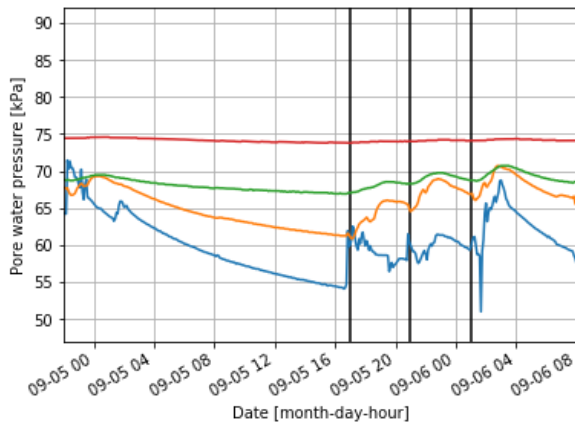


Figure 5.9: Second/middle ring at location of spade cell 1, chainage 4175

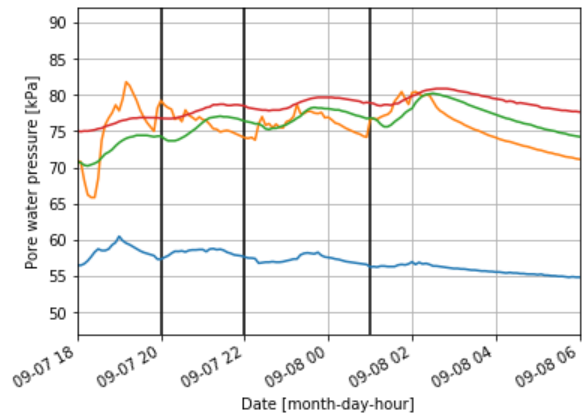


Figure 5.10: Second/middle ring at location of spade cell 3, chainage 4155

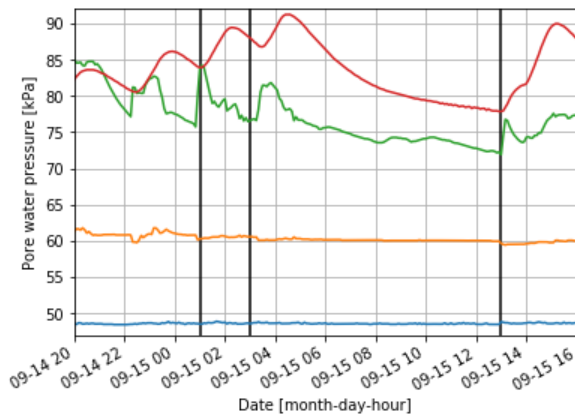


Figure 5.11: Second/middle ring at location of spade cell 5, chainage 4135

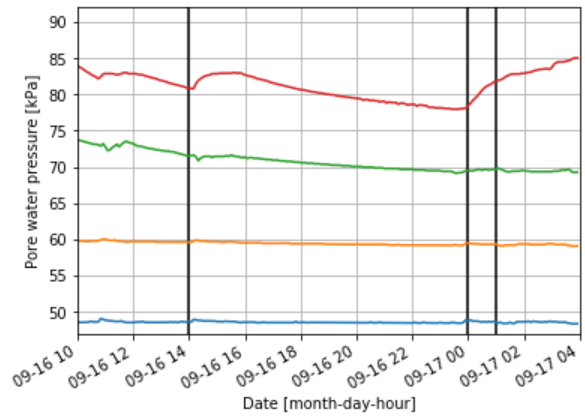


Figure 5.12: Second/middle ring at location of spade cell 7, chainage 4115

5.3 Face support pressure – Monitored TBM Data

5.3.1 Data interpretation

To interpret the applied face support pressures, TBM data provided by COMOL5 is used. The face support pressure is injected at four locations: 2 at the top of the TBM, 0.30 m. below the tunnel crown and 2 around the middle of the TBM, Figure 5.13.

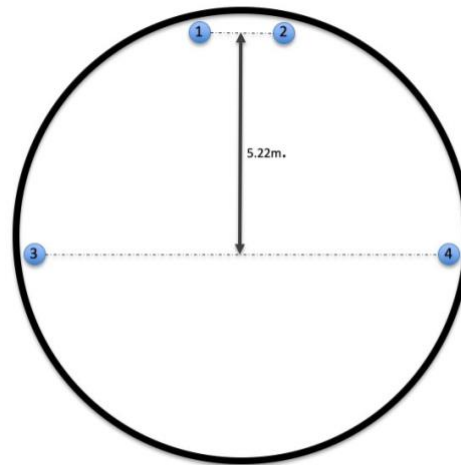


Figure 5.13: Schematic overview of face support pressure injection points

To determine the applied face pressure (fp) at the tunnel crown, the density of the slurry is required. The slurry density is determined by:

$$\text{Density slurry} = \frac{\frac{fp_{ip\ 3} + fp_{ip\ 4}}{2} - \frac{fp_{ip\ 1} + fp_{ip\ 2}}{2}}{\text{distance between injection points top and bottom}} = \frac{\frac{178\ kPa + 176\ kPa}{2} - \frac{121\ kPa + 118\ kPa}{2}}{5.23\ m} = 11.02\ kPa/m$$

With ip = injection point. The applied pressures which are used to determine the density of the slurry, are the pressures applied during the construction of ring 64.

The applied face support pressure at the tunnel crown is determined by:

$$\text{Applied face support pressure at tunnel crown} = \frac{fp_{ip\ 1} + fp_{ip\ 2}}{2} + 11.02\ kPa/m * 0.3\ m.$$

5.3.2 Data trends

Trends in the applied face support pressures are analysed for ring 3-103. The first 2 rings are not considered because they were built when the TBM was still in the start bell. Figure 5.14 shows the applied face support pressure for each ring and the cover of each ring. As expected the applied face support pressures show an increasing trend. This is expected because as the TBM is going deeper, the cover increases. An increasing cover roughly means an increase in total stress working on the tunnel face. (This could not be true if the soil profile varies a lot.) In the first part of the graph, the cover reduces. This is due to the fact the manmade overburden decreases faster than the TBM goes deeper into the ground. This means the general trends of the curves presented in Figure 5.14 confirm expectations.

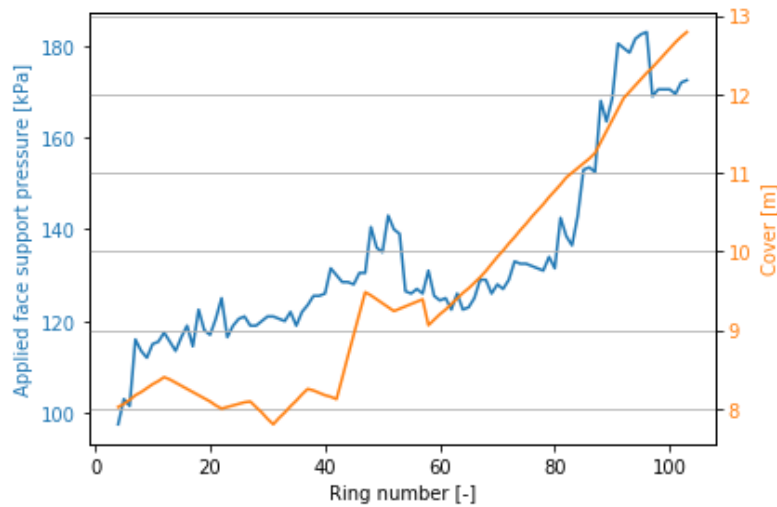


Figure 5.14: Applied face support pressures and covers for ring 3-103

5.4 Summary & Conclusions

From the field data analysis can be concluded the settlements and pore water pressure both show a thrust wave in front of the cutterhead. The settlement from the measurement field and the results of the spade cells validate this. This causes a decrease in settlement behind the cutterhead, being a positive thing.

From the spade cell measurement results it can be concluded that excess pore pressures are induced by the approaching and passing of a slurry TBM. The influence is dependent on the advance rate of the TBM. The influence of the TBM induces excess pore pressure between 20 and 40 meters in front of the TBM. When the advance rate is high, the excess pore pressure has less time to dissipate, which then can lead to a build-up of excess pore pressures in front of the face. The presence of excess pore pressure has a negative influence on the effectiveness of the face support pressure. This means a higher support pressure is required when excess pore water pressures occur. In order to determine how much more support pressure is required in such scenario, additional research will need to be conducted.

The applied face pressure behaviour coincides with the cover and in general does not show oddities.

The accuracy of all measurement devices is taken into account. The results of the settlement devices have an accuracy of 0.8 mm. The spade cells have an accuracy of around 1.0 kPa. The accuracy of the applied face pressure cannot be determined (within the time scope of this research).

Chapter 6

Case study

This chapter covers the case study. In the case study the three pillars are combined. Meaning this chapter elaborates on the results of the advanced numerical model, which will be compared with the field data and aims to find the relation between the advanced analytic face stability results with advanced numerical modelling results. For a more detailed outline of this chapter, please refer to §1.5.

NOTE: All mentioned relations result from the case study RijnlandRoute. It is not intended to suggest the results apply for all soft soil slurry TBM projects.

6.1 Relation between the advanced soil profile numerical model and the field data

The elaboration on the relation between the numerical model settlement prediction and the field data settlement results will mainly focus on the part of the trajectory around ring 65. The ring is built at KR4122, which means the cutterhead is at KR4113. Figure 6.1 shows the settlement curves of the rings 65, 67 and 69 and the face support pressure which is applied during the construction of ring 65. The two additional rings are elaborated on to broaden the area that is being analysed. Because the rings are close to each other, the soil profile as well as the cover on top of the tunnel do not vary much. As Figure 6.1 shows, behind the cutterhead the numerical prediction and field data settlement curves do match less compared to the curves in front of the cutterhead. They are not further elaborated on because this is not within the scope of this research. It is passively noted that they show similar trends up to the tail of the TBM, except for ring 65. Figure 6.2 shows similar curves as presented in Figure 6.1, however zoomed in on the settlements from the cutterhead to the front. In Figure 6.2, the measurement error of the settlement measurement devices of around 1.0 mm. is incorporated.

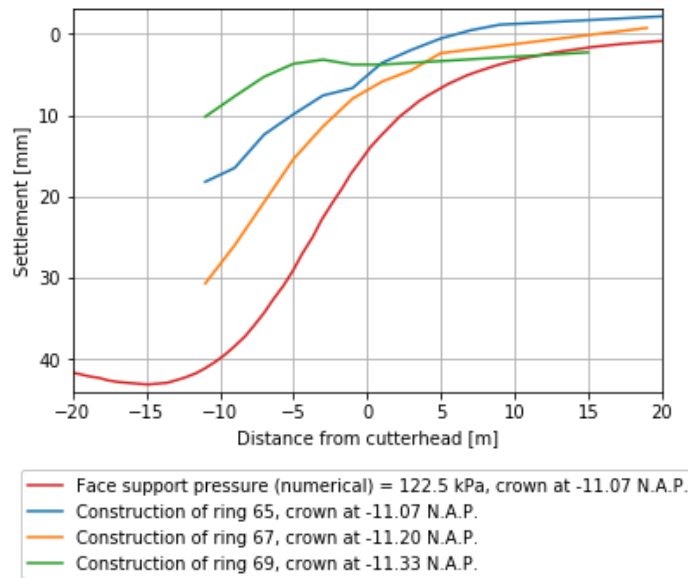


Figure 6.1: Settlement curves of ring 65, 67 and 69 and the settlement prediction by numerical modelling

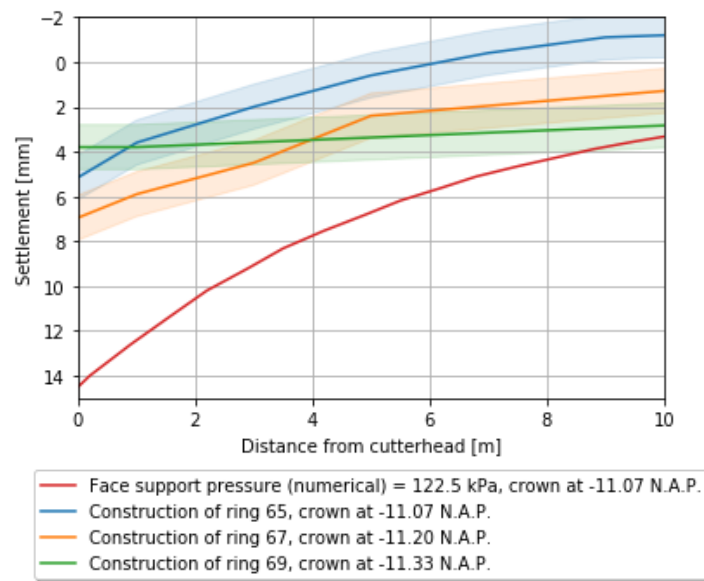


Figure 6.2: Settlement curves of ring 65, 67 and 69 including accuracy markers and settlement prediction by numerical modeling

Figure 6.2 shows quite a difference between settlements above the cutterhead, however the main focus lies in front of this the cutterhead. Since the research question is aimed to be able to find out the face stability during excavation, by use of settlement measurements ahead of the tunnel, Figure 6.3 zooms in further in front of the TBM. The difference between the numerical predicted settlement and the field data remains between 1 and 5 mm.

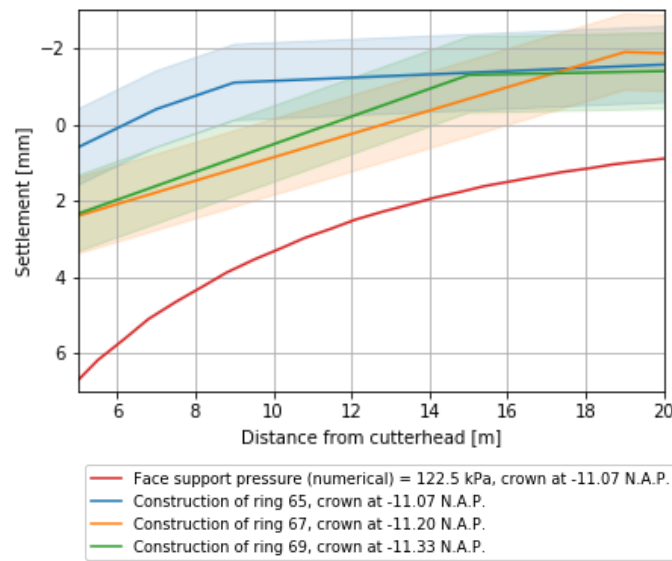


Figure 6.3: Settlements in front of the cutterhead

The fact that the field data results show less settlements, or even heave in front of the cutterhead, can be the result of the presence of excess pore water pressure. Figure 6.4 shows the (excess) pore water pressures measured at spade cell 7, at KR4115, and shows with vertical lines when the discussed rings have been built. During the construction of ring 65, the cutterhead was already 2 m. passed spade cell 7. Therefore it is likely the excess pore pressure is higher as presented in Figure 6.4. Similar reasoning accounts for ring 67 and 69. The influence of this excess pore pressure on the numerical modelling settlement prediction requires more research.

Another possible reason which induces the differences in predicted and measured settlements may have to do with the accuracy of the TBM data or inaccurate data interpretation by the subtraction of the measurements 1 week prior to the

moment of interest⁷. The method applied is following the methods of the project engineers of COMOL5. In a later phase of the research it was found out heave due to the approach of the TBM already occurs before 1 week prior to the passage. Which could be the reason why the amount of settlements is fewer for the field results in comparison with the numerical results. Hence it is recommend more research on when the heave is introduced ahead of the TBM in order to further increase accuracy.

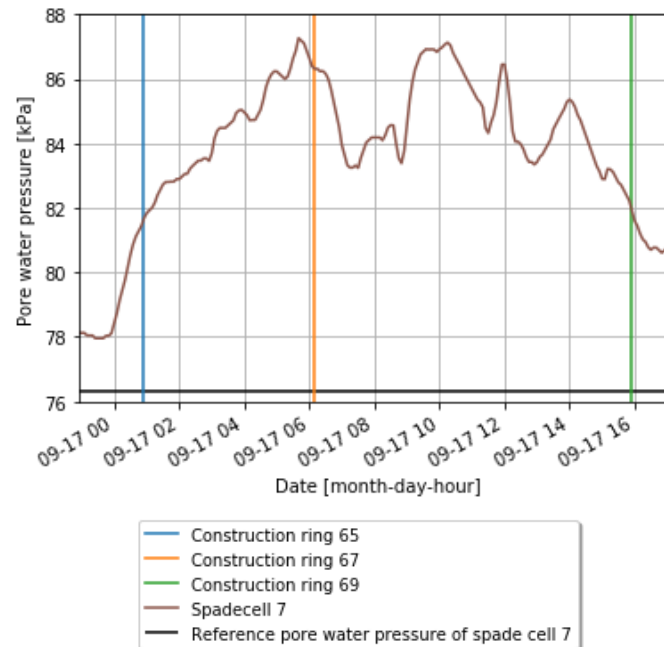


Figure 6.4: (Excess) Pore water pressure of the concerning rings noticed at spade cell 7, including the reference pore water pressure of spade cell 7 (at KR4115)

6.2 Relation between the advanced soil profile numerical model and the advanced soil profile analytic face stability

The comparison of the results of the numerical model and the results of the analytical calculation lead to a set of insights. Figure 6.5 presents the analytical limit face support pressures and a set of numerical face support pressures. The analytical limit pressures represent the limit pressures at the crown of the cutterhead. This accounts also for the numerical face support pressure. The results of the numerical face support pressures are extended by the settlements belonging to the applied face support pressures. Relations between the numerical and analytical method will mainly focus on the limit state face pressures.

⁷ The measurements from 1 week before are used to discard the influences on the settlements, other than the settlements induced by the TBM.

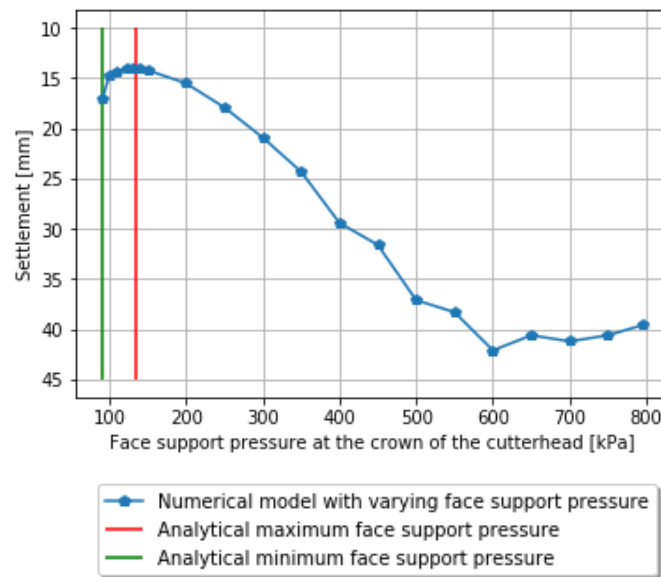


Figure 6.5: Settlements above the cutterhead vs. varying face support pressure at the crown including analytical face support pressure limits

6.2.1 Minimum face support pressure.

Figure 6.7 shows the minimum face support pressures are 91 kPa and 92 kPa for the numerical and analytical method respectively. This is of high accuracy, however the following points regarding inaccuracies must be taken into account:

- The result in Plaxis depends on the refinement of the mesh. The finer the mesh, the higher the minimum faces support pressure. Numerical models are built up from multiple elements. The composition of elements does not depend on the input of the model, such as structures and stratigraphy. An element provides a second-order interpolation of displacements. Each element contains the three local coordinates (ξ , η and ζ), as shown in Figure 6.6. Each of the nodes has three degrees of freedom, being in x, y and z direction. Each element contains 4 integration points, X (not the same x as from the coordinate system). When the boundary of the cutterhead (plate element in Plaxis) and soil are together in one element the integration point integrates their properties, leading to a distorted representation of amongst others the soil behaviour. This distorted soil behaviour leads to the soil being to be much stiffer and stronger than it would be in a non-numerical model. This behaviour leads to a lower face support pressure limit. This makes the result of the numerical minimum face support pressure lower than it is expected to be in reality. Which means the results is on the unsafe side.

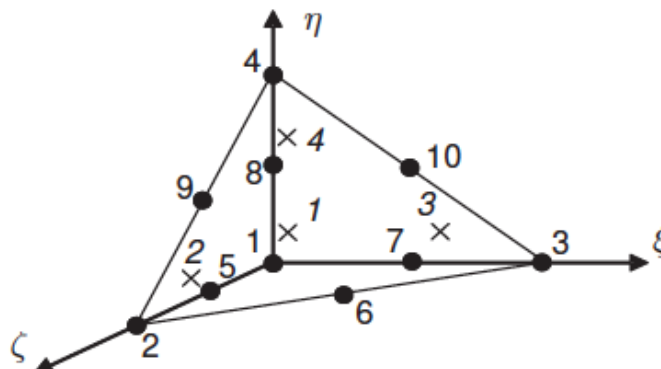


Figure 6.6: One element in a numerical model. Local numbering and positioning of nodes (•) and integration points (x) of a 10-node tetrahedral element [18]

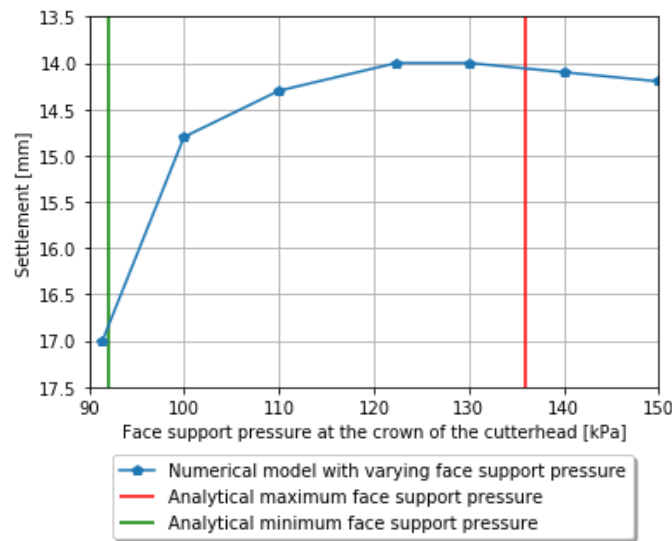


Figure 6.7: Settlements above the cutterhead vs. varying face support pressure at the crown including analytical face support pressure limits, zoom at low face support pressures

For both the analytical method as elaborated on in this research, meaning without safety factors, and the numerical method as elaborated on in this research, meaning a local refinement factor of the mesh of 0.125 and no tail void injection it holds that they are:

- On the unsafe side. The analytical method due to disregarding the safety factors and the numerical model due to its refinement which is not optimal.
- Both not considering the influence of tail void injection.

6.2.2 Maximum face support pressure

The maximum face support pressures of the numerical and analytical method differ greatly. The numerical maximum face support pressure is 792 kPa against 136 kPa for the analytical method.

The reason the numerically and analytically determined maximum face support pressures differ greatly is due the following reasons:

With a general approach the methods are 2D vs. 3D. The analytical methodology used in this case study is a commonly used method for soft soil slurry TBM projects. The method is based on a 2D column being pushed up, originating from the crown. The methodology does not coincide with the expected behaviour in the field but lies between two realistic approaches: blow-out and hydraulic fracturing. The used method is not as optimistic as a blow-out method, such as the Balhaus method, which has a global passive bursting failure mechanism, though not as conservative as a local active failure mechanism based on hydraulic fracturing. It is a simplified version of Balhaus.

On the other hand is Plaxis using a 3D approach, which has a passive global failure mechanism approach. This means the approach of determining the failure mechanisms of the analytical and numerical methods are completely different (in case of the maximum face support pressure). Due to the failure mechanisms discussed, it can be concluded the analytical approach suits better for the determination of the maximum face support pressure in case of a slurry TBM. Plaxis is more suitable for the determination of the maximum face support pressure in case of a EPB⁸ TBM, since the behaviour for the failure mechanism is similar to the soil behaviour in the field whilst using an EPB TBM.

Second, the maximum face support pressure of the analytical and the numerical method do not match because in the analytical method a vertical load from above is assumed. In the numerical method, which corresponds to the behaviour in the field, a horizontal load on a slice of ground in front of the TBM is assumed.

Observing the results presented in Figure 6.8, a set of mechanisms lead to relations and differences between the analytical and numerical approach. As elaborated on in this paragraph.

⁸ EPB = Earth pressure balanced. A TBM which uses the earth as counterbalance at the face of the TBM.

In Plaxis, from a face support pressure of 130 up to 600 kPa, a local active mechanism occurs. The soil in front of the tunnel face is being pushed forward, which leads to a settlement trough behind it. This does not coincide with the analytical global passive failure mechanism.

Heave is the result of a global passive mechanism, in both methods. The analytical method assumes a global passive mechanism is an expectable representation of hydraulic fracturing. Following this rationale, the assumption is made that the results of an analytical determination of the limit pressure should be comparable with the numerical method. This is however not the case, because the passive global failure mechanism in Plaxis comes back with way higher face support pressures compared to the analytical method.

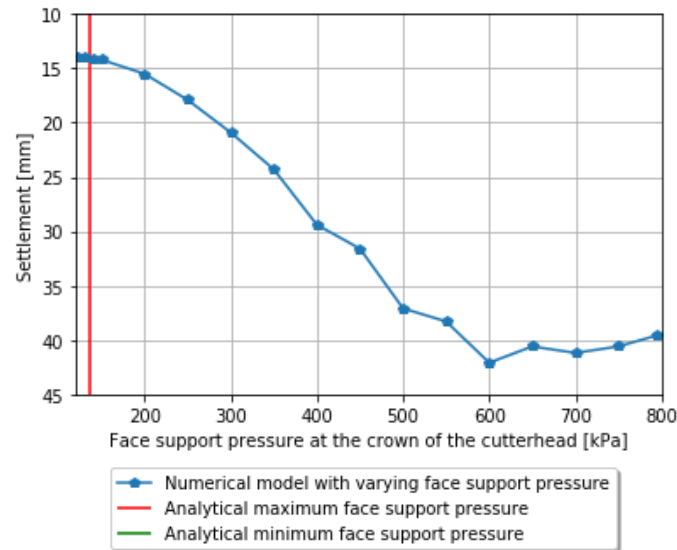


Figure 6.8: Settlements above the cutterhead vs. varying face support pressure at the crown including analytical face support pressure limits, zoom at high face support pressures

Chapter 7

Conclusions & Recommendations

This chapter covers the conclusions, the recommendations and answers the research question of this thesis. For a more detailed outline of this chapter, please refer to §1.5.

7.1 Conclusions

The main research question is whether it is possible to determine a relation between monitored settlements and the face stability of a slurry TBM by numerical modelling?

This cannot be answered with a simple yes or no, as the possibility to relate monitored settlement and the face stability of a slurry TBM by numerical modelling depends on whether the minimum or maximum face support pressure is considered.

For the **minimum face support pressure**, leading to a cave-in, the expected answer is **yes**. It is not a firm yes as, based on the data provided for this research, a relation is not found between the monitored settlements and the face stability by numerical modelling. This is simply because the TBM drive went very smoothly. No large face support pressure drops occurred, meaning: the minimum allowable face support pressure was not approached (neither numerically nor analytically).

The settlement profiles in front of the shield obtained from the monitored field data coincide with the trends and behaviour compared to the results obtained by numerical modelling. The input parameters of the numerical model, (nearly) correspond to the case study parameters: face support pressures, cover, soil profile and soil properties. The prediction of the amount of settlements as a result of the numerical modelling comes close to the monitored field data. However there is a discrepancy in the amount of settlements between the field data and the numerically predicted settlement curves. The difference in settlements is expected to originate from the presence of excess pore water pressures, inaccuracy of (measurement) equipment or human error in reading the provided data. Elaborating on the similar trends, it is possible the similarities in behaviour also accounts for lower applied face support pressures, close(r) to failure. Further research is required to find the answer to this. To be able to give a resounding yes to the research question with the help of further research and a focus on the minimum face support pressure, two paths can be followed:

One option is to gather more field data. The monitoring data must be gathered from a case study while the face stability is close to failure (cave-in). It is difficult to gain this data, because in practice contractors are not likely to lower the face support pressure to the minimum allowable face pressures because this increases the risk of a cave-in, which would mean a massive delay in construction time. To conclude if monitored settlements are a good, individual, method to determine the face stability of a slurry TBM, the answer is no in case solely consider project data and numerical modelling.

The second option is to incorporate physical modelling (centrifuge testing) into the research. By making a similar model with physical modelling, as is done in this research with numerical modelling, the results can be compared. If the results (and preferably the failure mechanism) coincide, for the range minimum face support pressure up to applied pressures from the case study, the liability of the results obtained by numerical modelling increases significantly.

Based on solely the numerical modelling results from this research, a practical cave-in warning number is found which can be used during construction. Based on the settlements curve for different face pressures, the TBM operator should get a warning a cave-in is approached at a slope of $m = -0.1$. The accuracy of this warning number can be increased by increasing the density of results of the settlement curve.

For the determination of the relation between monitored settlements and face stability by modelling when approaching the **maximum face support pressure**, leading to a blow-out or hydraulic fracturing, the answer is **no**. The maximum face support pressure found by numerical modelling is excessively higher than the analytically determined maximum face support pressure. The failure mechanism modelled by the two methods do not coincide. In numerical modelling a global failure mechanism occurs, a blow-out. In practice, hydraulic fracturing is more likely to occur in a soft soils slurry TBM project. Even though the analytical (DIN) method assumes a blow-out mechanism, the maximum face support limits do not coincide even slightly. The reason the results of the two methods are not comparable is amongst others the lacking ability of including the effect of hydraulic fracturing in the numerical model. Because it is not possible to model hydraulic fracturing, a realistic presentation of the on-site soil behaviour cannot be met. The behaviour as modelled in numerical modelling suits more projects performed by EPB TBM's, instead of slurry TBM's. From this can be concluded it is not possible to use numerical modelling in soft soil slurry TBM projects with the current state of the technological abilities of numerical modeling in Plaxis 3D.

Note: The above conclusions accounts for this specific case study with soft soils and a slurry TBM using the DIN analytical calculation method and Plaxis 3D software.

The answers to the sub-questions are listed below:

Is it possible to determine the relation between settlements and the face stability of a slurry TBM in an analytical way?

It is not possible to determine a relation between settlements and the face stability of a slurry TBM in an analytical way, as this does not take into account settlements.

Is it possible to determine the relation between settlements and the face stability of a slurry TBM by numerical modelling?

With support of the sub-research question answered below, it can be concluded that a relation between settlements and face stability can be determined by numerical modelling. When the minimum face support pressure is approached, there is an increase in settlements. When the face support pressure becomes below the minimum face support pressure, an active global failure mechanism occurs. When the face support pressure increases, originating from an ideal face support pressure, two trends are found. At first an increase in settlements occurs. These settlements arise as a result from a local active mechanism. As soon as the settlement increment switches to a decrease in settlement a global passive mechanism is activated, with as final result the reach of the maximum face support pressure. From this it can be concluded that the relation between settlements and face stability of a slurry TBM by numerical modelling can be determined. This can be done by performing a set of numerical models with a wide range of face support pressures and displaying the relating settlements above the cutterhead. The relation between the two is mainly useful for the face support pressures close to the minimum pressure limit, because this matches the behaviour of field data. The trends at high face support pressures do not coincide with the hypothesis as represented in Figure 1.13. This is due to the difference in soil behaviour between numerical modelling and behaviour of the soil in the field.

- ***What are appropriate boundary conditions to set up this specific model?***

The used dimensions for this research are a depth, $z \approx 1.5 \cdot \text{diameter of the tunnel (D)}$ below the tunnel invert, a width, $x \approx 6.5 \cdot D$ and a length, $y \approx 4.5 \cdot \text{length of the tunnel (L)}$. This results in the dimensions: $(x,y,z) = (-70, 200, -36)$. Elaborating on the results which show the area at which settlements are induced as a result of the minimum face support pressure applied are: $x = 0.7 \cdot D$, $y = 1.2 \cdot L$ and in case of the maximum face support pressure: $x = 2.3 \cdot D$, $y = 1.5 \cdot L$. This does not mean the boundaries should set to those dimensions. In fact that would have a negative influence on the results. Vertical model boundaries with their normal in x-direction are fixed in x-direction ($u_x=0$) and vertical model boundaries with their normal in y-direction are fixed in y direction ($u_y=0$). Even though the majority of the settlements are in z-direction, the fixities at the boundaries can influence the settlement behaviour. Therefore appropriate boundary conditions for this specific model could be set to $x = 2.5 \cdot D$, $y = 1.7 \cdot L$, hereby it is assumed 20% of D and L is a sufficient distance away from the boundary.

- **What are the influences of the soil profile parameters on the stability of the face of the TBM and the settlements?**

The influence of the soil profile parameters within the range of the low and high average characteristic values of the geotechnical parameter set is negligible. The fact that a variability in the soil parameters is of little influence is a pro. It means a little inaccuracy in the soil parameters is not changing the outcome of the numerical model significantly. Hereby the influence of the soil parameters within their characterised limits are of negligible influence on the stability of the face of the TBM and the settlements. It is of high importance to have an accurate soil profile.

- **Does the mortar pressure of the tail void injection influence the face stability/or settlements in front of the cutterhead?**

Yes, however the behaviour is not as predicted in the hypothesis. The tail void injection is of noteworthy influence up to 11 meter in front of the cutterhead of the TBM. Further away the influence is very little (+-1 mm.). When comparing values this little (+-1 mm.) with measurement results from the field, the inaccuracy of equipment should be taken into consideration. Instead of the expected active failure for a low mortar pressure at the tail void and a passive failure for a high mortar pressure, all values considered show active failure (settlement). It is possible that, alike the face support pressure, the expected passive failure behaviour occurs at much higher pressures in the numerical model. A change in mortar pressure within a reasonable range does neither change the amount of settlements at the cutterhead nor in front of it.

- **Does the taper of the TBM influence settlements (in front of the cutterhead)?**

Yes. In the hypothesis was expected that the zone of influence would be 0.5 times the diameter from the tail towards the back and to the front. Figure 7.1 shows this hypothesis is an underestimation. The zone of influence is almost 40 meters originating from the tail void. This means a zone of influence of 31 meters in front of the cutterhead. At the cutterhead the influence of the contraction is almost 5.0 mm. From 10 meters in front of the cutterhead and onwards, the influence is negligible. Because of the significant influence at the cutterhead, the plate contraction is not left out of the numerical model. Note: this conclusion has a specific application on the case study of this research.

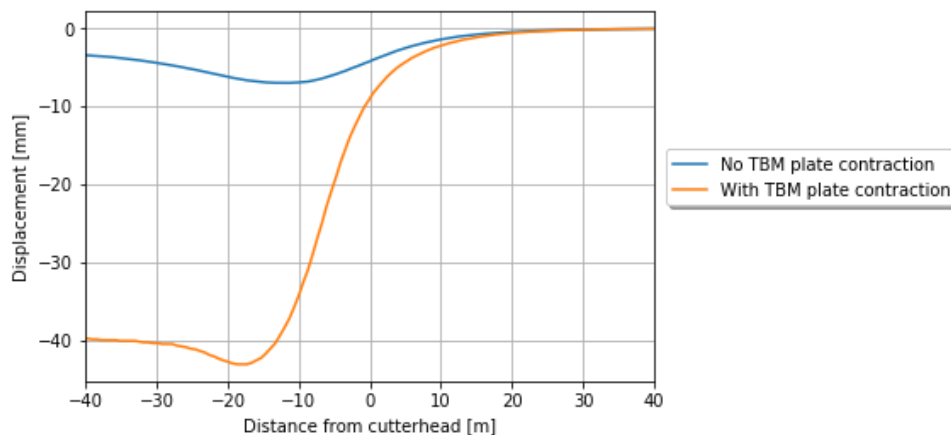


Figure 7.1: Settlements as a result of an active on inactive plate contraction representing the taper of the TBM

Can trends be found in the relation between applied face support pressures and measured settlements?

Following the answers as presented in the four sub-questions below it can be concluded a relation between measured settlements and applied face stability can be determined. This is however only for a specific part in the range of applied face support pressures which are not present in the data gathered from the case study as elaborated on in this research.

- **Do the measured settlements show trends?**

As expected the settlements show trends. The settlement curves in lateral direction show the shape of an Gaussian settlement trough, as expected. The fact heave is occurring which can mean the soil is being pushed away, not only in longitudinal direction, but also in transversal direction.

In longitudinal direction, as expected half a Gaussian settlement trough occurs. This only accounts for the tail void/end of the shield up to in front of the TBM. Behind the tail void, an increase in settlements occurs. The origin of the increase in settlements is not further investigated, because this is out of the scope of the research.

The measured settlements show the trend that at a standstill, an increase in settlement occurs. This is due to the high weight of the TBM in combination with the soft soil. This effect occurs mainly at the shield of the TBM, but also progresses to the front of the TBM. This does however damp out over distance.

Another trend is showing the TBM is pushing soil in front the TBM up by 0 to 10 mm. (in the investigated area of the case study). This leads to a reduction of the total settlements.

- ***Do the measured pore water pressures show trends?***

As expected in the hypothesis, indeed the results of the measured pore water pressures show trends. The trends show that excess pore water pressures are induced when the TBM is approaching and passing by. In the case study the zone of influence of the thrust wave in front of the cutterhead is up to 20 to 40 meters. Going forward from the cutterhead, the influence damps out.

A time related display of the results shows a reduction of excess pore pressure when the TBM is at a standstill or has a low advance rate. This is when the excess pore pressure has time to dissipate.

- ***Do the applied face support pressures show trends?***

The face support pressure shows an increasing trend over the progress of the TBM. This is expected because the depth of the TBM increases, meaning an increase in cover. In general an increasing cover means an increase in total stress working on the tunnel face.

In the first part of the TBM drive the cover reduces due to the manmade overburden. The overburden decreases faster than the TBM goes deeper into the ground. This gives a short, flattening of the applied face pressure curve.

- ***Can trends be found in the relation between applied face support pressure and measured settlements with support of numerical modelling?***

It is expected trends can be found in the relation applied face support pressure and measured settlements with support of numerical modelling for low face support pressures. This is due to the fact that the behaviour of high face support pressures in numerical modelling do not coincide with the soil behaviour in the field. As mentioned this is an expected trend, this could not be determined during this research. During the construction of the case study project: RijnlandRoute, face support pressures close to the minimum face support pressure have not been applied. Due to this, the predicted settlement behaviour of the numerical modelling could not be compared with matching situations from the field. The overall behaviour of the applied face support pressure settlement curves show a similar trend in behaviour compared to the numerical results when looking at the settlements from the tail to in front of the TBM. However with fewer settlements and sometimes heave. The reduction in settlements is expected to find its origin from the presence of excess pore water pressures, inaccuracy of (measurement) equipment or human error in the interpretation of the provided data.

7.2 Recommendations

This research has led to new insights, which, lead to recommendations for further research. The recommendations based on this research are:

- In the numerical model, further elaborate on the local mesh refinement factor while applying a limit state face support pressure. The goal is to gather more information about what level of local refinement is required for any specific case of interest.
- Gather field data with (approaching) limit states to study if the trends found by numerical modelling also occur in the field. If it is not possible to capture field data of this kind, similar behaviour could be simulated by performing a centrifuge test.
- If such research (with face support pressures close to the minimum face support pressure) is to be performed, it is recommended to normalise the results. Normalisation of the settlements can be done by describing the settlements as volume loss, and by relating face support pressures to the thickness of the cover. Note that results can only be used for projects in similar soil profiles with similar soil and hydraulic properties. Therefore it is recommended to perform this for projects at locations where the density of tunnelling projects is high.
- Excess pore pressures are prominent in the field data results. Since the trends of the settlement curves, numerical and field, coincide, but their amount of settlement do not, two recommendations are done regarding this topic:
 - o It is recommended to focus on the (excess) pore water behaviour in the numerical model to gain a better insight on its influence within numerical modelling soft soil slurry shield tunnelling projects;
 - o Determination of what the influence is of the excess pore pressures on the amount of settlements/heave occurring in front of the TBM is recommended. Not only could it lead to insight in if this is the cause of the difference in settlements as reported in this research, it could also lead to more insight on what the influence is of the excess pore water pressure on the face stability during a soft soil slurry TBM project.
- For further research it is recommended to match the geostatic pressure at the tunnel invert for calculation purposes. The reason settlements occur with slurry shield tunnelling is because it is very hard to meet the exact surrounding geostatic earth pressure. The reason this geostatic earth pressure cannot be met over the entire TBM face is because of the gradient of the face support slurry [14]. The gradient depends on the volumetric weight of support slurry. This gradient is linear, where the gradient of the soil is not (due to its heterogeneity). Mooney et al., 2016 investigated for which point the geostatic pressure must be met (invert, springline or tunnel crown) to minimize the amount of settlements. This turned out to be at the invert. This should be considered when interpreting the data from the TBM. This knowledge was only found after performing the calculations, but is worth mentioning as a recommendation for further research.
- The interpretation of data while providing for the comparison between numerical results and field data, it is recommended to first perform more elaborated research on when the heave is introduced ahead of the TBM in order to further increase accuracy of the comparison of the data.
- It is recommended to perform a similar research for the case study of the Rotterdamsebaan building on the conclusions and recommendations stemming from this research. The results of another case study could further validate the results of this research. If this validation occurs, a normalisation and guideline could be developed.

Bibliography

- [1] P.B. Attewell., J. Yeates, and A.R. Selby. *Soil Movements Induced by Tunnelling and their Effects on Pipelines and Structures*. Blackie, Glasgow, 1986.
- [2] T. Benz. *Small-strain Stiffness of Soils and Its Numerical Consequences*. Stuttgart, Germany: Inst. für Geotechnik, 2007.
- [3] A. Bezuijen, J.P. Puijksma, H.H. van Meerten. Pore pressures in front of tunnel, measurements, calculations and consequences for stability of tunnel face. In Adachi, T.K., 2001.
- [4] W. Broere. *Tunnel Face Stability & New CPT Applications*. PhD thesis, Delft University of Technology, 2001.
- [5] Internal documents provided by COMOL5 .
- [6] Z. Zizka and M. Thewes (Ruhr-University Bochum), *Recommendations for Face Support Pressure Calculations for Shield Tunnelling in Soft Ground*. Published by Deutscher Ausschuss für unterirdisches Bauen e.V. (DAUB) German Tunnelling Committee (ITA-AITES). Version 10/2016.
- [7] V. Fargnoli, D. Boldini & A. Amorosi. TBM tunnelling-induced settlements in coarse-grained soils: The case of the new Milan underground line 5. *Tunnelling and Underground Space Technology*, 38:336–347, 2013.
- [8] Geotechdata.info. 2013.
- [9] F.J. Kaalberg, J.A.T. Ruijgrok & R. De Nijs. TBM face stability & excess pore pressures in close proximity of piled bridge foundations controlled with 3D FEM. In *Proceedings of the 8th international symposium on geotechnical aspects of underground construction in soft ground*, pages 55-560. London, UK: Taylor & Francis., 2014.
- [10] J. Küpferle, Z. Zizka, B. Schoesser, A. Röttger, M. Alber, M. Thewes & W. Theisen. Influence of the slurry-stabilized tunnel face on shield TBM tool wear regarding the soil mechanical changes – Experimental evidence of changes in the tribological system. *Tunnelling and Underground Space Technology*, 74:206–216, 2018.
- [11] C.J. Lantinga. *Comparison of static and transient face stability*. Master's thesis, Delft University of Technology, 2018.
- [12] C. Lee, K. Chiang & C. Kuo. Ground movement and tunnel stability when tunneling in sandy ground. *Journal of the Chinese Institute of Engineers*, 27(7):1021–1032, 2004.
- [13] S. Möller. *Tunnel induced settlements and structural forces in linings*. PhD thesis, Universität Stuttgart, 2006.
- [14] M.A. Mooney, J. Grasmick, B. Kenneally & Y. Fang. The role of slurry TBM parameters on ground displacement: Field results and computational modelling. *Tunnelling and Underground Space Technology*, 57:257–264, 2016.
- [15] H. Mortier, B. Peerdeman & A. van der Put. Boren tussen de A4 en de A44. *CEMENT*, 5(5):2–3, 2017.
- [16] E. Ortiz-Ospina, M. Roser & H. Ritchie. *World Population Growth*. (2019, may 1st).
- [17] R.B. Peck. Deep excavations and tunnelling in soft ground. In *7th int. Conference Soil Mechanics and Foundation Engineering*, pages 225-290. Sociedad Mexican de Mecanica de Suelos, A.C., 1969.
- [18] Plaxis 3D-4 Scientific manual
- [19] D.M. Potts. Numerical analysis: A virtual dream or practical reality? *Géotechnique*, 53(6):535–573, 2003.

- [20] B. Ring & M. Comulada. Practical numerical simulation of the effect of TBM process pressures on soil displacements through 3D shift iteration. *Underground Space*, 3(4):297–309, 2018.
- [21] B. Schmidt. *Settlements and ground movements associated with tunnelling in soils*. PhD Thesis, University of Illinois, Urbana, 1969.
- [22] Soil Instruments. *Vibrating Wire Push-In Pressure Cell - Soil Instruments*. 2019.
- [23] M.N. Vu, W. Broere & J. Bosch. Structural Analysis for Shallow Tunnels in Soft Soils. *International Journal of Geomechanics*, 17(8), 2017.
- [24] tunnel.ita-aites.org. *Slurry Shield - About Tunnelling - ITA-AITES*. Retrieved in 2019.

Appendix

Appendix 1: Construction of the TBM to reach steady state situation

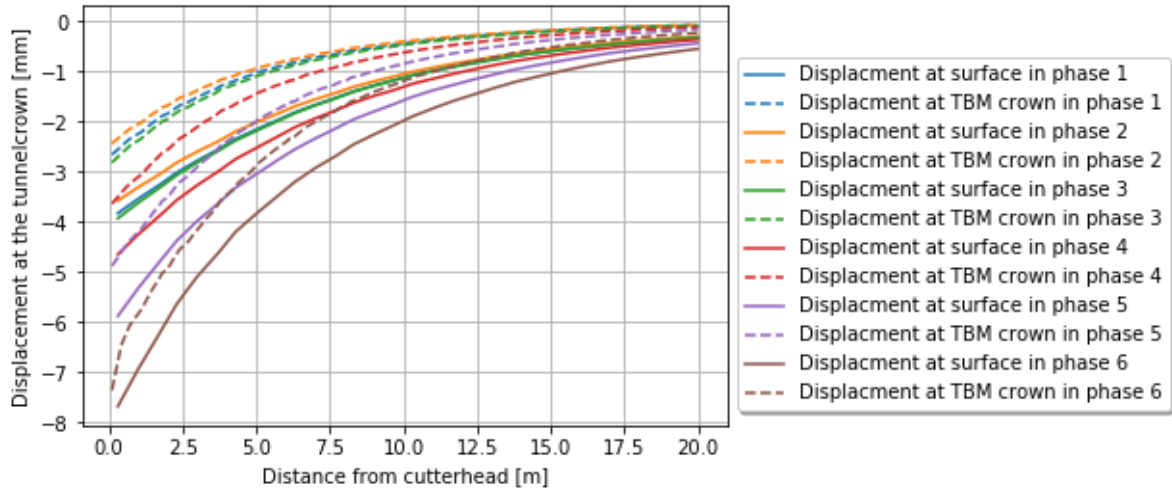


Figure A1.1: Displacements per phase of 1 model

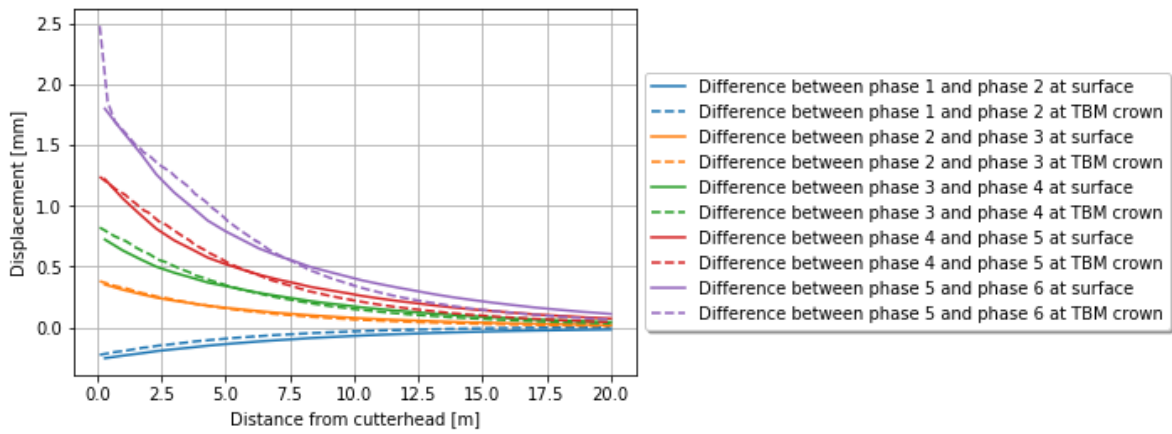
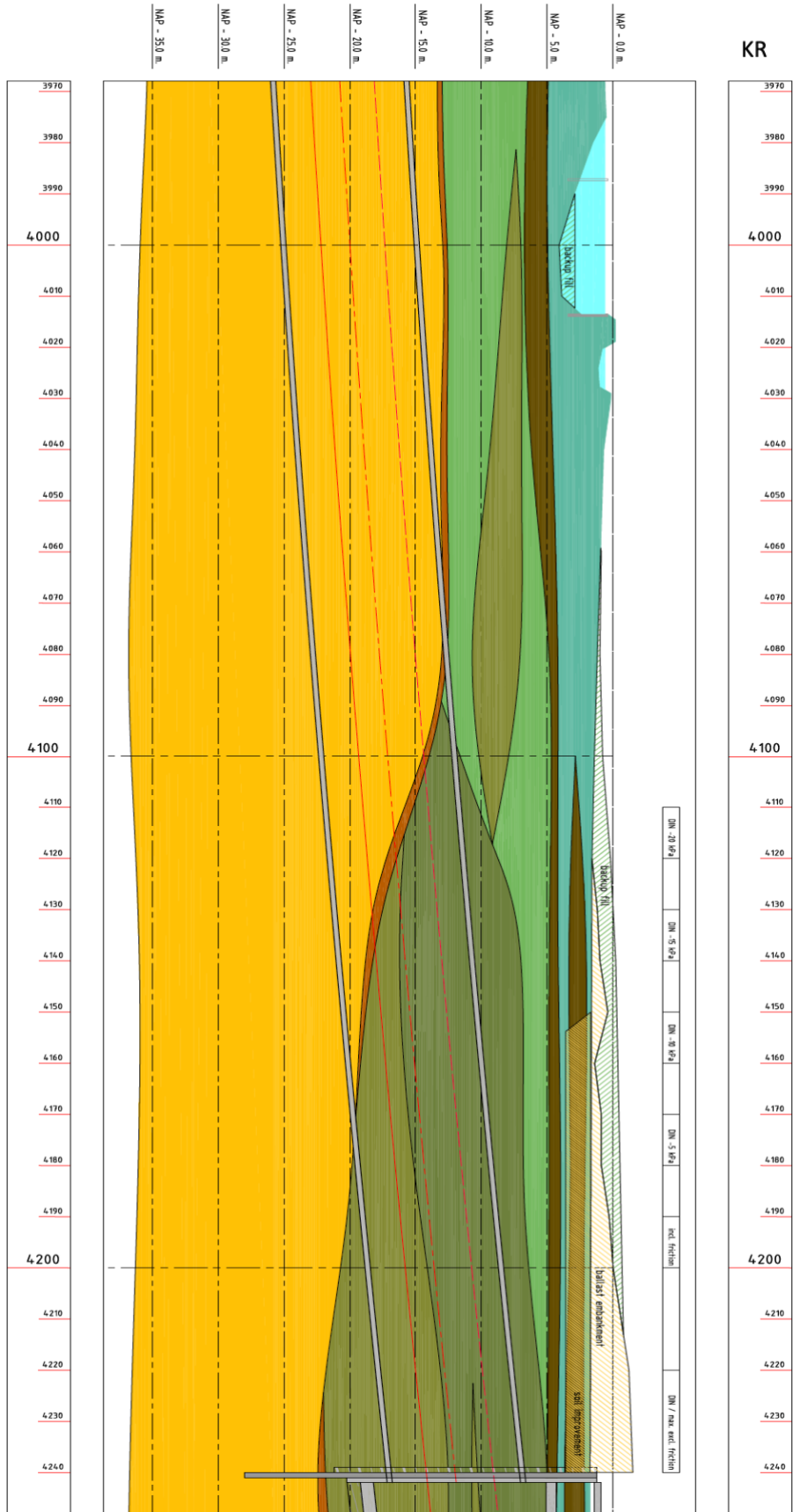


Figure A1.2: Displacements at two different face support pressures

Appendix 3: Soil profile at the eastern entrance [5]



Appendix 4: Reference pressure and small strain and K0 parameters

Layer	$\gamma_{0.7}$	G_{0ref}	p_{ref} [kPa]	OCR	POP
2A – Clay	$0.45 \cdot 10^{-3}$	$19.62 \cdot 10^3$	100.0	1.000	9.000
3 – Peat	$0.45 \cdot 10^{-3}$	$12.00 \cdot 10^3$	100.0	1.000	9.000
4C – Clay	$0.45 \cdot 10^{-3}$	$34.62 \cdot 10^3$	100.0	1.000	9.000
4D – Sand	$0.15 \cdot 10^{-3}$	$64.10 \cdot 10^3$	100.0	1.000	0.000
5 – Peat	$0.45 \cdot 10^{-3}$	$15.00 \cdot 10^3$	100.0	1.000	0.000
6 – Sand	$0.15 \cdot 10^{-3}$	$195.50 \cdot 10^3$	100.0	1.000	0.000

Appendix 5

Because there are multiple ways to determine the HS small strain parameters the method used is compared with a second method by Hardin & Black:

$$G_0^{ref} [MPa] = 33 * \frac{(2.97 - e)^2}{1 + e}$$

In this formula e is the void ratio [2].

Table A5.1 shows the different values for G_0 determined in by Hardin & Black and by the CIE4361 lecture slides. In the second column are the values, applied on the set of models elaborated in the rest of this chapter. The third column shows the multiplier value in case the CIE4361 value is modified to get a similar G_0 values as Hardin & Black gives. Due to the fact this multiplier value cannot reach below 1.0 as input in Plaxis a fourth column is added which results in a third value for G_0 . The outcome of the settlements when using Hardin & Black are compared with the ones when using the CIE4361 lecture slides. The results are shown in Figure A5.1 and Table A5.2. These show that at the locations which are of main interest for this research ($x=0$, $x=5$ and $x=10$) the difference is negligible in front of the face. At the face a difference of 0.2 mm. could be of significance later in the research and is kept in mind to calibrate the model later in the research. The values of the fourth lie between those values, due to the small differences no further investigation is done at this point in the research with respect to the small strain parameters.

Table A5.1: Estimation small strain parameters

	Hardin & Black		CIE4361 lecture slides		CIE4361 lecture slides after calibration with Hardin & Black		Plaxis input	
	Sand	Clay	Sand	Clay	Sand	Clay	Sand	Clay
$G_{0ref} = x * G_{ur}$ $x =$	-	-	1.5	9.0	0.9	10.4	1.0	10.4
G_{0ref} [kN/m ²]	11.60*10 ⁴	4.00*10 ⁴	19.55*10 ⁴	3.46*10 ⁴	11.60*10 ⁴	4.00*10 ⁴	13.04*10 ⁴	4.00*10 ⁴

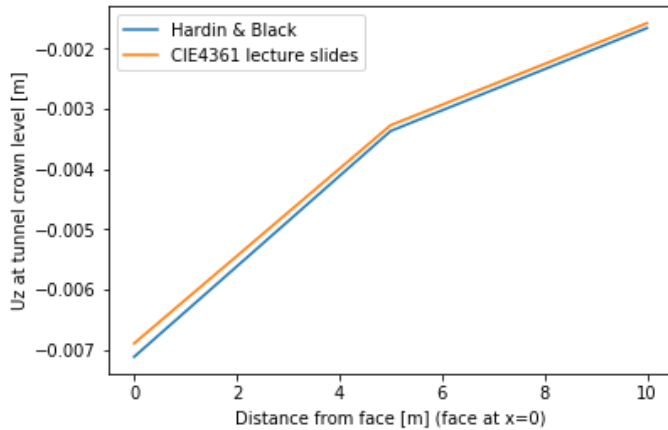


Figure A5.1: Displacement, U_z with varying Small Strain parameters

Table A5.2: Relative displacements of two different Small Strain parameters

Distance from face [m] Face at $x = 0$	ΔU_z , Hardin & Black – CIE4361 lecture slides [m]
0	-0.000222
5	-0.000096
10	-0.000081

Table A5.3: Input model set 1

Material set	Clay layer	Sand layer	unit
Identification	4C – Clay	6B - Sand	
Material model	HS small	HS small	
Drainage type	Undrained (A)	Drained	
General properties			
Top of layer	-1.6	-6.0	m. N.A.P.
γ_{unsat}	16.4	19.3	kN/m ³
γ_{sat}	16.4	19.9	kN/m ³
Advanced			
ϵ_{init}	1.3	0.6	-
Stiffness			
$E_{50\text{ref}}$	$2.6 * 10^3$	$76 * 10^3$	kN/m ²
E_{oedref}	$1.3 * 10^3$	$76 * 10^3$	kN/m ²⁸
E_{urref}	$9.0 * 10^3$	$305 * 10^3$	kN/m ²
Power (m)	0.80	0.55	-
Strength			
c'_{ref}	10.0	0.0	kN/m ²
Phi	22.5	36.5	°
Psi'	0.0	6.5	°
Small strain			
$\gamma_{0.7}$	$0.45 * 10^{-3}$	$0.15 * 10^{-3}$	-
$G_{0\text{ref}}$	$36.6 * 10^3$	$195.5 * 10^3$	kN/m ²
Advanced			
v'_{ur}	0.17	0.17	-
p_{ref}	100.0	100.0	kN/m ²
K_0 settings			
OCR	1.0	1.0	-
POP	9.0	0.0	kN/m ²

Appendix 6: Local refinement of the numerical model mesh

Figure 1 shows the meshes for increasing local refinement factors. On the left the mesh before excavation and on the right the displacement after excavation is presented. The failure plane (right hand side of the picture) visibly changes by increasing at a higher refinement factor.

Table shows the model properties in relation to the mesh. It also includes the displacement above and in front of the cutterhead. And the relative differences between the three levels of local refinement factors. The calculation time of the model did not increase significantly which made the choice to locally refine the mesh by the factor 0.125. The displacement at the face did not change much, but is only logical because the face support pressure was not near to a limit state.

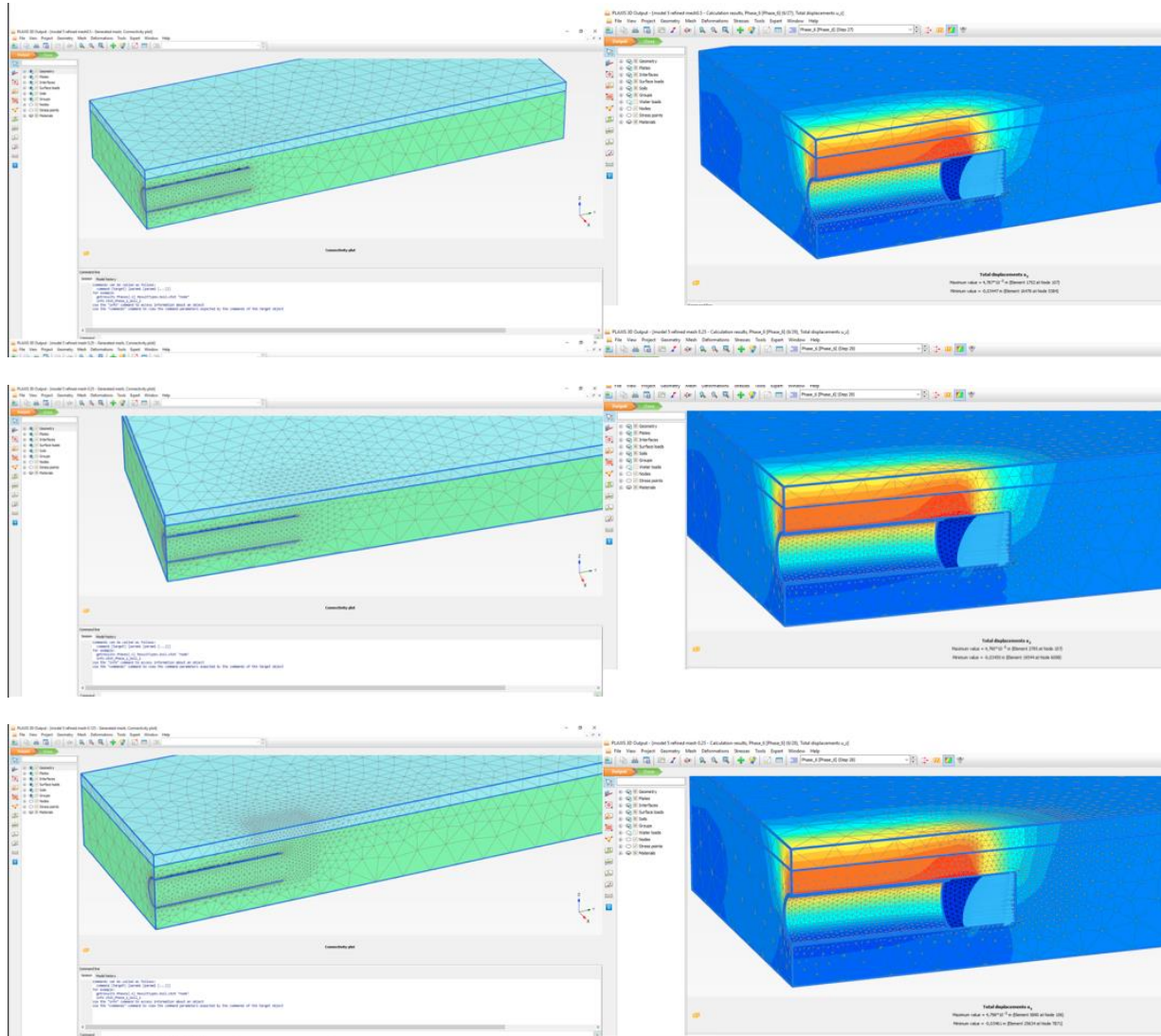


Figure A6.1: Local mesh refinement factor: Top: 0.5, middle: 0.25, bottom: 0.125

Table A6.1: Local mesh refinement model details

Mesh refinement at The cutterhead and ahead	0.5	0.25	0.125	Relative difference between local mesh refinements	
				0.5-0.25	0.25-0.125
Number of elements	20257	23649	32458	3392	8809
Number of nodes	33536	38593	51445	5057	12852
Settlements above the cutterhead [m]	-0.0083	-0.0082	-0.0081	$8.1939 * 10^{-5}$	$8.6223 * 10^{-5}$
Displacement at the crown of the cutterhead [m]	-0.0080	-0.0078	-0.0078	$1.0 * 10^{-4}$	$7.2107 * 10^{-5}$
Settlements ahead of the cutterhead [m]	-0.0038	-0.0039	-0.0038	$8.1826 * 10^{-5}$	$7.6468 * 10^{-5}$

Appendix 7: Failure mechanisms of the numerical modelling analysis

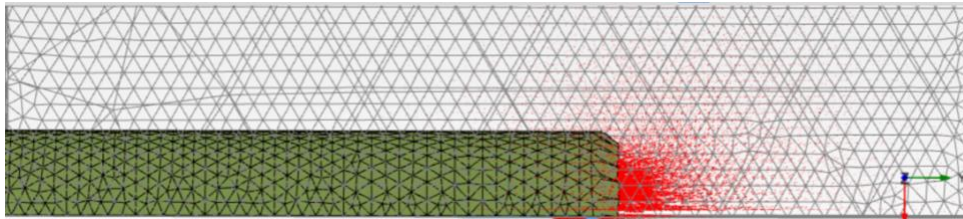


Figure A7.1: Top view on soil failure mechanism at the numerical lower face support pressure limit. Phase displacement, P_u

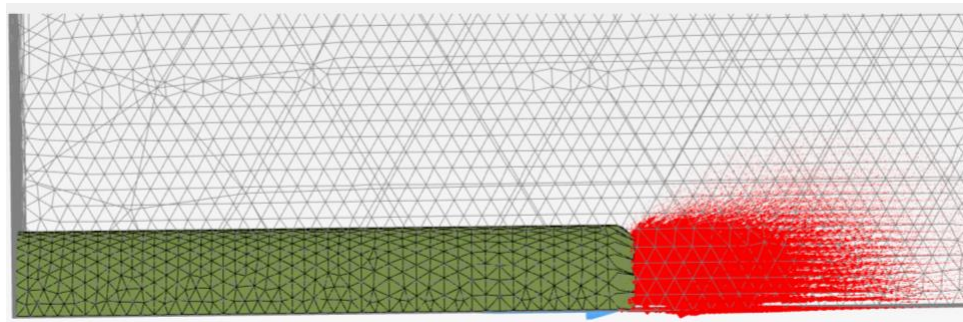
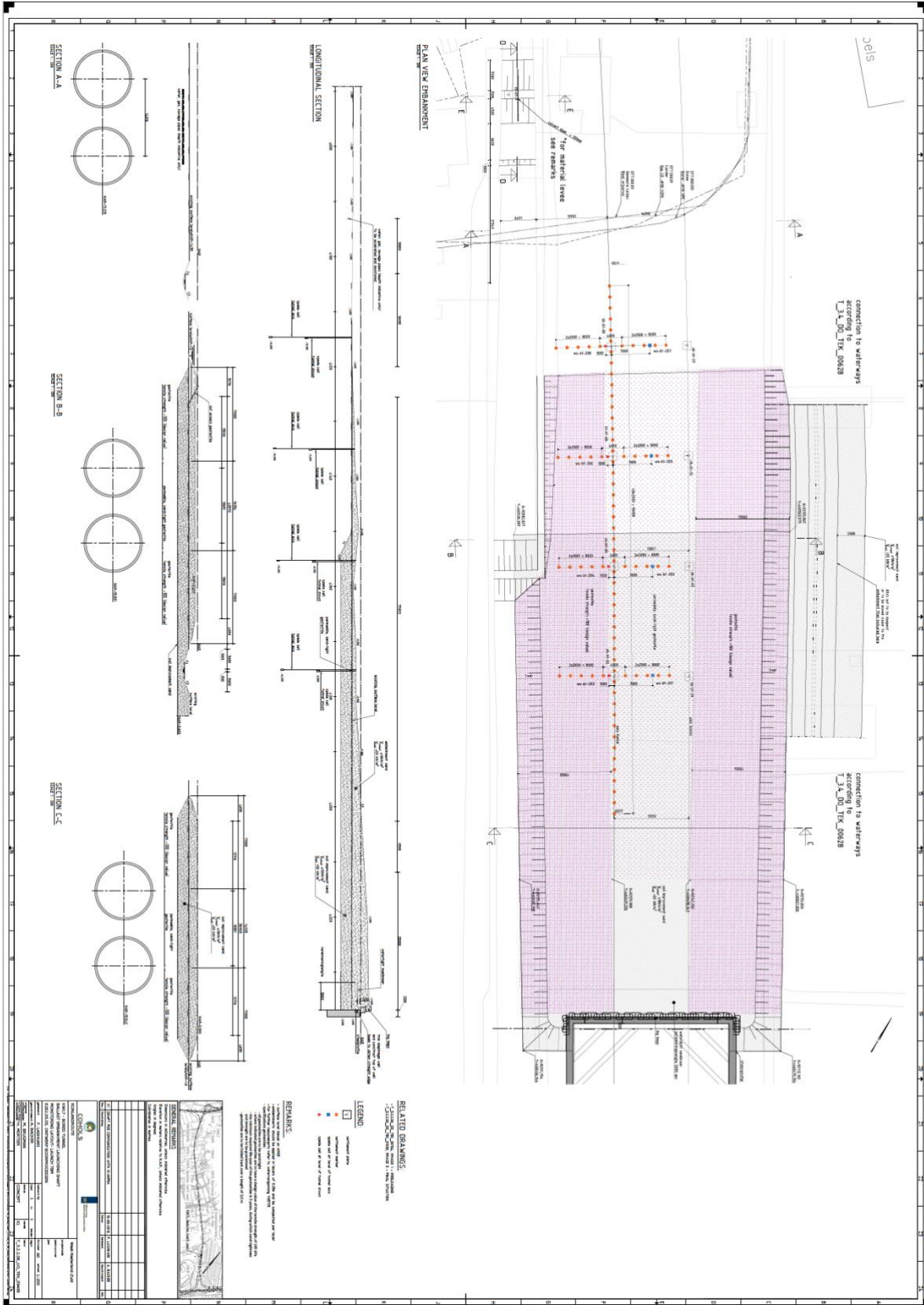


Figure A7.2: Top view on soil failure mechanism at the numerical upper face support pressure limit. Phase displacement, P_u

Appendix 8: Monitoring Layout – Launch TBM RijlandRoute [5]



Appendix 9: Accuracy settlement device

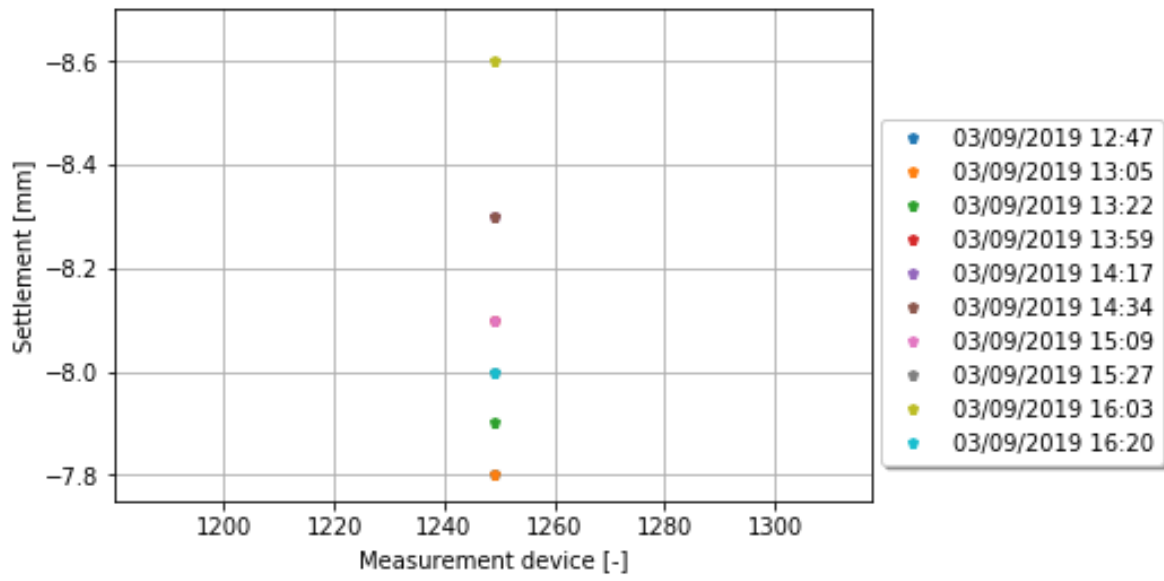


Figure A9.1: Accuracy settlement device (01249-Z) → can easily be extended if preferred

Appendix 10: Accuracy spade cells above the southern tube (1, 3, 5, 7)

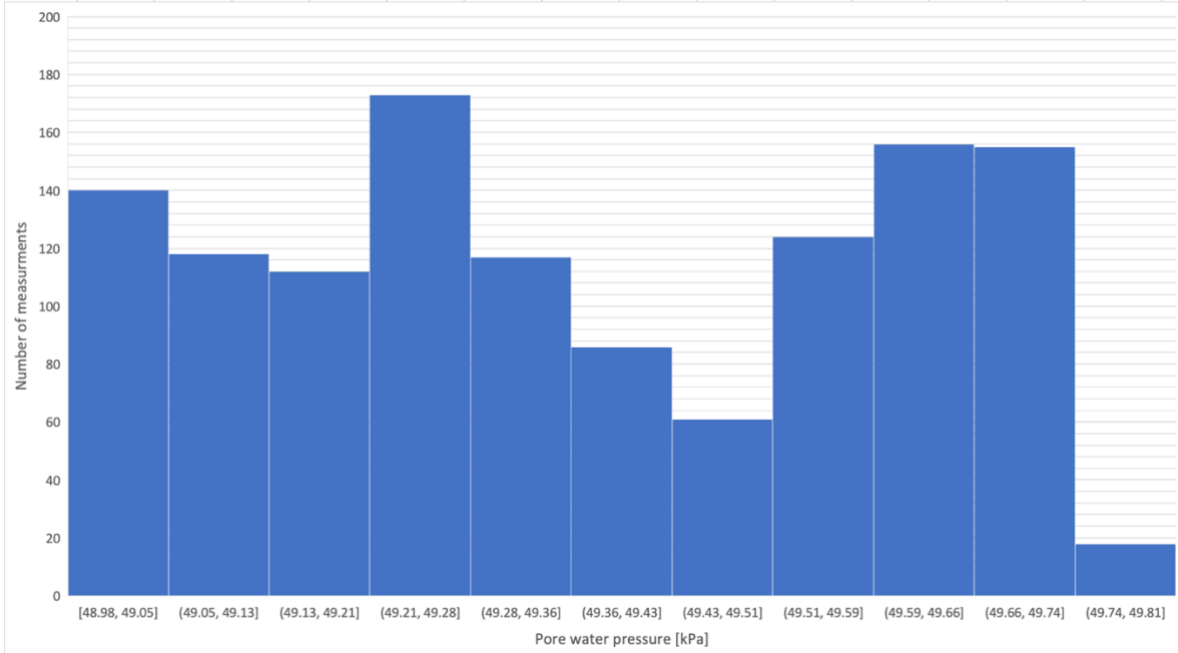


Figure A10.1: Accuracy spade cell 1

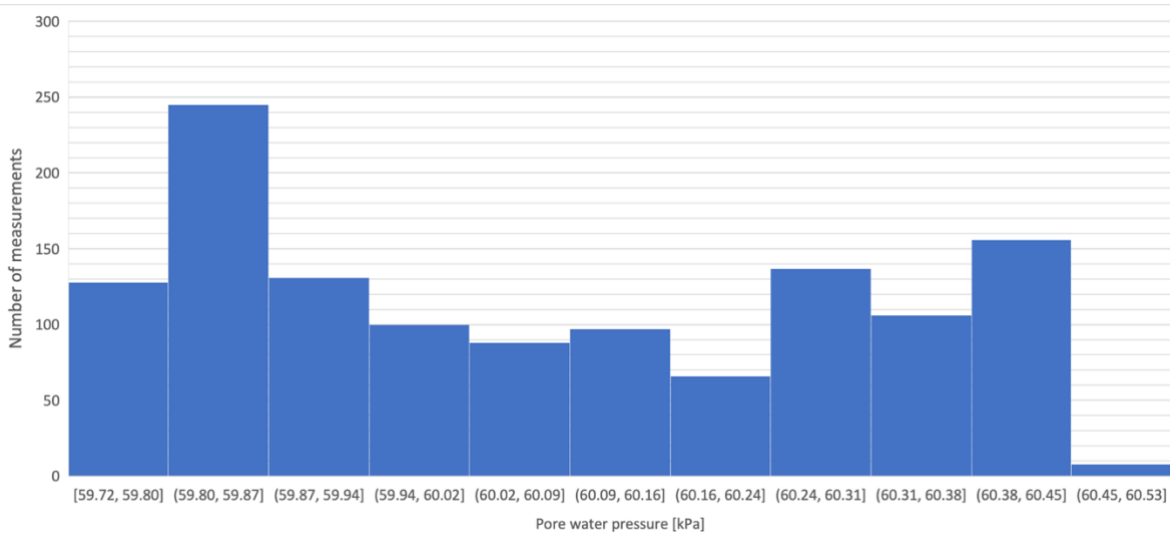


Figure A10.2: Accuracy of spade cell 3

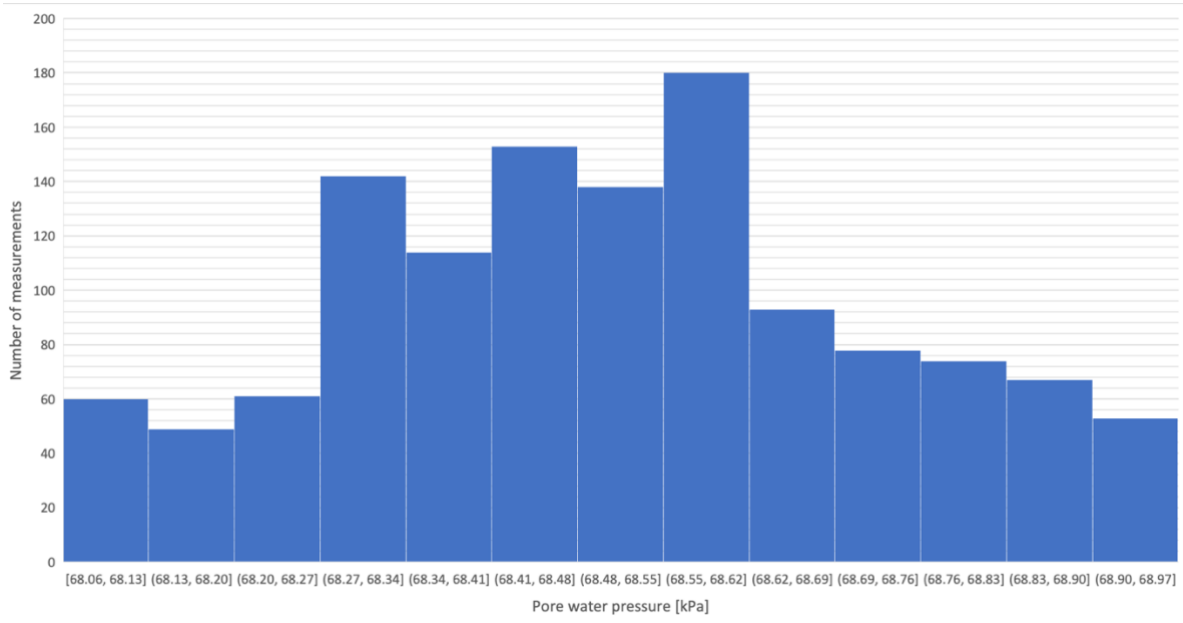


Figure A10.3: Accuracy spade cell 5

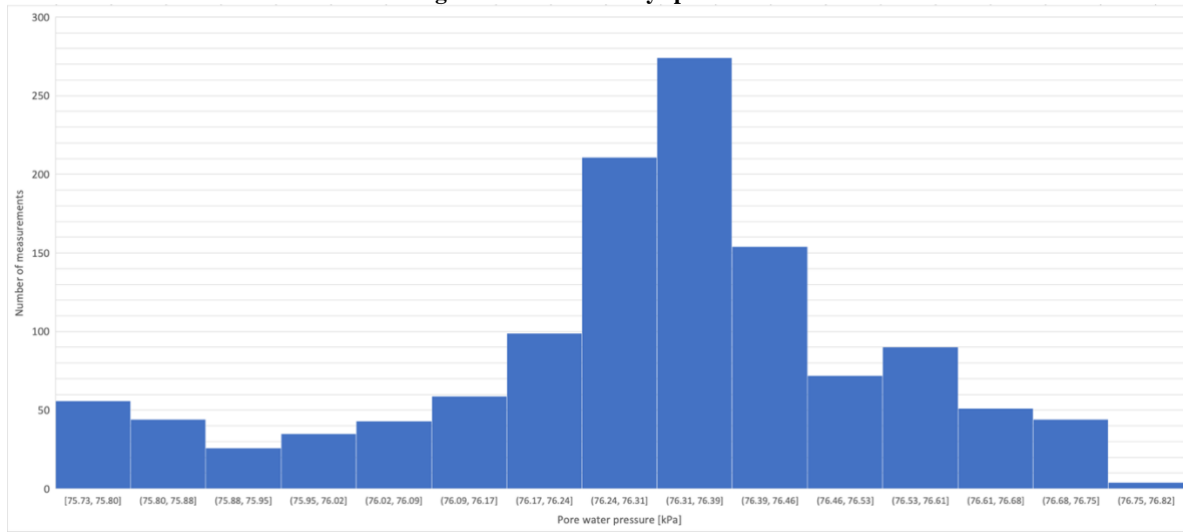


Figure A10.4: Accuracy of spade cell 7

Appendix 11: Face support pressure

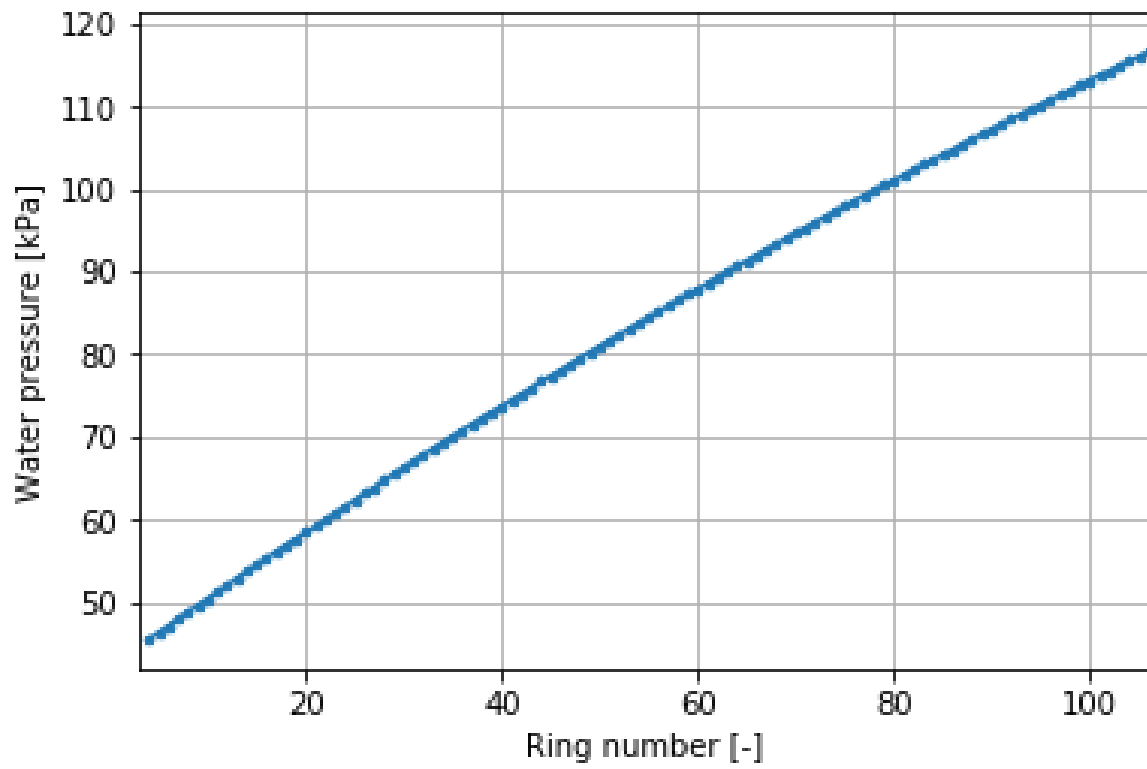


Figure A11.1: Water pressure distribution over the rings 3 to 106